

UNIVERSITY OF CALGARY

An Investigation of the Interactions between Organic Contaminants and Various Humic  
Acids by DSC Analysis

by

Michelle Laplante

A THESIS

SUBMITTED TO THE FACULTY OF GRADUATE STUDIES  
IN PARTIAL FULFILLMENT OF THE REQUIREMENTS FOR THE  
DEGREE OF MASTER OF SCIENCE IN CHEMICAL ENGINEERING

DEPARTMENT OF CHEMICAL AND PETROLEUM ENGINEERING

CALGARY, ALBERTA

SEPTEMBER, 1998

© Michelle Laplante 1998



National Library  
of Canada

Acquisitions and  
Bibliographic Services

395 Wellington Street  
Ottawa ON K1A 0N4  
Canada

Bibliothèque nationale  
du Canada

Acquisitions et  
services bibliographiques

395, rue Wellington  
Ottawa ON K1A 0N4  
Canada

*Your file Votre référence*

*Our file Notre référence*

The author has granted a non-exclusive licence allowing the National Library of Canada to reproduce, loan, distribute or sell copies of this thesis in microform, paper or electronic formats.

The author retains ownership of the copyright in this thesis. Neither the thesis nor substantial extracts from it may be printed or otherwise reproduced without the author's permission.

L'auteur a accordé une licence non exclusive permettant à la Bibliothèque nationale du Canada de reproduire, prêter, distribuer ou vendre des copies de cette thèse sous la forme de microfiche/film, de reproduction sur papier ou sur format électronique.

L'auteur conserve la propriété du droit d'auteur qui protège cette thèse. Ni la thèse ni des extraits substantiels de celle-ci ne doivent être imprimés ou autrement reproduits sans son autorisation.

0-612-35019-3

Canada

## **ABSTRACT**

Knowledge of the interactions between organic contaminants and the organic phase of soil is necessary for the development of predictive models describing the fate of contaminants in soil remediation processes such as thermal desorption. The organic phase of soil can be subdivided in humic acid (HA), fulvic acid (FA) and humin.

This research investigates the interactions between three humic acids (one HA extracted from soil and two commercial HAs) and three different classes of organic contaminants (PAHs, aliphatic hydrocarbons and polar organics) using differential scanning calorimetry (DSC). Chemical characterization of the humic acids were completed by total acidity tests and analysis by nuclear magnetic resonance (NMR) spectroscopy. Differences in the interactions between the HA and the contaminant as observed in the DSC thermograms were explained with respect to the chemical structure of the humic acid. It was determined that HA structure, contaminant type and contaminant concentration played a significant role in contaminant-HA interactions.

## **ACKNOWLEDGEMENTS**

I would like to express my gratitude to the large number of people who contributed to this work in a number of different ways. First, I would like to thank my supervisor, Dr. Anil Mehrotra, for giving me the opportunity to work on this project and for his continuous support and guidance.

Environmental projects require multidisciplinary knowledge and therefore I would like to thank those people whose expertise in various areas of science and engineering were invaluable to this work. Particularly, I would like to thank Dr. Salim Abboud of the Alberta Research Council, Dr. Nancy Okazawa of the Department of Chemical Engineering, and Aldo Bruccoleui of the Department of Chemistry. I would also like to acknowledge the TGA work provided by Mr. Les McLeod of Shell Canada. As well, funding for this project from the Natural Sciences and Engineering Research Council (NSERC) is gratefully acknowledged.

The technical work provided by Bruce Miles, Jake Neudorf, Claudine Curnow and Mike Grigg was greatly appreciated. Their dedication kept this project on track.

Finally, I would like to thank my fellow graduate students, friends and family for their moral support during my time at the University of Calgary. In particular, I would like to thank Darryl Wensley for his continuous encouragement throughout this project, and my family, Kristie, Pat and Denis for their love and support in all of my endeavours.

**FOR  
DENIS, PAT, KRISTIE  
AND  
DARRYL**

## **TABLE OF CONTENTS**

<b>APPROVAL PAGE</b>	<b>ii</b>
<b>ABSTRACT</b>	<b>iii</b>
<b>ACKNOWLEDGEMENTS</b>	<b>iv</b>
<b>DEDICATION</b>	<b>v</b>
<b>TABLE OF CONTENTS</b>	<b>vi</b>
<b>LIST OF TABLES</b>	<b>xi</b>
<b>LIST OF FIGURES</b>	<b>xii</b>
<b>NOMENCLATURE</b>	<b>xiv</b>
<b>Chapter 1: INTRODUCTION</b>	<b>1</b>
1.1 General Description	1
1.2 Scope of Study	3
<b>Chapter 2: LITERATURE REVIEW AND BACKGROUND</b>	<b>6</b>
2.1 Thermal Desorption Process	6
2.2 Soil Organic Matter	7
2.2.1 Non-humic Substances	8
2.2.2 Humic Substances	8
2.2.3 Breakdown of Humic Substances	10
2.2.4 Chemical Structure of Humic Acid	11
2.3 Sorption of Organic Contaminants	13
2.3.1 Adsorption Isotherms	15
2.3.2 Partitioning	17
2.3.3 Miscible/Immiscible Interactions	19
2.3.4 Critics of Partitioning	19
2.3.5 Site Specific Bonding	20

2.4	Thermal Analysis Techniques	21
2.4.1	Differential Thermal Analysis	22
2.4.2	Differential Scanning Calorimetry	22
2.4.3	Thermogravimetric Analysis	23
2.5	Use of Thermal Analytical Techniques in Soil Analysis	24
2.5.1	Determination of Chemical Components of Humic Materials	24
2.5.2	Determination of Physical Properties of Humic Materials	26
2.5.3	Determination of Miscible/Immiscible Interactions between Humic Material and Organic Contaminants	26
2.6	Summary	34
<b>Chapter 3:</b>	<b>EXPERIMENTAL</b>	<b>36</b>
3.1	Materials	36
3.1.1	Organic Chemicals	
3.1.2	Soil Samples	36
3.2	Schnitzer Procedure for Extraction of Humic Acid Fraction from Soils	38
3.2.1	Separation of Humin	38
3.2.2	Separation of Humic Acid	40
3.2.3	Cleaning of Humic Acid Fraction	41
3.2.4	Drying of Humic Acid	42
3.2.5	Comparison to Maguire's Procedure	42
3.3	DSC Measurements	42
3.3.1	Crucible Design	44
3.3.2	Sample Size	44
3.3.3	Sample Preparation	45
3.3.4	Heating Rate	46
3.3.5	Calibration	48
3.3.6	Interpretation of DSC Thermograms	48
3.4	Characterization of Humic Materials	49
3.4.1	Ash Content	49
3.4.2	Reactive Functional Group Analysis	50
3.4.2.1	Total Acidity	50
3.4.2.2	NMR Analysis	51
3.4.3	Mass Loss Experiments	53

3.5	DSC Thermograms for Pure Contaminants	53
3.5.1	Anthracene	55
3.5.2	Fluorene	57
3.5.3	Dodecane	57
3.5.4	Hexadecane	60
3.5.5	O-chlorophenol	60
<b>Chapter 4:</b>	<b>CHARACTERIZATION OF HUMIC ACID</b>	<b>64</b>
4.1	Ash Content	64
4.2	Chemical Functional Groups	65
4.2.1	Total Acidity	67
4.2.2	NMR Spectroscopy Results	69
4.3	Humic Acid DSC Thermograms	73
4.3.1	Dehydration	73
4.3.2	Cleavage of Terminal Functional Groups	77
4.3.3	Breakdown of Aromatic Structure	78
4.4	TGA Analysis	78
4.4.1	Mass Loss Experiments	78
4.4.2	Differential Mass Loss Curves	80
4.5	Summary	82
<b>Chapter 5:</b>	<b>DSC RESULTS FOR HUMIC ACID CONTAMINANT MIXTURES</b>	<b>84</b>
5.1	Anthracene on Humic Acid	84
5.1.1	Anthracene on HA(ML)	84
5.1.2	Anthracene on HA(F)	87
5.1.3	Anthracene on HA(A)	91
5.1.4	Constant Concentration of Anthracene on HA(ML), HA(F) and HA(A)	93
5.2	Fluorene on Humic Acid	94
5.2.1	Fluorene on HA(ML)	95
5.2.2	Fluorene on HA(F)	97
5.2.3	Fluorene on HA(A)	99
5.2.4	Constant Concentration of Fluorene on HA(ML), HA(F) and HA(A)	101



5.3	Discussion of PAH and Humic Acid Results	103
5.3.1	Effect of Humic Acid Structure	104
5.3.2	Effect of PAH Structure	105
5.3.3	Effect of PAH Concentration	106
5.4	Dodecane on Humic Acid	107
5.4.1	Dodecane on HA(ML)	107
5.4.2	Dodecane on HA(F)	109
5.4.3	Constant Concentration of Dodecane on HA(ML) and HA(F)	111
5.5	Hexadecane on Humic Acid	112
5.5.1	Hexadecane on HA(ML)	112
5.5.2	Hexadecane on HA(F)	114
5.5.3	Constant Concentration of Hexadecane on HA(ML) and HA(F)	116
5.6	Discussion of Straight Chain Aliphatic and Humic Acid Results	117
5.6.1	Effect of Humic Acid Structure	117
5.6.2	Effect of Aliphatic Structure	118
5.6.3	Effect of Aliphatic Concentration	119
5.7	O-chlorophenol on Humic Acids	119
5.7.1	O-chlorophenol on HA(ML)	119
5.7.2	O-chlorophenol on HA(F)	121
5.7.3	Constant Concentration of O-chlorophenol on HA(ML) and HA(F)	121
5.8	Discussion of Polar Organic and Humic Acid Results	123
5.9	Cooling Thermograms	125
5.10	Summary	125
<b>Chapter 6:</b>	<b>CONCLUSIONS AND RECOMMENDATIONS</b>	<b>129</b>
6.1	Conclusions	129
6.2	Significance of Results to the Thermal Desorption Process	132
6.3	Recommendations for Future Work	133
<b>Chapter 7:</b>	<b>REFERENCES</b>	<b>135</b>

<b>Appendix A: CALCULATIONS FOR DATA PROCESSING</b>	<b>140</b>
A.1 Calculations	140
A.2 Data Processing	141
A.3 BASIC Program	142

## **LIST OF TABLES**

<b><u>Table</u></b>	<b><u>Title</u></b>	<b><u>Page</u></b>
3.1	Properties of Contaminant Hydrocarbons	37
3.2	Number and type of Contaminant Humic Acid DSC Experiments	47
4.1	Experimental Values for Physical and Chemical Characteristics of Humic Acids	66
4.2	Average Total Acidity	66
4.3	% TOC in Various Organic Functional Groups in HA(F) and HA(ML) by $^{13}\text{C}$ -NMR Analysis	71

## LIST OF FIGURES

<u>Figure</u>	<u>Title</u>	<u>Page</u>
2.1	Breakdown of Soil Organic Matter	9
2.2	Typical Structure of Humic Acid	12
2.3	Important Functional Groups in Humic Acid	14
2.4	The Four Types of Adsorption Isotherms	16
2.5	Phase Diagrams for Fluorene and Humic Acid	28
2.6	Predicted Results for Fluorene-Humic Acid in a Miscible System	29
2.7	Predicted Results for Fluorene-Humic Acid in an Immiscible System	31
2.8	DSC Thermograms for Prepared Binary Mixtures of Fluorene	32
2.9	DSC Thermograms for Prepared Binary Mixtures of Anthracene	33
3.1	Schematic of Dilute Alkali Extraction Method	39
3.2	Schematic of DSC Measuring Cell	43
3.3	Chemical Shifts for Common Organic Groups	54
3.4	DSC Thermograms for Equivalent Anthracene Concentration on Glass Beads	56
3.5	DSC Thermograms for Equivalent Fluorene Concentration on Glass Beads	58
3.6	DSC Thermograms for Equivalent Dodecane Concentration on Glass Beads	59
3.7	DSC Thermograms for Equivalent Hexadecane Concentration on Glass Beads	61

3.8	DSC Thermograms for Equivalent O-chlorophenol Concentration on Glass Beads	62
4.1	NMR Spectrum for HA(F)	70
4.2	NMR Spectrum for HA(ML)	70
4.3	DSC Thermograms for Clean HA(ML)	74
4.4	DSC Thermograms for Clean HA(F)	75
4.5	DSC Thermograms for Clean HA(A)	76
4.6	% Mass Loss of Humic Acid with Temperature by TGA	79
4.7	Differential Mass Loss of Humic Acids with Temperature by TGA	81
5.1	DSC Thermograms for Anthracene in HA(ML)	85
5.2	DSC Thermograms for Anthracene in HA(F)	88
5.3	DSC Thermograms for Anthracene in HA(A)	92
5.4	DSC Thermograms for Fluorene in HA(ML)	96
5.5	DSC Thermograms for Fluorene in HA(F)	98
5.6	DSC Thermograms for Fluorene in HA(A)	100
5.7	DSC Thermograms for Dodecane in HA(ML)	108
5.8	DSC Thermograms for Dodecane in HA(F)	110
5.9	DSC Thermograms for Hexadecane in HA(ML)	113
5.10	DSC Thermograms for Hexadecane in HA(F)	115
5.11	DSC Thermograms for O-chlorophenol in HA(ML)	120
5.12	DSC Thermograms for O-chlorophenol in HA(ML)	122
5.13	DSC Cooling Thermograms	123

## NOMENCLATURE

$\Delta H$	enthalpy change (J/g or mWs/mg)
$A$	constant for determination of $E_{rel}$
$B$	constant for determination of $E_{rel}$
$C$	equilibrium concentration (kmol/kg)
$E(T)$	calorimetric sensitivity ( $\mu V/mW$ )
$E_{ln}$	temperature independent component of $E$ ( $\mu V/mW$ )
$E_{rel}$	temperature dependent component of $E$ ( $\mu V/mW$ )
$f_{oc}$	fractional mass of carbon
$K_{oc}$	normalized partitioning coefficient
$K_{ow}$	octanol-water partitioning coefficient
$K_p$	partitioning coefficient
$m$	sample mass (mg)
$Q$	cumulative heat flow (W/g)
$\dot{Q}$	heat flow per unit mass (mW/mg)
$q$	mols of sorbate/kg sorbent (kmol/kg)
$T$	temperature ( $^{\circ}C$ )
$U$	DSC measurement signal ( $\mu V$ )
DSC	differential scanning calorimetry
DTA	differential thermal analysis
TGA	thermogravimetric analysis
TOC	total organic carbon

FA	fulvic acid
HA	humic acid
HA(F)	Fluka humic acid
HA(A)	Aldrich humic acid
HA(ML)	extracted humic acid
PAH	polyaromatic hydrocarbon
SOM	soil organic matter

## Chapter 1

### INTRODUCTION

#### 1.1 General Description

The type and the extent of the sorption of organic contaminants on soil play an important role in the fate of these contaminants in the environment. In particular, researchers have recognized that these interactions are dominated by the interaction between organic contaminants and soil organic matter (SOM). A number of mechanisms have been put forth to explain these interactions; however, a partitioning of the contaminant in the organic phase of soil is the mechanism favoured by most researchers. Attempts have been made to quantify these interactions in hopes of creating models to describe the interaction between soil and organic contaminants. These models are useful for describing the transport of chemicals in the environment and predicting the effectiveness of soil remediation processes such as thermal desorption.

Thermal desorption is a soil remediation process in which soils contaminated with organic contaminants are heated to volatilize the contaminants. Troxler et al. (1993) showed that the organic content or humic content of the soil is an important soil characteristic influencing the application of thermal desorption.

The humic content of the soil is the stable organic portion of the soil consisting of large macromolecular polymers of chemically resistant organic materials such as cellulose, hemicellulose and lignin. These humic substances can be further subdivided



into humic acid (HA), fulvic acid (FA), and humin, each of which has slightly different physical and chemical characteristics.

Previous work in our laboratory by Maguire (1994) investigated thermal interactions between polycyclic aromatic hydrocarbons (PAHs) and the humic fractions of soil, specifically, humic acid, fulvic acid, and humin. Maguire (1994) attempted to explain soil-contaminant interactions in terms of miscible and immiscible behaviour. Maguire (1994) found that PAHs tended to form miscible mixtures with humic acid and immiscible mixtures with fulvic acid and humin. Due to the unique behaviour with humic acid, this work will elaborate on the findings of Maguire, 1994 and focus on the interactions between organic contaminants and the humic acid fraction of soil.

Humic acid (HA) is a very heterogeneous substance and has different chemical structures depending on the type of soil. A number of authors have stressed the importance of the structure and composition of HA on the binding of organic contaminants and stress the implications of this on the formation of predictive models for the fate of pollutants in the environment (Gauthier et al., 1987; Garbarini and Lion, 1986). Often, dissimilarities in HA's ability to sorb nonionic organic contaminants can be attributed to differences in polarity or hydrophobicity of the humic acid (Kile et al., 1995). Therefore, it is expected that different types of organic contaminants will interact differently with different humic acids at different concentrations.

## 1.2 Scope of the Study

The technique of differential scanning calorimetry (DSC) is used to study the interactions of three different humic acids (one extracted HA and two commercial HAs) and three different classes of organic contaminants (PAHs, aliphatic hydrocarbons and polar hydrocarbons) at various concentrations. This study is an extension of the work performed by Maguire (1994) in this laboratory, as a means of further understanding the implications of humic content on the thermal desorption process. In particular, the main objectives of this work are to:

- 1) to elaborate on the data presented by Maguire (1994) to understand solid-liquid and liquid-vapour transition behaviour of humic acid and organic contaminants at various concentrations;
- 2) to investigate the importance of chemical composition of humic acid on humic acid-organic contaminant interactions;
- 3) to investigate the importance of the type of contaminant on the sorption characteristics on different humic acids; and,
- 4) to determine the effect of contaminant concentration on the sorption characteristics of different humic acids.

Chapter 2 of this thesis presents a literature review and background knowledge for this investigation. First, thermal desorption, the main application of this work, is discussed, followed by a description of the chemical and physical characteristics of soil organic matter and its components. A review of the sorption mechanisms of organic compounds on humic substances, including physical adsorption, partitioning,

4

miscible/immiscible interactions, and site specific bonding, is given. Finally, a summary of thermal analytical techniques, and their applicability to the study of humic substances is presented.

Chapter 3 describes the experimental work used to achieve the objectives of this research. The experimental section can be broken down into five parts. The materials section describes the contaminants and humic acids used in this study and describes the chemical characteristics of the contaminants. The Schnitzer extraction procedure was used to extract humic acid from soil and is described in detail in this chapter. Differential scanning calorimetry (DSC) was the analytical tool used in this investigation and considerations for vaporization experiments using DSC is discussed. Chemical characterization methods used in this work including, ash content, total acidity tests, NMR spectroscopy and mass loss experiments are also described. This chapter is concluded with DSC thermograms obtained for the pure contaminants.

Chapter 4 presents the results obtained for the characterization of humic acids. In particular, the relative polarity of each humic acid is investigated in terms of the concentration of specific organic functional groups. Wherever possible, the results obtained are compared to expected literature values. DSC thermograms for the clean humic acids are also illustrated in this chapter.

Chapter 5 summarizes the results obtain from DSC thermograms of humic acid-contaminant mixtures. The importance of the chemical structure of the contaminant compared to the chemical structure of the different humic acids is emphasized. The results obtained are compared to those presented by Maguire (1994).

Chapter 6 presents a summary of the conclusions of this study along with some recommendations.

## **Chapter 2**

### **LITERATURE REVIEW AND BACKGROUND**

#### **2.1 Thermal Desorption Process**

Thermal desorption is an ex-situ soil remediation process in which a contaminated soil is heated in order to volatilize organic contaminants into an exhaust gas. Combustion or soil incineration has long been the thermal remediation process of choice; however, the desire to lower costs and the need to avoid challenges with tightly regulated air emission standards have led to thermal remediation technologies that avoid combustion (Valenti, 1994).

Thermal desorption is effective in reducing concentrations of a wide range of petroleum contaminants including gasoline, diesel fuel, jet fuels, kerosene, heating oils and lubricating oils. Thermal desorption can be applied to most petroleum constituents that are volatilized at temperatures up to 650 °C (Friend, 1996). The process can also find applications to contamination by wood-treating processes, creosote contaminated soil, synthetic rubber processing wastes and paint wastes. Thermal desorption has been proven effective in treating contaminated soils, sludges and various filter cakes, and has been chosen as the remediation technique for a number of US Superfund sites (Laforanara et al., 1991).

Thermal desorption as a remediation process is gaining acceptance as a viable alternative to soil incineration and is considered an innovative technique. Research is

7

very active in this area, particularly in the areas of fundamental studies and testing of bench, pilot and commercial scale systems. Smith (1997) investigated the feasibility of treating several contaminated industrial samples by thermal desorption using a bench scale batch thermal desorber. Laformara et al. (1991) gave a summary of data collected from various pilot and full-scale thermal desorbers. Maguire (1994) and Mehrotra et al. (1996) investigated the thermal interactions between humic materials and polyaromatic hydrocarbons and attempted to explain the soil-contaminant interactions in terms of miscible and immiscible behaviour. This research presents the implications of miscible or immiscible systems on the temperature required for complete removal of a given contaminant from the whole soil (Mehrotra et al., 1996).

Troxler et al. (1993) identified a number of critical success factors necessary for effective soil remediation by thermal desorption. These factors include: site, waste and soil characteristics; regulatory requirements; process equipment design; and operating characteristics. In terms of soil characteristics, humic content or organic content of the soil has a large effect on the sorptive capacity of organic contaminants to the soil (Garbarini and Lion, 1986). Therefore, an understanding of the thermal interactions between the organic phase of soil and organic contaminant is important for the optimization of the thermal desorption process.

## **2.2 Soil Organic Matter**

It has long been recognized that soil organic matter is a major factor in controlling the physical and chemical properties of soils. These properties include buffering

capacity, metal binding capacity, sorption of hydrophobic organic compounds, stability of aggregates of soil particles and water holding capacity (Wershaw, 1993). Soil organic matter (SOM), or humus, includes the total of the organic material in the soil excluding undecayed plant and animal tissues, their partial decomposition products and the soil biomass.

### 2.2.1 Non-humic Substances

SOM can be subdivided into a number of different components as illustrated in Figure 2.1. First, SOM can be subdivided into both humic and nonhumic substances. Nonhumic substances are organic compounds that have recognizable physical and chemical properties, and belong to known classes of biochemistry (i.e. amino acids, carbohydrates, fats, waxes, resins, and organic acids). These compounds become incorporated in the soil due to the biodegradation of plant and animal tissues. Most of this material is further biodegraded by microorganisms to carbon dioxide as part of the carbon cycle and therefore have short residence times in the soil (Schnitzer, 1982).

### 2.2.2 Humic Substances

Humic substances, on the other hand, are the part of soil organic matter that consists of resynthesis products of partially oxidized nonhumic substances. These larger molecules are polymers of more chemically resistant organic materials such as cellulose, hemicellulose and lignin, and are stable parts of the soil. They are a series of relatively

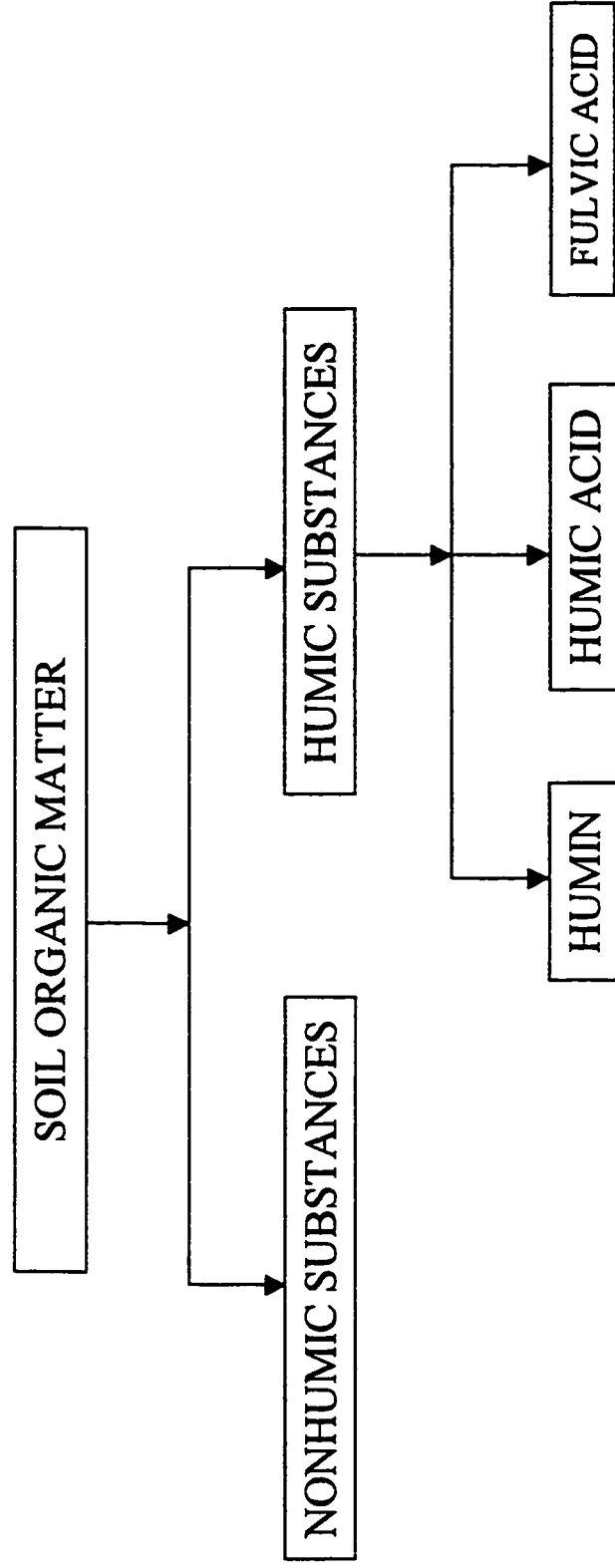


Figure 2.1: Breakdown of Soil Organic Matter



high molecular weight substances formed from secondary synthesis reactions and are generally characterized as being rich in oxygen containing functional groups such as COOH, phenolic or enolic OH, alcoholic OH, and C=O of quinones (Stevenson, 1994). This process is called humification. These molecules are considered to be coiled, long-chain structures of two- or three-dimensional cross-linked macromolecules whose negative charge is primarily derived from ionization of acidic functional groups. A formal definition of humic substances give by Sparks (1995) is “general category of naturally occurring, biogenic, heterogeneous organic substances that can generally be characterized as being yellow to black in colour, of high molecular weight, and refractory”. Humic substances are considered to be amphiphilic which means that they consist of separate hydrophobic (non-polar) and hydrophilic (polar) segments.

Tan (1985) presented scanning electron microscopy images of the macromolecular structure of humic substances. Five major types of structures were noted: small spheroids, flattened aggregates of spheroids, linear, chainlike assemblies of aggregates, flattened filaments and perforated sheets. A computer-simulated three-dimensional model of a humic substance is presented in Schnitzer and Schulten (1995). This model shows a large three-dimensional structure in which anthropogenic substance can be trapped and bound within void spaces.

### 2.2.3 Breakdown of Humic Substances

Humic substances can be further sub-divided into humic acid (HA), fulvic acid (FA), and humin. The structure of the three humic fractions are very similar; however,

they vary in molecular weight, ultimate analysis and functional group content (Schnitzer, 1978).

Humic acid is the dark-coloured organic material that can be extracted from soil by dilute alkali and other reagents, but is insoluble in dilute acids. Humic acid has a molar mass between 3000 and 10000 kg/kmol.

Fulvic acid is the soil organic matter fraction that is soluble in both alkali and acid. Fulvic acid has a molar mass between 500 and 5000 kg/kmol. The O/C ratios in soil HA and FA are 0.5 and 0.7, respectively. The properties of humic acid and fulvic acid often overlap leading to the belief that fulvic acid is derived from the oxidation of humic acid. The transition from humic acid to fulvic acid is accompanied by a decrease in molecular weight, a loss of carbon, hydrogen and nitrogen, and an increase in oxygen (Schnitzer and Desjardins, 1962).

Humin is the alkali insoluble fraction of soil organic matter. Humin is thought to consist of: 1) humic acids so intimately bound to mineral matter that the two cannot be separated; 2) highly condensed humic matter with a high C content and thereby insoluble in alkali; and 3) fungal melanins and parafinic substances.

#### 2.2.4 Chemical Structure of Humic Acid

A diagram of the structure of humic acid is shown in Figure 2.2. Because of the large number of component molecules combined with the numerous types of linkages which bind these molecules together, accurate structural formulas for humic substances are unavailable. Therefore, each fraction (HA, FA, humin) must be regarded as



consisting of a series of molecules of different sizes, with few having the same structural configuration or array of reactive functional groups (Stevenson, 1992). Fractionation of humic substance into humic acid, fulvic acid and humin reduces the heterogeneity of humic substances and allows for the observation of more common physical and chemical properties. Figure 2.3 shows the common functional groups found in humic substances.

### **2.3 Sorption of Organic Contaminants**

Adsorption is defined as the accumulation of a substance or material at an interface between the solid surface and the bathing solution. Sorption is a general term, which includes adsorption, that is used when the retention mechanism at the surface is unknown (Sparks, 1995). Sorption mechanisms are very important in the interactions between organic contaminants and soil organic matter.

The reactivity of SOM is very high and, therefore, plays a very important role in chemical processes occurring in the soil. Due to the high specific surface and cation exchange capacity, SOM is an important sorbent of plant macronutrients and micronutrients, heavy metal cations and organic materials. There are a number of different mechanisms with which ionic and non-ionic compounds can be adsorbed on the soil. The sorption characteristics of organic contaminants on soil organic materials have been discussed in literature. The dominant theory of interaction between soil organic material and nonionic organic substances is a partitioning process between the aqueous phase and the hydrophobic surface phase of the humic material.

Functional Group	Structure
<b><u>Acidic Groups</u></b>	
Carboxylic	$R-C=O(-OH)$
Enol	$R-CH=CH-OH$
Phenolic OH	$Ar-OH$
Quinine	$Ar=O$
<b><u>Neutral Groups</u></b>	
Alcoholic OH	$R-CH_2-OH$
Ether	$R-CH_2-O-CH_2-R$
Ketone	$R-C=O(-R)$
Aldehyde	$R-C=O(-H)$
Ester	$R-C=O(-OR)$
<b><u>Basic Groups</u></b>	
Amine	$R-CH_2-NH_2$
Amide	$R-C=O(-NH-R)$

Figure 2.3: Important Functional Groups in Humic Acid (Sparks, 1995)

### 2.3.1 Adsorption Isotherms

A common procedure for the evaluation of sorption mechanisms between soil organic matter and organic contaminants is through equilibrium adsorption experiment and adsorption isotherms. An isotherm is a plot of the variation of the solid-phase concentration versus the solution phase concentration under equilibrium conditions. Researchers explain the interactions between the SOM and organic contaminants using four general types of isotherms (S, L, H and C) as illustrated in Figure 2.4. The S-type curve is characterized by an increasing slope with increasing adsorptive concentration followed by an eventual decreasing to zero slope. This indicates a low affinity for the adsorbate at low concentrations with increasing affinity at higher concentrations. The L-shaped or Langmuir isotherm is characterized by a decreasing slope as concentration increases, thus indicating a decrease in affinity at higher concentrations. The H-type isotherm indicates very strong adsorbent-adsorbate interactions. Finally, the straight line of the C-type isotherm is indicative of a partitioning mechanism whereby the adsorptive molecules are distributed or partitioned between the interfacial phase and the bulk solution phase without specific bonding between the adsorbent and the adsorbate (Sparks, 1995). S-, L- and C-type isotherms are all observed in literature related to the sorption of organic contaminants to soil organic matter; however, the C-type isotherms are most common leading many researchers to suggest a partitioning mechanism for the interaction between SOM and organic contaminants.

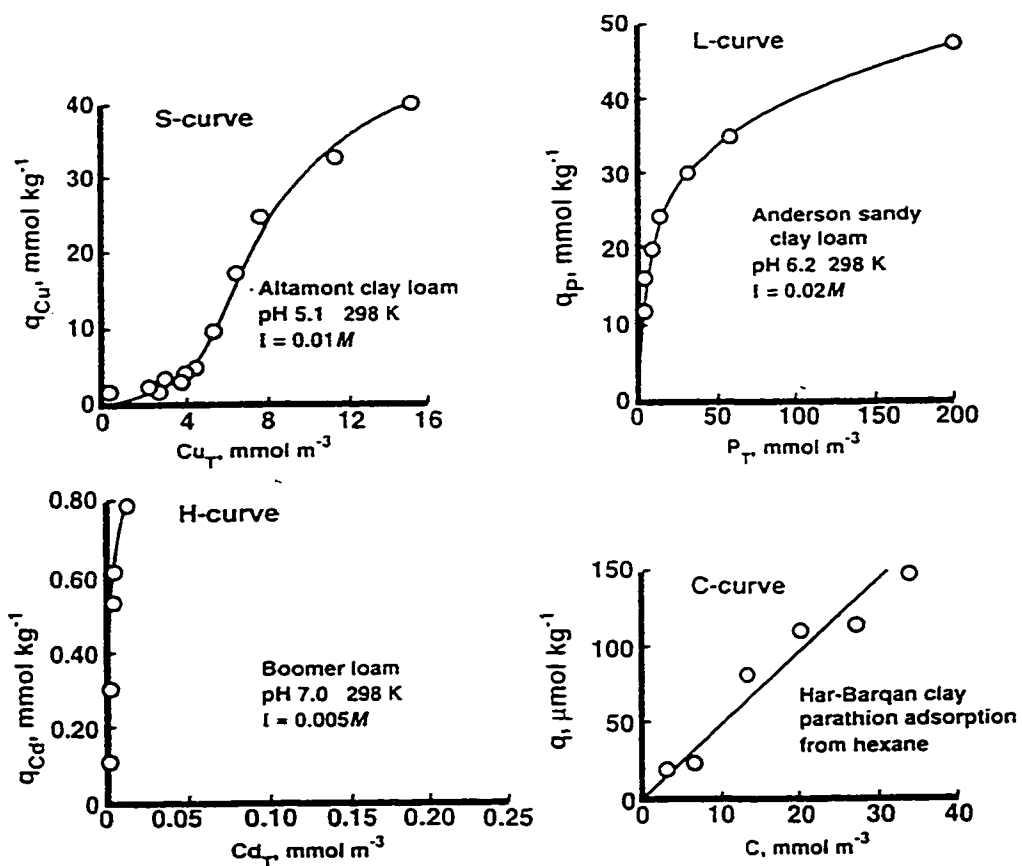


Figure 2.4: The Four Types of Adsorption Isotherms (Sparks, 1995)

### 2.3.2 Partitioning

Lambert (1967) first proposed partitioning between the soil organic matter and organic compounds as being analogous to liquid-liquid phase equilibria. This partitioning occurs on the specific hydrophobic SOM surfaces by weak solute-solvent interactions. These important hydrophobic sites on humic substances include fats, waxes, resins and aliphatic side chains. Because water is not a good competitor for these sites, organic molecules tend to accumulate at these sites. The partitioning would give rise to linear isotherms as exhibited by adsorption of nonpolar or slightly polar molecules by soils (Weed and Weber, 1975).

Lambert (1967) suggested that the role of soil organic matter is similar to that of an organic solvent in solvent extraction and that the partitioning of a neutral organic compound between soil organic matter and water should correlate well with its partitioning between water and an immiscible organic solvent. Thus the concept of partitioning coefficients could be used to describe the interaction between organic matter and organic contaminants. This concept has gained widespread acceptance (Voice et al., 1983).

The partitioning coefficient,  $K_p$ , is defined as the slope of the C-type isotherm or, similarly, the ratio between the activities of a solute in two bulk phases according to the equation:

$$q = K_p C \quad (2.1)$$



where  $q$  is the amount of adsorption in kmol/kg, and  $C$  is the equilibrium concentration in kmol/kg.

Karickhoff et al. (1979) investigated partition coefficients for pyrene and methoxyclor on organic matter. A plot of  $K_p$  as a function of fractional mass of organic carbon,  $f_{oc}$ , indicated a linear increase of  $K_p$  with  $f_{oc}$ . Therefore, it is useful to normalize the partitioning coefficient with fractional organic content according to the equation:

$$K_{oc} = \frac{K_p}{f_{oc}} \quad (2.2)$$

Many researchers have found that  $K_{oc}$  is nearly the same for a variety of soils and a given nonionic organic compound, leading to numerous correlations between the  $K_{oc}$  value of a contaminant and its corresponding octanol-water partition coefficient ( $K_{ow}$ ) or its water solubility ( $S_w$ ). Some of these correlations are presented in Garbarini and Lion (1986), Briggs (1973) and Voice et al. (1983). These correlations allow for predictions of the fate of organic contaminant in many cases where accurate values for sorption in the given soil system are not available. Using these correlations, Onken and Traina (1997) were able to match calculated  $K_{oc}$  values with experimental values of  $K_{oc}$  for the sorption of pyrene and anthracene to humic acid-mineral complexes. They also identified C-type adsorption isotherms indicative of the partitioning mechanism.

### 2.3.3 Miscible/Immiscible Interactions

Maguire (1994) expanded on the concept of partitioning between the SOM and nonionic organic compound by introducing the importance of miscible and immiscible interactions between organic fractions of soil and polycyclic aromatic hydrocarbons (PAH). This work was performed in our laboratories at the University of Calgary.

Maguire's results showed distinct differences between the interactions between different organic fractions and PAHs. The humic acid fraction exhibited miscible behaviour with the PAHs investigated, whereas the fulvic acid and humin fractions exhibited immiscible behaviour (Mehrotra et al., 1996). The importance of these findings to thermal desorption lies in the fact that complete removal of a hydrocarbon contaminant may only occur at temperatures higher than the boiling temperature of the contaminant if miscible behaviour occurs between the contaminant and the humic substance. Conversely, if immiscible behaviour occurs, the contaminant will vaporize at or below the bubble point temperature (Mehrotra et al., 1996).

### 2.3.4 Critics of Partitioning

Some researchers have challenged the concept of partitioning as the primary sorption mechanism. Using the Langmuir equation (L-type) of adsorption, Mingelgrin and Gerstl (1983) showed that, at the low concentrations used in the sorption experiments, a linear isotherm, similar to the ones used to support a partitioning mechanism, should result. MacIntyre and Smith (1984) have echoed this concern.

In general, a surface will display attraction for adsorbates of chemical nature similar to its own. However, when considering a heterogeneous surface such as that found in organic matter, general measures of similarity such as polarity, hydrophobicity or any other single measure of similarity may not always predict the extent of adsorption (Mingelgrin and Gerstl, 1983). Therefore, it is stated that theoretically, as well as practically, surface uptake of organic contaminants by organic matter in the soil cannot be simply defined as adsorption or partitioning, but rather as a continuum of possible interactions starting with fixed site adsorption and ending with true partitioning between three dimensional phases.

Mingelgrin and Gerstl (1983) state that reliance on prediction models based solely on partitioning data “may lead to serious misconceptions regarding the nature of the interactions of non-ion compounds in soils and to erroneous predictions regarding the fate of such compounds there, thus creating possible economic and ecological damage.”

#### 2.3.5 Site Specific Bonding

Lambert (1967) stated that “sorption of chemicals in soil is an extremely complex phenomenon and any explanation of what is, in fact, occurring should reflect this complexity.” Therefore, a simple partitioning process for the interaction between soil organic matter and organic contaminants may be too simplistic; however, it does not need to be disregarded. Graber and Borisover (1998) refer to site-specific interactions between organic compounds and soil organic matter that may occur at limited surface sites or at limited interior sites. This is in contrast to true partitioning in ideal systems in which

molecules are distributed throughout the sorbent bulk. For example, the presence of carboxyl, hydroxyl and amino groups on organic matter suggests hydrogen bonding will function as a bonding mechanism for organic molecules which contain similar functional groups.

Another theory recently proposed is a rubbery/glassy polymer model in which most of the partitioning occurs in the rubbery phase, whereas physical adsorption by “hole filling” occurs in the glassy phase (Xing and Pignatello, 1997). This model considers the SOM to be a mixture of macromolecules consisting of rubbery and glassy components spanning a range of glass transition temperatures. The rubbery section is characterized by a relative ease of molecular motion and behaves similarly to a fluid within which simple Brownian motion and Fickian diffusion of solute molecules occurs. Thus, the phase partitioning theory is compatible with this “rubbery” section. The glassy section is characterized as containing fixed free-volume microvoids within which sorbing materials are adsorbed and immobilized. This glassy section is more condensed, highly cross-linked, and more aromatic thus having reduced molecular mobility (Leboeuf and Weber, 1997).

## **2.4 Thermal Analysis Techniques**

Thermal analysis is a valuable technique which gives information concerning physical parameters such as energy, mass and evolved volatiles as a function of temperature. Thermal analysis has been used as a research tool for over a century to examine the rate and temperature at which materials undergo physical and chemical

changes. The three most common techniques used in evaluating the thermal properties of soil are differential thermal analysis (DTA), differential scanning calorimetry (DSC), and thermogravimetric analysis (TGA).

#### 2.4.1 Differential Thermal Analysis

Differential thermal analysis (DTA) is a thermal analysis technique in which a sample and an inert reference are subjected to a controlled heating program where the temperature difference between the sample and the reference material is measured. The difference in temperature between the sample and the reference is attributed to energy-emitting (exothermic) or energy-absorbing (endothermic) transitions occurring within the sample. Although the transition temperatures are observable using DTA, calorimetric measurements are not.

#### 2.4.2 Differential Scanning Calorimetry

The recognition of the need to have direct calorimetric measurements of energies of transition lead to the development of differential scanning calorimetry (DSC). DSC is very similar to DTA; however, in a DSC system the differential energy required to keep both the sample and the reference at the same temperature is measured. During an endothermic transition in the sample, the energy absorbed by the sample is replenished by an increased energy input to the sample which is precisely equivalent in magnitude to the

energy absorbed in the transition. Thus, the precise energy required for the transition is measurable. Watson et al. (1964) gives a good comparison of DTA and DSC.

DSC is commonly used in laboratories to characterize polymers, elastomers, organic materials and other materials in terms of properties such as melting points, glass transition temperatures, and percent crystallinity. Most of these experiments are done in the solid or liquid phase since determination of boiling points with DSC has traditionally delivered unacceptable results due to pre-boiling vaporization. However, DSC is gaining popularity for use in the vapour phase with the development of pressure DSC and the development of standard procedures (TA Instruments, 1994). For example, determination of boiling points at different pressures using pressure DSC yields boiling point shifts which can be used to obtain quantitative vapor pressure information. Cassel and DiVito (1994) describes the application of DSC for boiling point and vapor pressure determination.

#### 2.4.3 Thermogravimetric Analysis

Thermogravimetric analysis (TGA) is another popular thermal analysis technique in which the change in mass of a sample is measured as a function of temperature. Therefore, in order to yield useful information, any physical or chemical changes in the sample must be accompanied by the evolution of volatiles. Thermal changes within the organic phase of soil usually involve the cleavage and volatilization of terminal functional groups. Therefore, TGA is applicable for the thermal study of soil organic compounds.

Goodrum and Siesel (1996) found that TGA was a useful tool in determining boiling points and vapour pressures of organic compounds using the same techniques as developed for pressure DSC to reduce pre-boiling vaporization of the sample. Goodrum (1997) found that vapour pressure data of the short-chain triglycerides, tricaproin and tricaprylin could be determined with errors less than 6% for pressures from ambient down to 20 mmHg.

## **2.5 Use of Thermal Analytical Techniques in Soil Analysis**

Soil is a complex mixture of mineral and organic matter varying in physical, chemical and biological properties. For this reason, no pertinent data are available in literature concerning differential thermal analysis of whole soils. With the improved knowledge of extraction and purification techniques of humic and fulvic acids and related compounds from soils, thermal analytical techniques are receiving increased research attention (Tan et al., 1986).

### **2.5.1 Determination of Chemical Components of Humic Materials**

Schnitzer and Kodama (1972) described three thermal events resulting from the thermal study of humic substances. The first event is observed as an endothermic peak resulting from the dehydration of bound water, and it occurs up to a temperature of about 200 °C. The second thermal event is an exothermic reaction occurring primarily between 250 °C and 280 °C in which elimination of functional groups occurs. Finally, the

decomposition of the “nuclei” of the organic fractions occurs as another exothermic peak at temperatures over 400 °C. In order to obtain a better understanding of the specific mechanisms involved in the decomposition of the organic “nucleus”, it is necessary to identify the reaction products. However it is believed that mass loss above this temperature is due to the breakdown of the aromatic structure of the humic acid.

Flaig et al. (1975) found that the main decomposition reactions of humic acid occur at 340-370 °C and at 400-420 °C. This decomposition reaction was attributed to decarboxylation and cleavage of terminal functional groups accompanied by the cleavage of acetyl groups and demethylation of methoxyls. Any decomposition reaction observed above 450 °C was attributed to decomposition of the aromatic structure of the humic acid.

In another thermal decomposition study using TGA by Schnitzer and Hoffman (1964), humic substances obtained from two different soil regions ( $A_o$  and  $B_h$ ) were investigated. It was found that the  $B_h$  fulvic acid was more thermally stable than the  $A_o$  humic acid. The  $A_o$  fraction showed decomposition reactions at 280 °C and 540 °C. It was determined that the decarboxylation of the sample started above 150 °C and was complete at 250 °C, and decomposition of the phenolic hydroxyl group started at 150 °C and was maximum at 200 °C. By 400 °C, both functional groups were completely released. The  $B_h$  sample was much more resistant as decarboxylation started at temperatures above 250 °C and was complete by 450 °C. The elimination of hydroxyl groups increased up to 300 °C and rapidly decreased until 450 °C.



These examples of thermal studies of humic materials show the great variability in thermal stability of different humic materials, especially between humic acid and fulvic acid. Research has been conducted to distinguish humic acids from fulvic acids using DTA or DSC. Tan et al. (1986) reported humic acid and fulvic acid as having strong exothermic reactions around 400 °C and 500 °C, respectively. However, these temperatures can be shifted to higher or lower temperatures depending on the characteristics of the organic fraction.

#### 2.5.2 Determination of Physical Properties of Humic Materials

Leboeuf and Weber (1997) used DSC to observe the glass transition point of humic acid. At the glass transition temperature,  $T_g$ , there is a continuity of enthalpy, entropy and volume, but not in the constant-pressure heat capacity. Because the rubbery state allows greater molecular motion, it has a greater ability to disperse heat and thus exhibits a higher heat capacity. This measurement is observable using DSC. The range of  $T_g$  for humic acids in this study was between 43°C and 62 °C.

#### 2.5.3 Determination of Miscible/Immiscible Interactions between Humic Material and Organic Contaminants

Maguire (1994) used DSC to investigate thermal interactions between humic fractions and PAHs. This work was completed in our laboratory in the Chemical Engineering Department at the University of Calgary. Using the assumption of completely miscible and completely immiscible binary systems, Maguire (1994)

presented a qualitative simulation of DSC thermograms for each case. Example calculations for fluorene-humic acid mixtures are presented here.

Phase diagrams for completely miscible and immiscible fluorene-humic acid mixtures are shown in Figures 2.5a and 2.5b, respectively. The cumulative heat energy ( $Q$ ) required to raise the temperature from just below the normal boiling point of the contaminant to the estimated boiling point of humic acid was calculated for both the miscible and immiscible cases. Differentiation of the cumulative heat energy with respect to time ( $-dQ/dt$ ) gave the respective simulated DSC plot. Presented here are simulated DSC plot for fluorene on humic acid assuming miscible and immiscible behaviour presented by Maguire et al. (1995).

Figure 2.6 shows the predicted results for the fluorene-humic acid system for fluorene fractions of 0.05 to 0.85, assuming a completely miscible system, as presented by Maguire et al. (1995). In Figure 2.6a, the cumulative heat energy increased steadily until the bubble point temperature was reached, as seen in Figure 2.5a, at which point the heat flow increased rapidly due to the heat of vaporization. In Figure 2.6b, the model calculations indicated that for a completely miscible system, a plot of the differentiated heat flow ( $-dQ/dt$ ) versus temperature ( $T$ ) would show no vaporization peak regardless of fluorene feed concentration. Since this plot was analogous to a DSC thermogram, a corresponding DSC thermogram in which no vaporization peak occurs within the range of bubble points of the contaminant and the humic material would indicate miscible behaviour between the contaminant and the humic material. These results also imply that, in the case of a miscible mixture, temperatures above the pure contaminant boiling point may be required for complete removal of the contaminant (Maguire et al., 1995).

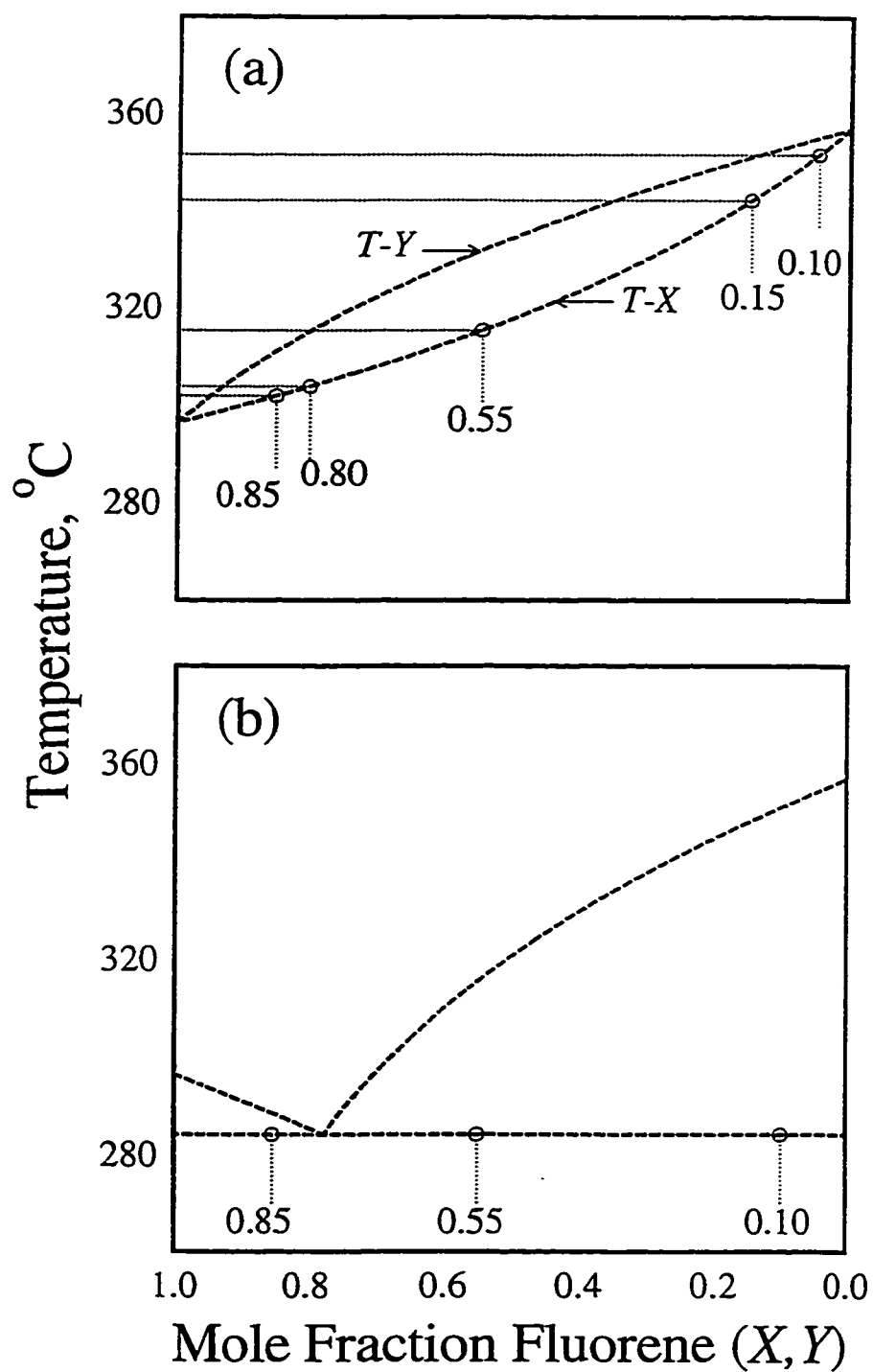


Figure 2.5: Phase Diagrams for Fluorene and Humic Acid. (a) Miscible case. (b) Immiscible Case.

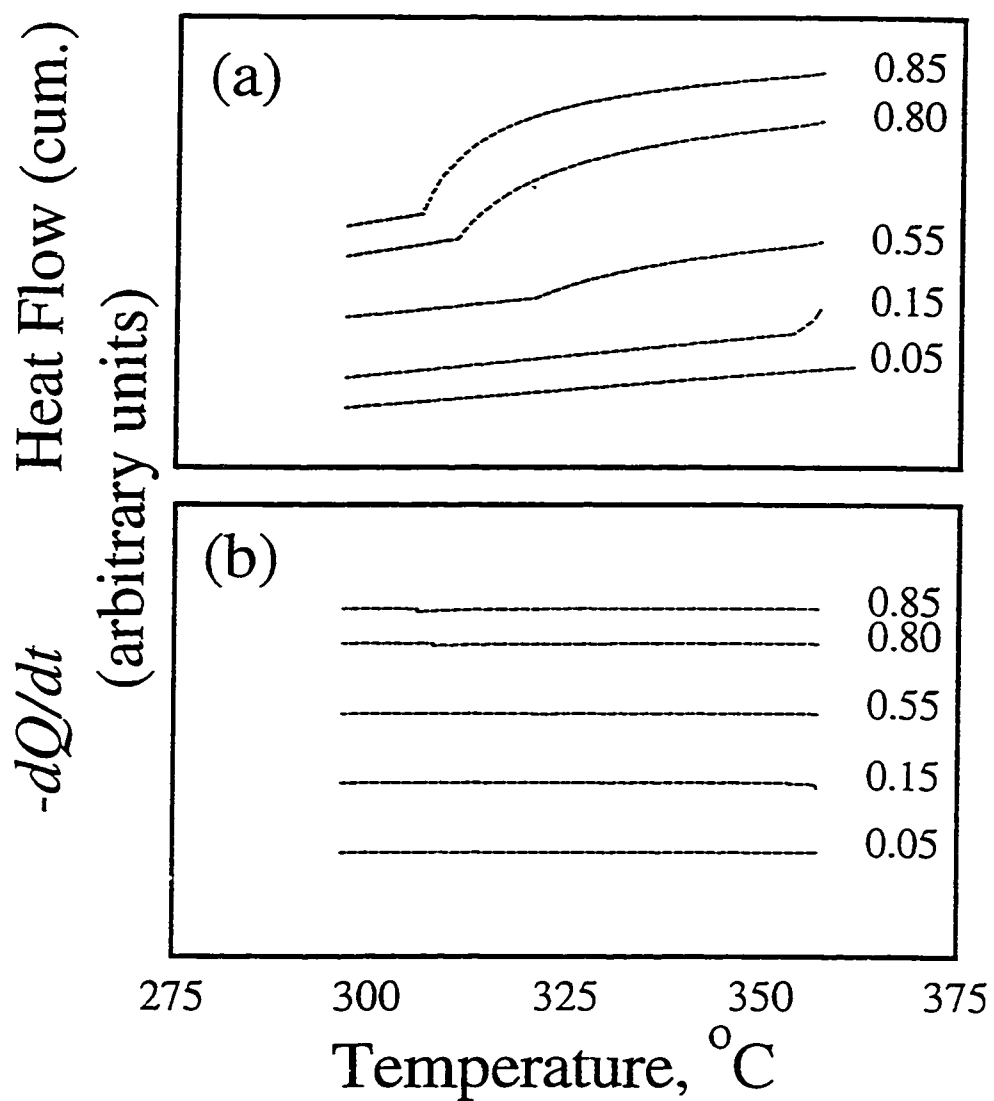


Figure 2.6: Predicted Results for Fluorene-Humic Acid in a Miscible System (Maguire et al., 1995)

In comparison, Figure 2.7 shows the predicted results for the fluorene-humic acid system for fluorene fractions of 0.10 to 0.85, assuming a completely immiscible system, as presented by Maguire et al. (1995). In Figure 2.7a, the cumulative heat energy increased sharply at the three phase temperature, as seen in Figure 2.5b, for all fluorene concentrations presented, and increased sharply again at the bubble point of pure HA or fluorene. In completely immiscible systems, the three-phase liquid-vapor mixture will remain constant until one of the components is completely volatilized. Therefore, the second peak occurred at the bubble point temperature of the humic acid or organic contaminant depending on whether the initial concentration of the mixture was to the right or left of the three-phase point. As shown in Figure 2.7b, the model indicated that for a completely immiscible system, two peaks should result on a DSC thermogram. These peaks should correspond to the sharp increases in  $Q$  shown in Figure 2.7a, with the first occurring at the three-phase temperature of the binary phase diagram and the second occurring at the bubble point temperature of either pure fluorene or HA. These results indicate that at low contaminant concentrations, complete removal of the contaminant may be accomplished at the three-phase temperature, which is lower than the pure contaminant boiling point.

Figures 2.8 and 2.9 show some experimental DSC thermograms presented by Maguire et al. (1995) for fluorene on humic fractions and anthracene on humic fractions, respectively. As seen in Figure 2.8a, no fluorene vaporization peaks were observed for all three fluorene concentrations presented. In comparison, as seen in Figure 2.8b and 2.8c, distinct fluorene vaporization peaks were observed for the 3% and 4% fluorene concentrations for both fulvic acid and humin. The lack of a distinct vaporization peak

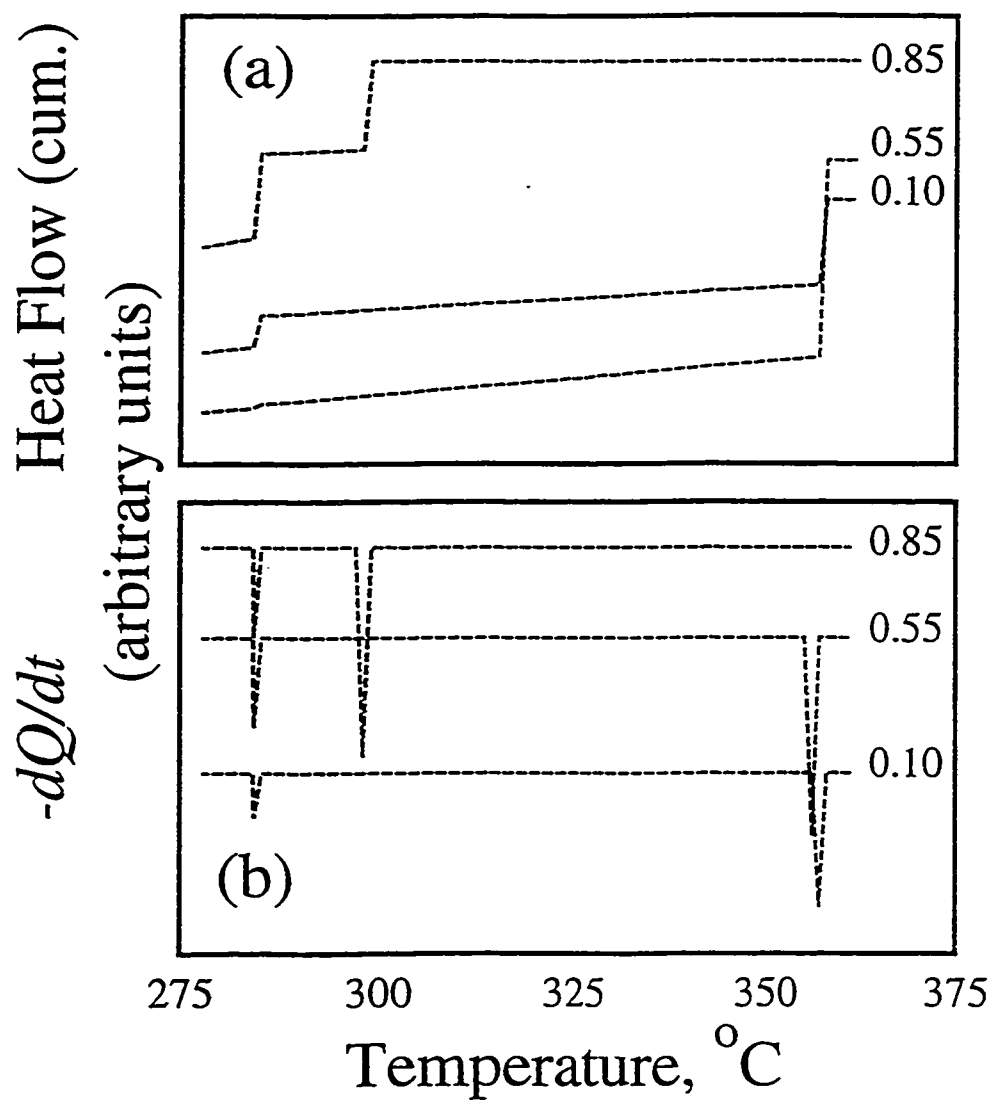


Figure 2.7: Predicted Results for Fluorene-Humic Acid in an Immiscible System (Maguire et al., 1995)

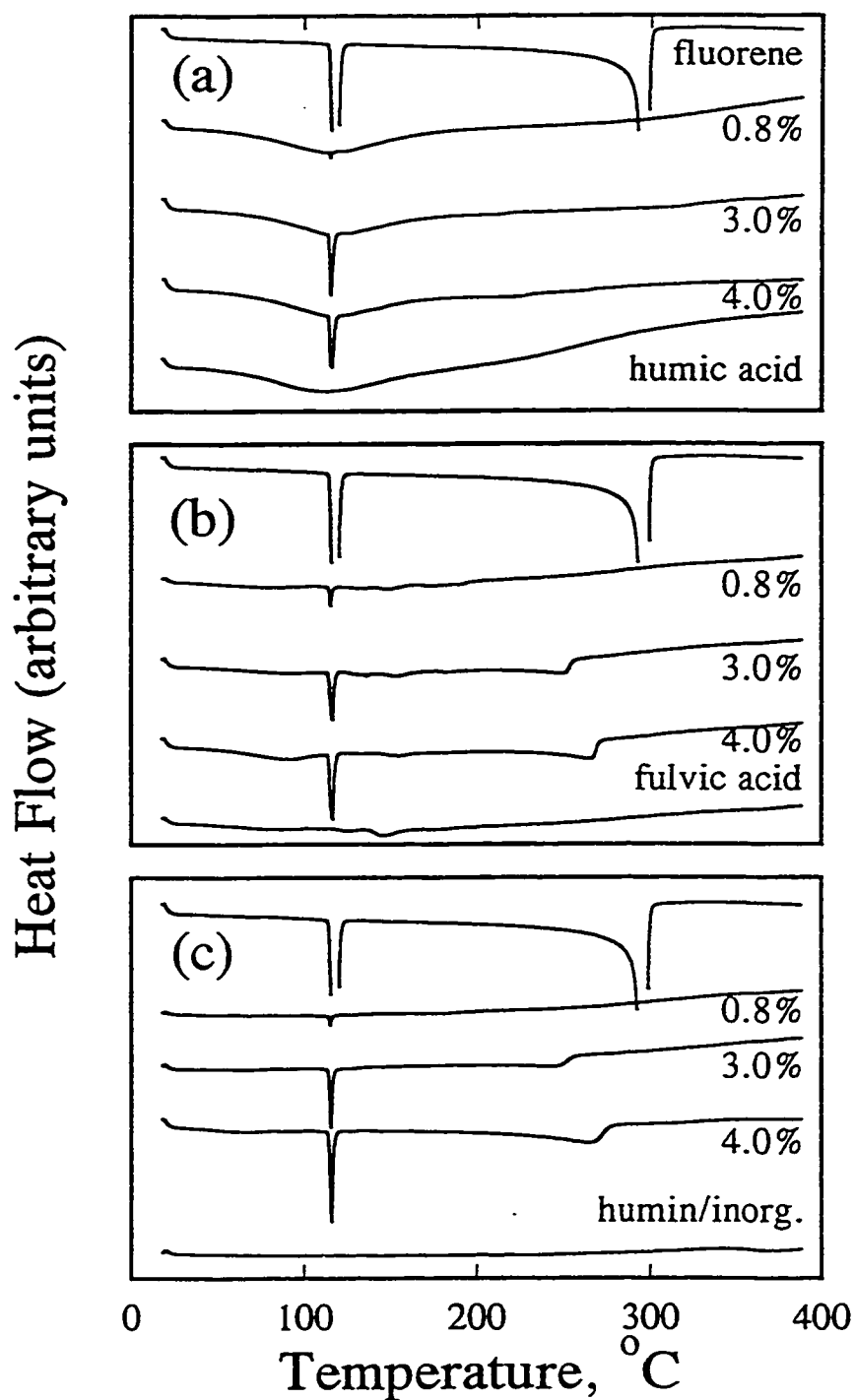


Figure 2.8: DSC Thermograms for Prepared Binary Mixtures of Fluorene. (a) Fluorene + HA. (b) Fluorene + FA. (c) Fluorene + Humin (Maguire et al., 1995)

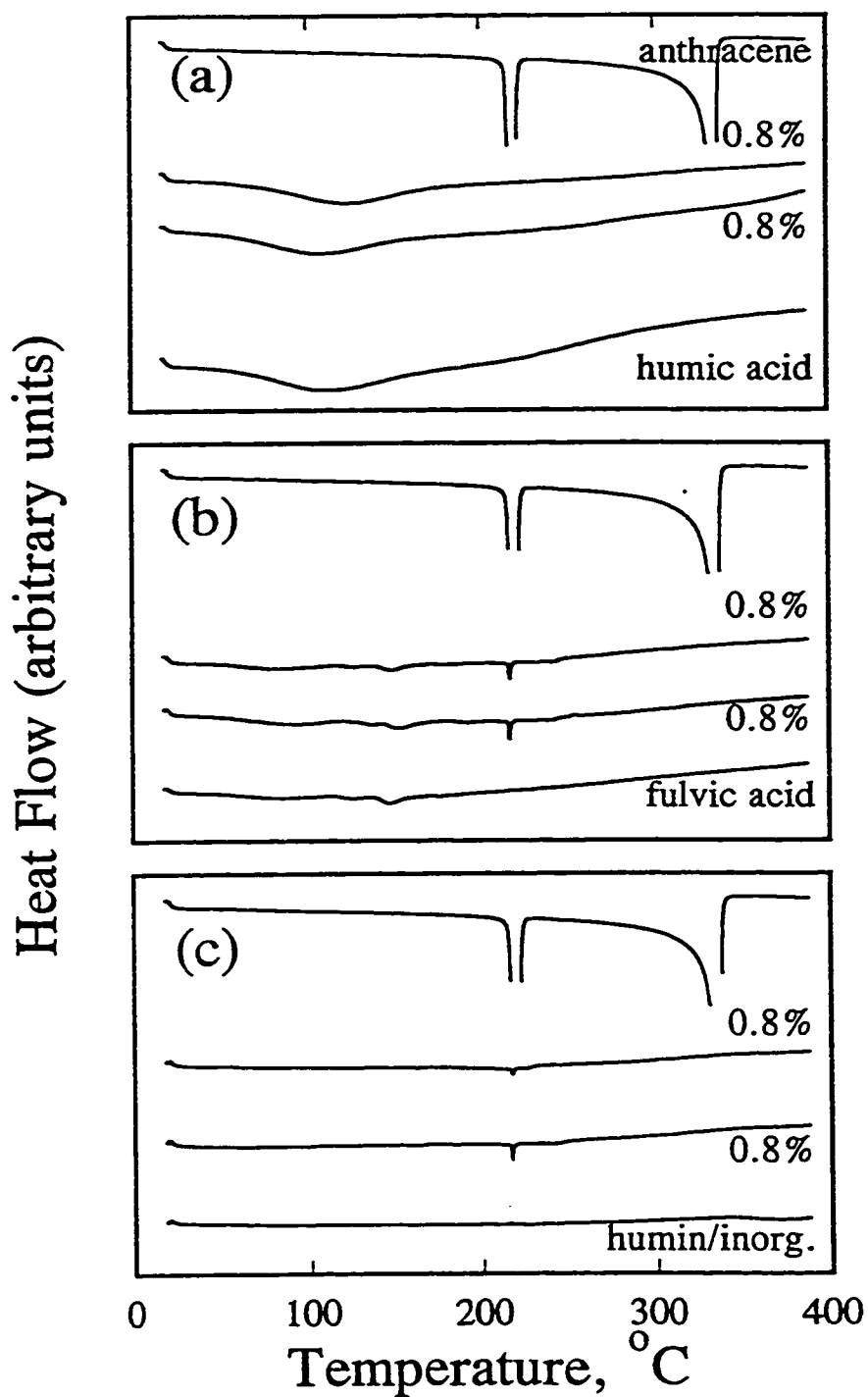


Figure 2.9: DSC Thermograms for Prepared Binary Mixtures of Anthracene. (a) Anthracene + HA. (b) Anthracene + FA. (c) Anthracene + Humin (Maguire et al., 1995)



for 0.8% fluorene on fulvic acid or humin is likely due to the small fluorene concentration. According to the model described above, the results presented in Figure 2.8 indicated that fluorene exhibited miscible behaviour with humic acid and immiscible behaviour with fulvic acid and humin.

Figures 2.9a-2.9c show the experimental DSC thermograms presented Maguire et al. (1995) for 0.8% anthracene on humic acid, fulvic acid and humin, respectively. Like the results presented for fluorene on humic fractions, the results presented in Figure 2.9 indicated that anthracene forms a miscible mixture with humic acid and an immiscible mixture with fulvic acid and humin.

## 2.6 Summary

The interactions of humic materials and organic contaminant is clearly a complicated issue; however, understanding of these interactions is important for improved commercial success of thermal desorption as a soil remediation process. Although many researchers have criticized the complete partitioning theory as being overly simplistic, partitioning still plays an important role in the interaction between humic substances and organic contaminants. Current research does not dispute the partition theory, but emphasizes the importance of the chemical and physical properties of humic substances on different interaction mechanisms.

The large amount of research concerning humic acid structure shows a great variety in the chemical and physical properties of different humic acids. Chemical functional group analysis and  $^{13}\text{C}$ -NMR analysis are effective at discerning these

differences. Most of the variability lies in the relative hydrophobic and hydrophilic sections of the humic macromolecules.

Because thermal desorption is a process involving the evolution or release of volatiles, thermal analytical techniques such as TGA, DTA, and DSC can simulate thermal activities occurring between the humic material and organic contaminants during the thermal desorption process. Particularly, valuable information concerning miscible and immiscible interactions between humic substances and PAHs has been reported using DSC.

## Chapter 3

### EXPERIMENTAL

#### 3.1 Materials

##### 3.1.1 Organic Chemicals

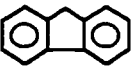

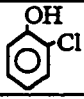
Three classes of organic chemicals were used to contaminate the soil fractions: polyaromatic hydrocarbon (PAH), straight chain aliphatic hydrocarbon, and polar organic hydrocarbon. The PAHs used in these experiments were fluorene ( $C_{13}H_{10}$ ) and anthracene ( $C_{14}H_{10}$ ). The straight chain aliphatics used were dodecane ( $C_{12}H_{26}$ ) and hexadecane ( $C_{16}H_{34}$ ). The polar organic used was o-chlorophenol ( $ClC_6H_4OH$ ). All chemicals were obtained from Aldrich Chemical Company, Inc. The chemical properties of these chemicals are shown in Table 3.1.

All of the chemical contaminants were dissolved in methylene chloride prior to mixing with soil fractions for even distribution on the surface of the soil fraction.

##### 3.1.2 Soil Samples

Both commercial and extracted humic acids were used in these experiments. The commercial humic acids used were Fluka humic acid (HA(F)) and Aldrich humic acid (HA(A)).

Table 3.1: Properties of Contaminant Hydrocarbons

	Fluorene	Anthracene	Dodecane	Hexadecane	o-Chlorophenol
Molar Mass (kg/kmol)	166.22	178.23	170.33	226.43	128.56
Purity (%)	98	97	99+	99	98+
Normal (@ 1 atm) Boiling Point (°C)	297.3	342.0	214.5	287.5	175.0
Calgary (@ 0.9 atm) Boiling Point (°C)	289.9	335.8	211.3	281.8	169.9
Melting Point (°C)	114.0	216.5	-9.6	18.5	7.0
Flash Point (°C)	-	-	74	135	64
Chemical Formula	C <sub>13</sub> H <sub>10</sub>	C <sub>14</sub> H <sub>10</sub>	C <sub>12</sub> H <sub>26</sub>	C <sub>16</sub> H <sub>34</sub>	ClC <sub>6</sub> H <sub>4</sub> OH
Heat of Vaporization (kJ/kg)	319.5	317	256	229	318.2
Structural Formula			CH <sub>3</sub> (CH <sub>2</sub> ) <sub>10</sub> CH <sub>3</sub>	CH <sub>3</sub> (CH <sub>2</sub> ) <sub>14</sub> CH <sub>3</sub>	

The soil used for extraction of humic acid was obtained from the Alberta Research Council in Edmonton. The soil used was a relatively fertile grassland soil of the order Chernozem and series Malmo. The soil was obtained from the A<sub>h</sub> horizon which is a very dark brown to black in colour. Soil from the A horizon forms at or near the surface in the zone of maximum removal of materials in solution and suspension and maximum in situ accumulation of organic matter. Therefore, this horizon is high in organic matter. The A<sub>h</sub> horizon is the A horizon occurring closest to the surface and, due to the large amount of biological activity, has accumulated organic matter (Bowser et al., 1962). This soil was ground to less than 2 mm and was then used for the extraction of humic acid, fulvic acid and humin using dilute alkali under nitrogen atmosphere.

### **3.2 Schnitzer Procedure for the Extraction of Humic Acid Fraction from Soil**

Alkali extraction is a widely used soil extraction method due to its large extraction yield of up to 80% (Stevenson, 1994). The procedure followed is the Schnitzer procedure as described in Schnitzer (1982). A flowsheet of the extraction technique is shown in Figure 3.1. The soil sample extraction work was carried out by the writer in the laboratories of the Alberta Research Council in Edmonton.

#### **3.2.1 Separation of Humin**

Approximately 1 kg of soil was ground to less than 2 mm in diameter. 90 g of this soil was added to each of 13 1L Nalgene bottles. 900 mL of 0.1 M NaOH was added

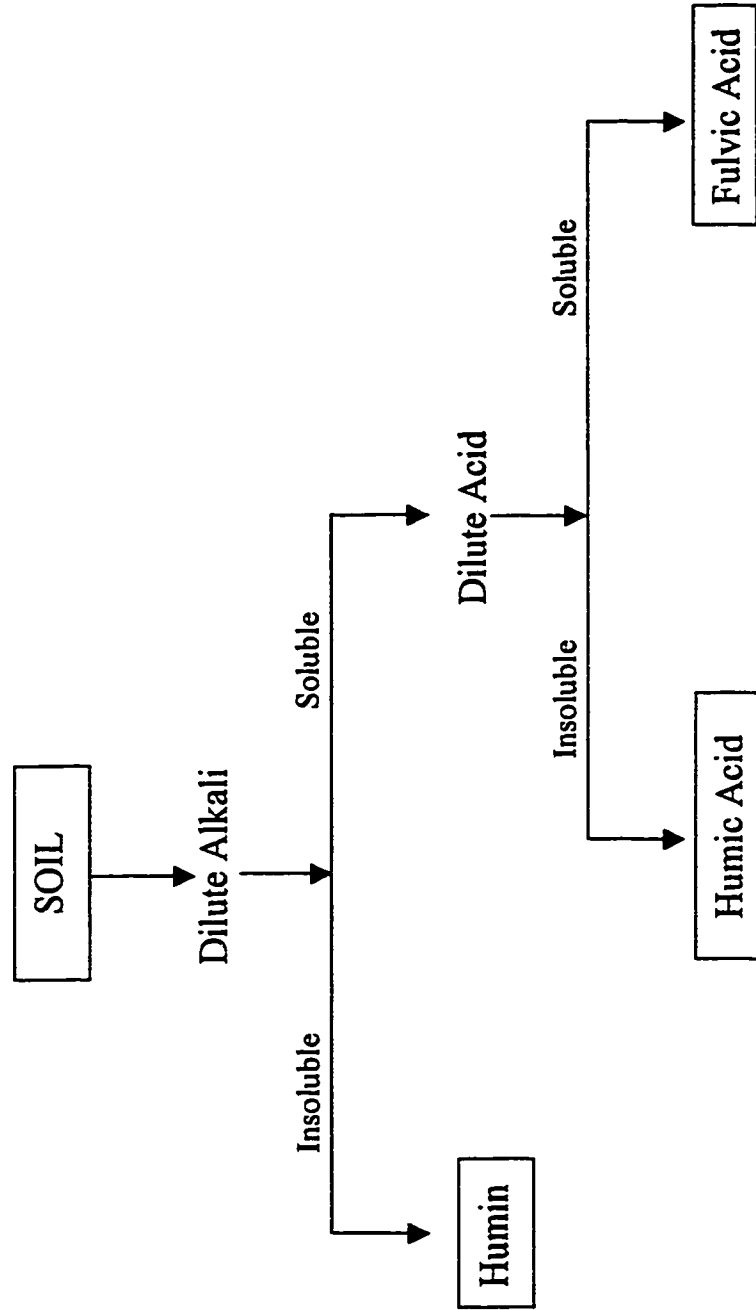


Figure 3.1: Schematic of Dilute Alkali Extraction Method (Schnitzer, 1982)

to each bottle. After the addition of NaOH, nitrogen was bubbled through the mixture for 5-6 minutes to remove the dissolved oxygen as the breakdown of humic acids by autoxidation is enhanced in the presence of O<sub>2</sub> in alkaline environments. Nitrogen was bubbled through the slurry until no more O<sub>2</sub> was evolved as determined by a lighted match test. The bottles were sealed tightly and left to shake overnight.

The bottles were then removed from the shaker and the contents were transferred to 200 mL Nalgene centrifuge bottles. The samples were centrifuged for 30 minutes at 12000 rpm using a Beckmann centrifuge Model J2-21. The centrate containing dissolved humic and fulvic acids was decanted from the undissolved humin fraction and was filtered using a Whatman #1 filter paper.

The pH of the centrate was adjusted to less than 2 to precipitate the dissolved HA. The precipitated HA was allowed to settle for approximately 12 hours at a cool temperature (approximately 4°C).

A second extraction of humic and fulvic acid was performed by adding 750 mL of 0.1 M NaOH to the 1L Nalgene bottles containing the humin residue. Again, nitrogen was bubbled through the mixture and was left to shake overnight. The samples were centrifuged and the humic acid was precipitated from the centrate as described above.

### 3.2.2 Separation of Humic Acid

After the HA settling procedure, the clean FA fraction in solution was removed from the top using suction. The rest of the HA from the HA-FA fraction was separated

by centrifugation as described above. The FA fraction was filtered using a Whatman #1 filter and set aside.

### 3.2.3 Cleaning of Humic Acid Fraction

5 mL of HCl was mixed in 1 L of distilled water. 100 mL of this solution was added to each bottle containing humic acid precipitate. 0.5 mL of concentrated hydrofluoric acid was added to each bottle. Schnitzer and Wright (1957) reported that dilute HCl extracts carbon associated with easily soluble iron and aluminum. HF is effective in reducing the ash content of humic acids because of its ability to dissolve hydrated clay minerals and to form complexes with di- and trivalent cations released by the dilute HCl. The bottles were left to shake on the shaker overnight. The acid wash was centrifuged and then decanted from the samples. This process was repeated 2 more times.

After the acid washings, the humic acid residue was washed with water. 100 mL of distilled water was added to each bottle and left to shake overnight. The wash water was removed by centrifugation and then decanted. The wash water was tested for  $\text{Cl}^-$  ions using  $\text{AgNO}_3$ . Three washes were completed. Later analysis showed that the washing procedure reduced the ash content from 30% to 14%.



#### 3.2.4 Drying of Humic Acid

The HA slurry produced after washing was frozen and then thawed to release the humic acid particles from the thick slurry. The clean water was decanted from the mixture and the resulting solid HA was air dried under vacuum.

The humic acid produced in this procedure is referred to as HA(ML) in this study.

#### 3.2.5 Comparison to Maguire's Procedure

Maguire (1994) also performed humic acid extractions in this laboratory. Maguire (1994) also used the Schnitzer procedure; however, cleaning with dilute HCl-HF solution was not performed in Maguire's work. Since cleaning with dilute HCl-HF significantly reduces the ash content of the humic acid, the ash content of the humic acid in this work is much lower than that in the work of Maguire (1994). References in this work to the humic acid used in Maguire (1994) will be HA(VM).

### **3.3 DSC Measurements**

Thermal interactions between the humic acids and the organic contaminants were investigated using a Mettler DSC12E. The instrument was controlled and the data was collected using a PC and system software TA89E. The DSC12E allowed for measurements from  $-40\text{ }^{\circ}\text{C}$  and  $400\text{ }^{\circ}\text{C}$  at atmospheric pressure. A schematic representation of the DSC12E measuring cell is shown in Figure 3.2. A standard method

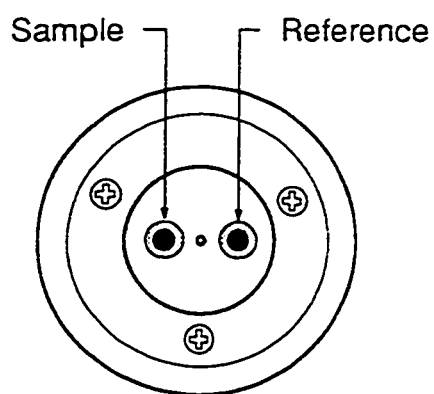
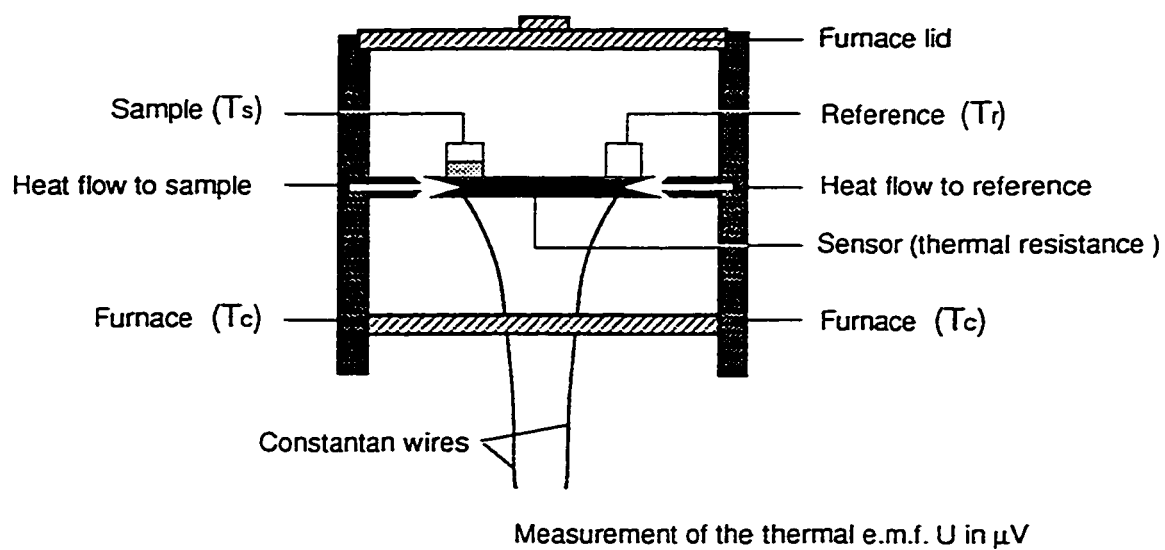


Figure 3.2: Schematic of DSC Measuring Cell

for vaporization experiments using differential scanning calorimetry should consider sample vessel design, sample size, sample preparation and heating rate.

### 3.3.1 Crucible Design

The samples were placed in 40  $\mu\text{L}$  mechanically sealed aluminum crucibles with two small pinholes in the lid. Aluminum is the standard material for these crucibles due to the high heat transfer properties of aluminum which lead to a correspondingly high sensitivity to heat flow. Using a capped crucible with two small pinholes (as done in these experiments) prevents the immediate vaporization of the sample and significant vaporization does not occur until close to the boiling point of the organic contaminant. The pinholes in the lid of the crucibles serve to prevent self-pressurization of the crucible as the sample vaporizes. Self-pressurization causes the sample pressure to be greater than the cell pressure thus causing a boiling point elevation (Seyler, 1976). The holes act to create a more controlled diffusion path preventing early vaporization and producing a sharper endotherm (TA Hotline, 1994). This is a common and accepted procedure for performing DSC for boiling point determination.

### 3.3.2 Sample Size

In order to achieve valid boiling point measurements, the sample must undergo isothermal boiling within the temperature range. Isothermal boiling will occur only with an optimal sample size. For samples that are too large, superheating and partial self

cooling occurs before isothermal boiling is reached. If the sample is too small, insufficient sample remains at the boiling point and therefore the establishment of reflux conditions necessary for isothermal boiling cannot be established (Seyler, 1976). The volume of the sample is also important. The sample should just cover the bottom of the DSC crucible to ensure uniform heat transfer.

For these experiments, humic acid samples of 7.8 mg were measured directly into the aluminum crucibles. It was found that this size of sample just covered the bottom of the crucible. The humic acid samples were directly contaminated in the crucible by injection with a given amount of contaminant dissolved in methylene chloride.

Contaminant concentrations were low (3-10 mass %). Higher concentrations were considered not of much practical value in terms of expected contaminated soils conditions and lower concentrations would be difficult to detect using DSC. Because of the relatively low contaminant concentrations used, reflux conditions were not achieved and isothermal boiling was not attainable in these experiments. Therefore, each thermogram was compared to a reference thermogram consisting of glass beads contaminated with an equivalent amount of organic contaminant. The reference was placed on the glass beads since this increases the liquid surface area and reduces pre-boiling vaporization due to sample retention caused by surface tension. (Seyler, 1976)

### 3.3.3 Sample Preparation

Each of the contaminants investigated was dissolved in methylene chloride and was added to a 40  $\mu\text{L}$  aluminum crucible containing 7.8 mg of humic acid using a 10  $\mu\text{L}$

syringe. Methylene chloride was used because, as shown in Maguire (1994), it did not interact with the contaminant and vaporized quickly from the surface of the sample.

A 10 mass% solution of fluorene was used for contamination whereas 5 mass% solutions of each of dodecane, hexadecane, and o-chlorophenol were used for contamination. Only a 1% solution of anthracene was used due to its limited solubility in methylene chloride. Humic acid-contaminant mixtures were made using HA(F), HA(ML) and HA(A) and each of fluorene, dodecane, and hexadecane at concentrations of 3%, 7% and 10% by mass. 3% and 7% by mass concentrations of humic acid-contaminant mixtures of the above three humic acids and anthracene were made. A summary of the experiments completed is shown in Table 3.2.

The methylene chloride was allowed to evaporate from the surface of the humic acid mixture, leaving the contaminant behind. Aluminum lids with two pinholes were then cold welded to the crucibles using a mechanical crucible sealer. The samples were then left to sit for approximately 24 hours. Maguire (1994) stated that experiments did not show apparent variation due to the time of adsorption between 24 and 168 h. This was also reported by Lighty et al. (1988). Due to the relatively high vapor pressure of o-chlorophenol, samples contaminated with o-chlorophenol were run immediately after contamination.

#### 3.3.4 Heating Rate

Slow heating rates amplify pre-boiling vaporization. For the case of vaporization experiments, Cassel and DiVito (1994) suggested heating rates of 5-10 °C/min; whereas

Table 3.2: Number and Type of Contaminant-Humic Acid DSC Experiments

	HA(ML)		HA(F)		HA(A)	
	Mass%	# Exp	Mass%	# Exp	Mass%	# Exp
Anthracene	3 7	2 2	3 7	2 2	3 7	2 2
Fluorene	3 7 10	2 2 2	3 7 10	2 2 2	3 7 10	2 2 2
Dodecane	3 7 10	2 3 3	3 7 10	2 2 2	- - -	- - -
Hexadecane	3 7 10	2 2 2	3 7 10	2 2 2	- - -	- - -
O-chlorophenol	3 7	4 2	3 7	2 3	- -	- -

Syler (1976) suggests heating rates of 10-20 °C/min for optimal results. Based on these findings and for consistency with previous work done in our laboratory (Maguire, 1994), a heating rate of 10 °C/min between temperatures of 20 °C and 390 °C was used.

### 3.3.5 Calibration

The system software TA89E calculated the calibration constants required for the calculations. Calibration was carried out using a known quantity of pure indium sample. Approximately 6 mg of indium was placed in an aluminum crucible with a perforated lid. The calibration was run between 150 °C and 160 °C at a heating rate of 1 °C per minute. The calibration constant or calorimetric sensitivity,  $E_{in}$ , was calculated at the melting point of indium (156.6 °C) using the following equation:

$$E_{in}(\mu V / mW) = \frac{\text{area of melting peak } (\mu V \cdot s)}{\text{weight of indium (mg)} \times \text{heat of fusion of indium (mW} \cdot s/\text{mg)}} \quad (3.1)$$

where the heat of fusion of indium = -28.43 J/g.

### 3.3.6 Interpretation of DSC Thermograms

During DSC analysis, thermal events occurring in a sample can be observed by different amounts of energies being added to the sample or the reference in order to keep them both at the same temperature. The energy added to the sample or reference is equal

in magnitude to the amount of energy absorbed or emitted by the sample. These energy transitions are observable as deviations from the base line of a heat flow versus temperature plot.

The thermograms presented are plots of heat flow in W/g versus temperature. The convention used in these experiments is a negative peak for endothermic transitions and a positive peak for exothermic transitions.

### **3.4 Characterization of Humic Materials**

#### **3.4.1 Ash Content**

The ash contents of the commercial and extracted humic acids were determined using the ASTM test method (D 2974-87). The humic samples were heat dried in an oven overnight at 110 °C to eliminate bound water and then cooled to room temperature in a dessicator. The dried samples were weighed into ceramic crucibles and incinerated in a muffle furnace at 750 °C overnight. The remaining residue is the ash or inorganic content of the sample. The samples were then cooled in a dessicator and the ash was weighed. The mass loss and ash content of each sample were calculated.



### 3.4.2 Reactive Functional Group Analysis

#### 3.4.2.1 Total Acidity

The total acidity of each of the humic acids (Fluka, Aldrich and HA(ML)) was determined using the barium hydroxide (Baryta Absorption) method. This method is an indirect potentiometric method based on the release of  $H^+$  from acidic functional groups, which ionize up to the pH of the  $Ba(OH)_2$  solution. The HA sample is allowed to react with an excess  $Ba(OH)_2$  after which the unused reagent is titrated with standard acid. The reaction is described by:



where R is the humic acid macromolecule and H is the proton of a COOH or acidic OH group.

The method described by Schnitzer (1982) was used. A 0.2N  $Ba(OH)_2$  solution was made up using  $CO_2$ -free distilled water. Between 50 and 100 g of each type of humic acid was added to a 125 mL Erlenmeyer flask in duplicate. 20 mL of the 0.2N  $Ba(OH)_2$  was added to each flask. As well, two blanks were set up using 20 mL of  $Ba(OH)_2$  only. The air was displaced from each flask with nitrogen and sealed with a rubber stopper. The flasks were shaken for 24 hours at room temperature. The contents were then filtered using a Buchner funnel under vacuum and washed using  $CO_2$ -free distilled water. The filtrate plus washing was titrated potentiometrically with 0.1N HCl

to pH 8.4. This was a deviation from Schnitzer's procedure which called for titration using 0.5N HCl. The lower concentration was used to increase the accuracy of the titration results. The total acidity of the sample was calculated by:

$$\frac{(\text{Volume blank} - \text{Volume sample}) \times (\text{Normality acid}) \times 1000}{\text{Weight of sample}} \quad (3.3)$$

$= \text{meq total acidity/g of humic material}$

#### 3.4.2.2 NMR Analysis

Solid state CPMAS  $^{13}\text{C}$ -NMR (cross polarization, magic angle spinning  $^{13}\text{C}$  nuclear magnetic resonance) analysis was performed on HA(ML) and HA(F) samples in the Department of Chemistry at the University of Calgary using the procedure described by Cook (1997). This procedure combines ramped amplitude CP, high sample spinning rates and high field strength. Relative concentrations of aliphatic, carbohydrate, carbon singly bonded to two oxygens (O-C-O), phenolic, aromatic, carboxyl and ketonic groups were observed.

$^{13}\text{C}$ -NMR is a frequently used and widely accepted approach for the characterization of organic matter (Stott and Martin, 1990).  $^{13}\text{C}$ -NMR has replaced  $^1\text{H}$ -NMR for the investigation of the structure of humic substances due to a number of advantages. First, the carbon skeleton of the humic substance is observed rather than the adjacent protons thus allowing for the detection of functional groups such as ketones and fully functionalized aromatic rings. Second, the carbon nuclei are spread over a wider range of chemical shifts so that individual signals may be observed even when carbons

have only a small difference in structural environments. Finally, the line widths of signals in  $^{13}\text{C}$ -NMR are narrower than in  $^1\text{H}$ -NMR thus reducing signal overlap (Cook, 1997).

Cross polarization (CP) and magic angle spinning (MAS) techniques were used. CP is a technique which reduces line broadening. CP results in the transfer of net magnetization from the abundant  $^1\text{H}$  spins to the less abundant  $^{13}\text{C}$  spins thus enhancing resolution due to the increase in net  $^{13}\text{C}$  magnetization. Magic angle spinning (MAS) further decreases line broadening by reducing or eliminating dipolar  $^{13}\text{C}$ - $^1\text{H}$  interactions by spinning the sample at the so called “magic angle” of  $54.7^\circ$  (Stevenson, 1994). Ramp CP allows for the use of higher spinning rates and higher field strengths which result in enhanced sensitivity.

NMR spectroscopy is an analytical technique which relies upon the interactions of electromagnetic radiation with nuclear, atomic or molecular species. A chemical shift ( $\delta$ ) measured in ppm is the parameter from which structural information is obtained according to the equation:

$$\delta = \frac{\nu_{\text{sample}} - \nu_{\text{reference}}}{\nu_{\text{reference}}} \times 10^6 \quad (3.4)$$

where  $\nu$  is the frequency of electromagnetic radiation of the sample or reference. The basis for NMR analysis is that the frequency at which nuclei resonate (i.e.  $^{13}\text{C}$  in the case of  $^{13}\text{C}$ -NMR) is determined by the chemical environment of the nuclei. A number of chemical shifts corresponding to specific chemical  $^{13}\text{C}$  functional groups important in the

analysis of humic substances are shown in Figure 3.3. These groups along with their chemical shifts consist of aliphatic (0-50), carbohydrate (50-96), O-C-O (96-108), aromatic (108-145), phenolic, (145-162), carboxyl (162-190) and ketonic (190-220) groups (Cook and Langford, 1998).

### 3.4.3 Mass Loss Experiments

Mass loss experiments were done using thermogravimetric analysis (TGA) at the Shell Research Centre in Calgary. Samples of HA(ML) and HA(F) were prepared in mechanically sealed aluminum crucibles using the same protocol as for DSC. The heating program used was the also same as that used for DSC measurements to ensure comparable results between DSC and TGA. The mass and rate of mass loss were measured as a function of temperature.

### **3.5 DSC Thermograms for Pure Contaminants**

DSC thermograms were completed for each equivalent concentration for every contaminant used in this study, and are shown in Figures 3.4-3.8. For each pure contaminant DSC run, 12.4 mg of glass beads were measured into a DSC crucible. The same volume of contaminant-methylene chloride solution was added to 12.4 mg of glass beads as was added to 7.8 mg of humic acid to achieve the given contaminant concentration. It was assumed that there were no chemical interactions between the contaminant and the glass beads. This way, each humic acid-contaminant mixture could

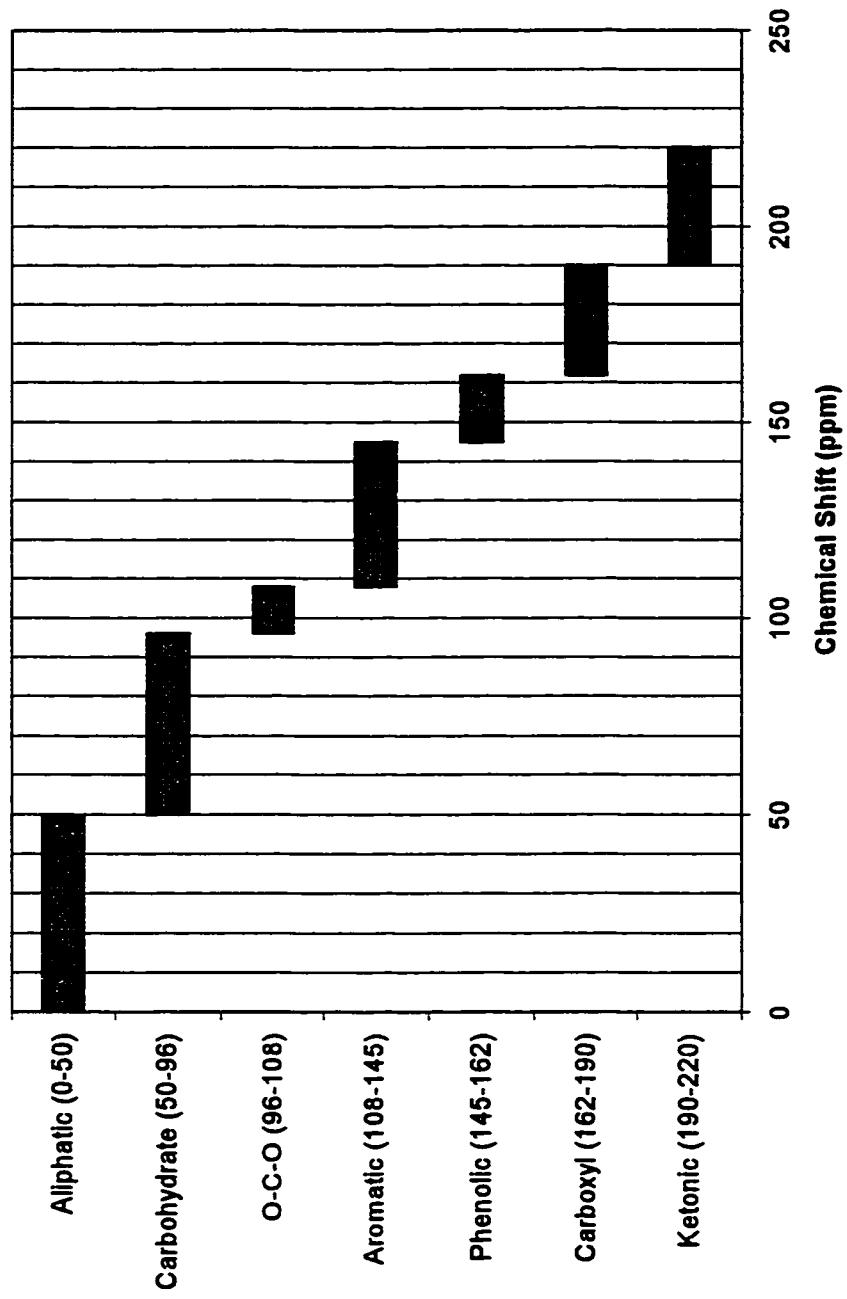


Figure 3.3: Chemical Shifts for Common Organic Groups

be compared to the equivalent glass-contaminant mixture. Differences between the two curves could then be attributed to interactions between the humic acid and the contaminant.

### 3.5.1 Anthracene

Figure 3.4 shows DSC thermograms for 3% and 7% equivalent masses of anthracene on glass beads. One run is shown for 3% equivalent anthracene and two runs are shown for 7% equivalent anthracene. From the duplicate run for 7% equivalent anthracene, it appears that the repeatability of the experiment is not good in terms of the actual heat flow values; however, the repeatability is acceptable in terms of the temperatures of peak locations.

The first sharp peak represents the melting point of anthracene. The melting point coincides at 216°C for all runs and all concentrations of anthracene. The second peak represents vaporization of anthracene. The endpoint of vaporization varies with concentration of contaminant. As the concentration of anthracene increases from 3% to 7%, the end point of vaporization also increases from approximately 250°C to 270°C. Vaporization of anthracene is complete before the Calgary boiling point of pure anthracene of 336°C. This indicates preboiling vaporization and is a function of the small amount of contaminant used in this study. Because of this “shift” in vaporization peaks as a function of concentration, humic acid-contaminant DSC thermograms will be compared to the equivalent glass-contaminant DSC thermogram.

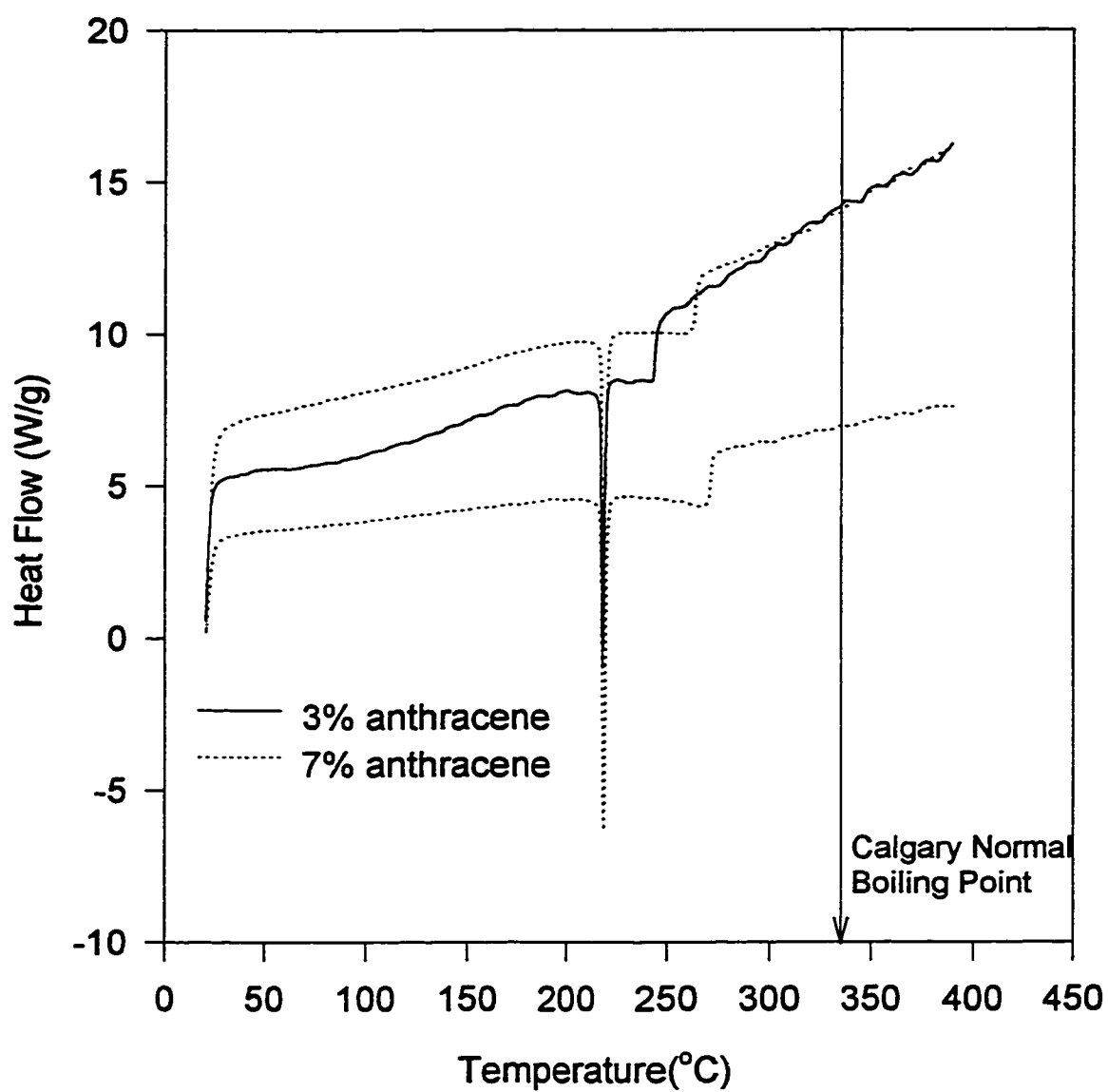


Figure 3.4: DSC Thermograms for Equivalent Anthracene Concentrations on Glass Beads

### 3.5.2 Fluorene

Figure 3.5 shows DSC thermograms for 3%, 7%, and 10% equivalent masses of fluorene on glass beads. The first sharp peak is the melting endotherm and coincides at 116°C for all runs and all concentrations. Again, from duplicate runs, it can be observed that the repeatability of the experiments is not good in terms of the actual heat flow values, but is good in terms of the temperature of peak locations.

Due to the small amount of fluorene sample, the endpoint of vaporization varies with amount of fluorene. The endpoint of vaporization occurs at 216°C, 247°C, and 250°C for 3, 7, and 10 equivalent %, respectively. These temperatures are much lower than the normal Calgary vaporization temperature of 290°C.

### 3.5.3 Dodecane

Figure 3.6 shows DSC thermograms for 3%, 7%, and 10% equivalent masses of dodecane on glass beads. Duplicate runs for dodecane are not available. Only vaporization peaks are observable for dodecane since dodecane is a liquid at room temperature. Again, due to the small amount of dodecane and the effects of pre-boiling vaporization, the temperature of the endpoint of vaporization increases as the equivalent concentration increases from 3% to 10%. The endpoint of vaporization occurs at 150°C, 175°C, and 178°C for 3, 7, and 10 equivalent %, respectively. These temperatures are much lower than the normal Calgary boiling point of 211°C.



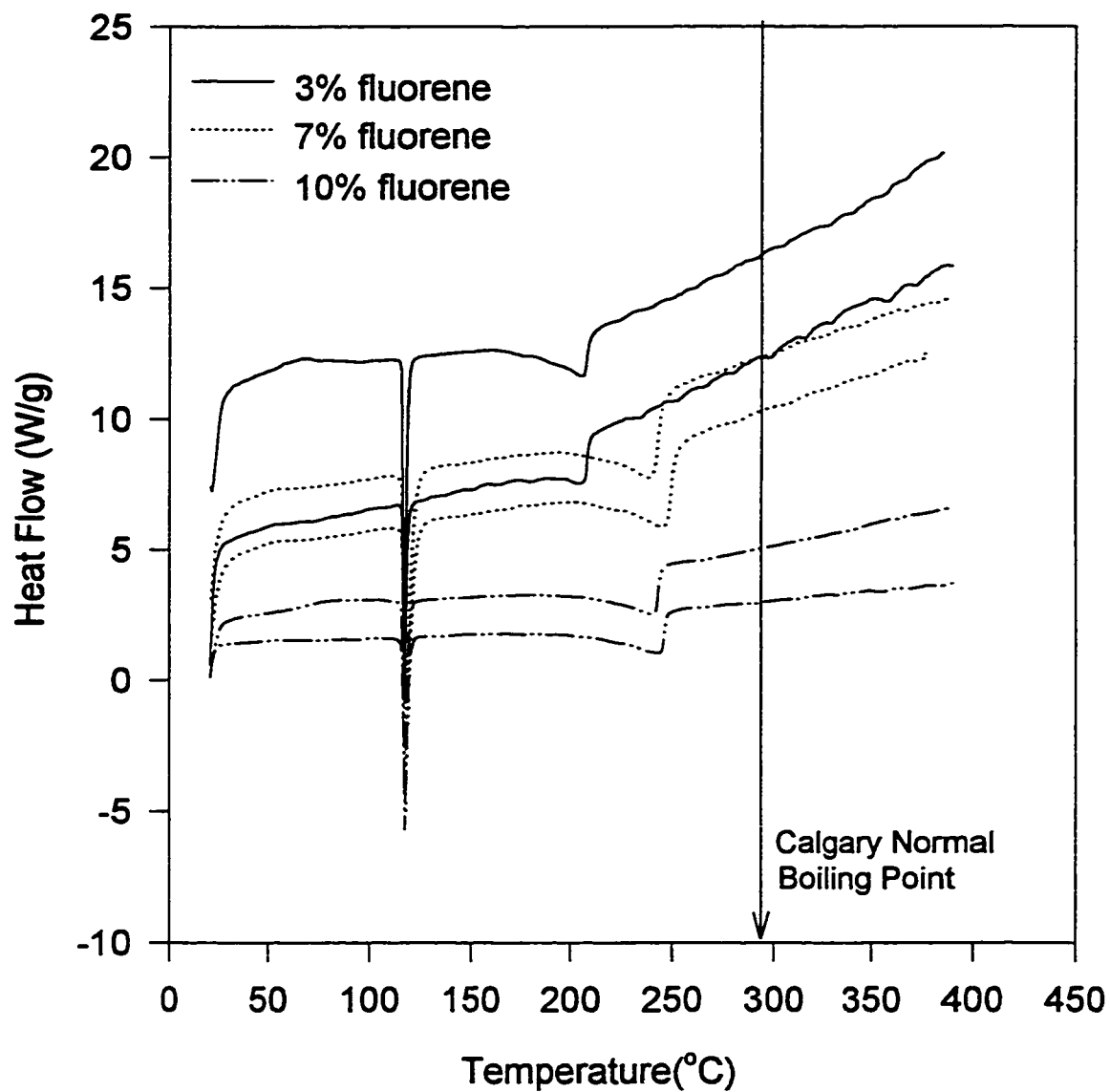


Figure 3.5: DSC Thermograms for Equivalent Fluorene Concentrations on Glass Beads

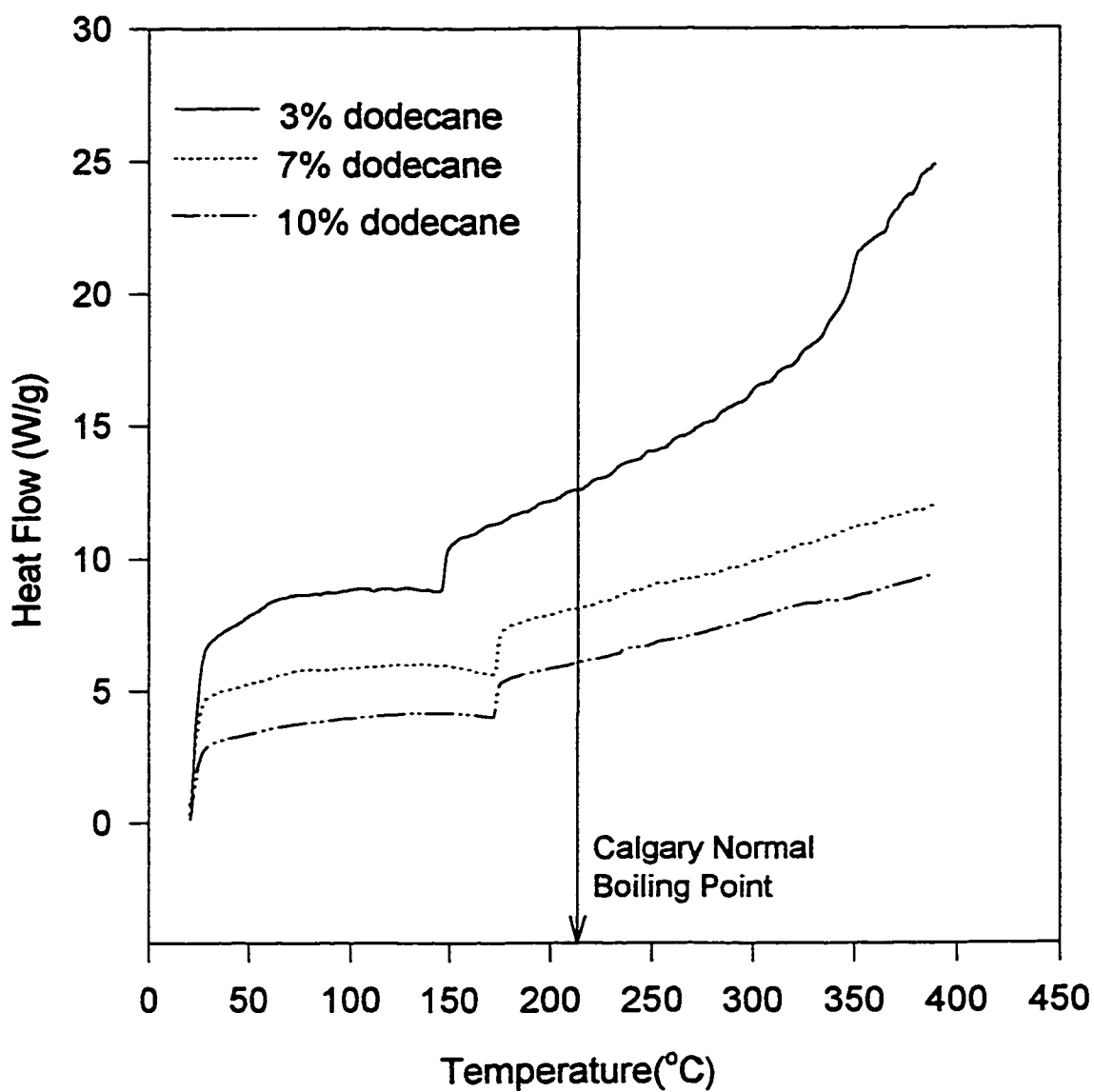


Figure 3.6: DSC Thermograms for Equivalent Dodecane Concentrations on Glass Beads

#### 3.5.4 Hexadecane

Figure 3.7 shows DSC thermograms obtained for 3%, 7%, and 10% equivalent masses of hexadecane on glass beads. Like the previous DSC thermograms of pure contaminants, duplicate runs on each concentration of dodecane show that the repeatability of the experiments is not good in terms of the actual heat flow values, but is good in terms of the temperature of peak locations.

Melting peaks are not observed on the hexadecane thermograms since hexadecane is a liquid at room temperature. Decomposition of the hexadecane can be observed by an exothermic peak starting at approximately 198°C. This exothermic peak is immediately followed by an endothermic vaporization peak.

Again, due to the small amount of hexadecane and the effects of pre-boiling vaporization, the temperature of the endpoint of vaporization increases as the equivalent concentration increases from 3% to 10%. The endpoint of vaporization occurs at 214°C, 240°C, and 259°C for 3, 7, and 10 equivalent %, respectively. These temperatures are much lower than the normal Calgary boiling point of 287°C.

#### 3.5.5 O-chlorophenol

Figure 3.8 shows DSC thermograms for 3% and 7% equivalent masses of o-chlorophenol on glass beads. Again, duplicate runs on each concentration of o-chlorophenol show that the repeatability of the experiments is not good in terms of the actual heat flow values, but is good in terms of the temperature of peak locations.

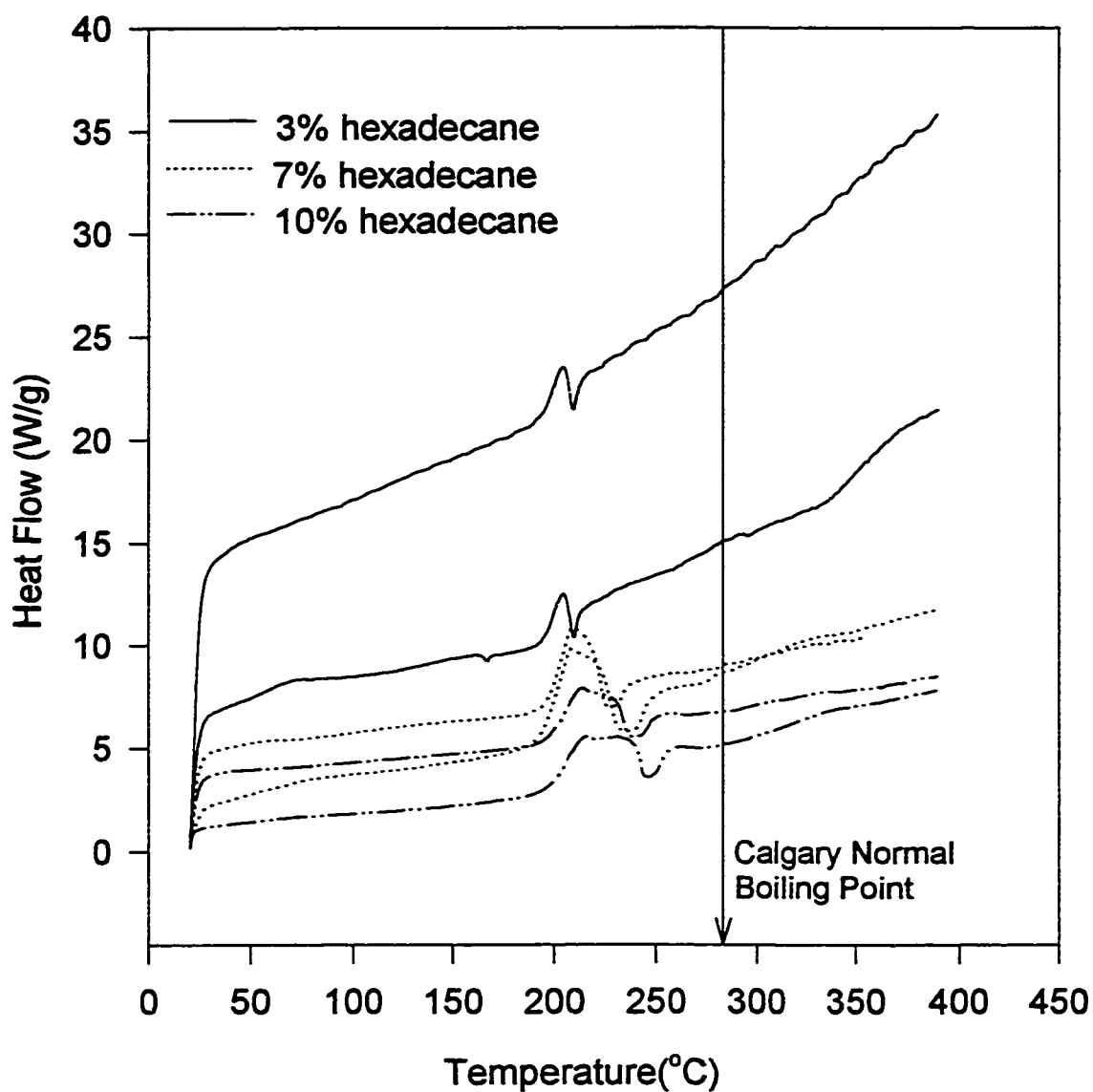


Figure 3.7: DSC Thermograms for Equivalent Hexadecane Concentrations on Glass Beads

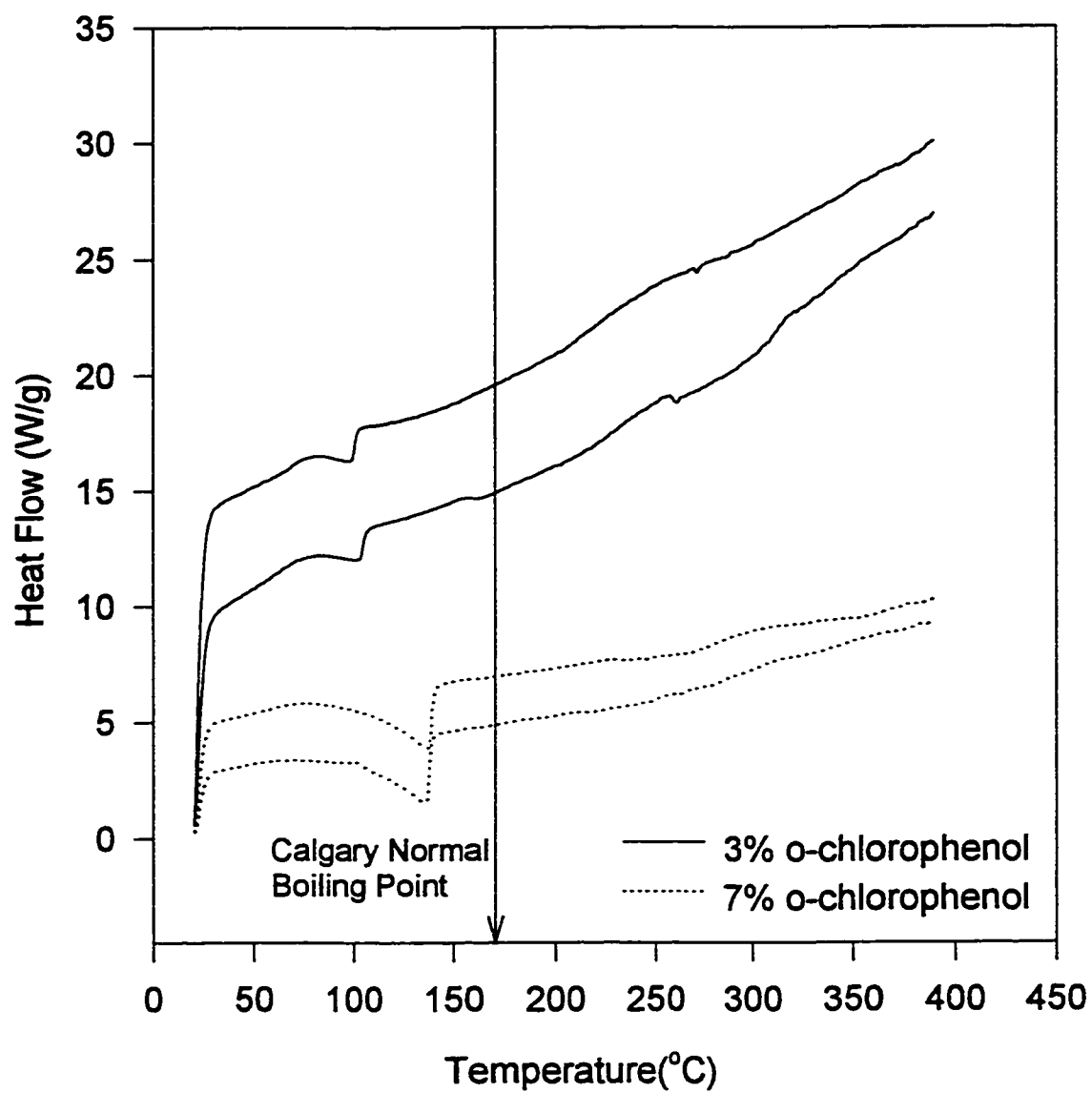


Figure 3.8: DSC Thermograms for Equivalent O-chlorophenol Concentrations on Glass Beads

Only vaporization peaks are observable for o-chlorophenol since o-chlorophenol is a liquid at room temperature. Again, due to the small amount of o-chlorophenol and the effects of pre-boiling vaporization, the temperature of the endpoint of vaporization increases as the equivalent concentration increases from 3% to 7%. The endpoint of vaporization occurs at 104°C and 143°C 3 and 7 equivalent %, respectively. These temperatures are much lower than the normal Calgary vaporization temperature of 275°C.

## CHAPTER 4

### CHARACTERIZATION OF HUMIC ACID SAMPLES

#### 4.1 Ash Content

To study the chemical properties of soil organic matter, it must first be separated from its inorganic matrix of sand, silt and clay. The solubility of humic substances in alkali is due to the disruption of bonds holding organic matter to inorganic soil components and the conversion of acidic components to their soluble salt forms (Stevenson, 1994). These bonds include electrostatic bonds, hydrogen bonds, hydrophobic bonding, and physical bonds such as van der Waals and dipole interactions. Since organic anions are normally repelled from negatively charged clay surfaces, adsorption of humic and fulvic acids by clay material occurs when polyvalent cations are present on the exchange complex. These polyvalent cations are able to maintain neutrality at the surface by neutralizing both the charge on the clay and the acidic functional groups of the organic matter (Stevenson, 1994).

During extraction of humic substances from soil, humic acid becomes contaminated with hydrated clay materials and the insoluble salts of the polyvalent cations used to bond the humic acid to the clay. This inorganic portion of the extracted humic acid fraction is referred to as the ash content. Hydrofluoric acid is effective in reducing the ash content of humic acids because of its ability to dissolve hydrated clay minerals and to form complexes with di- and trivalent cations.

The ash contents of HA(ML), HA(F) and HA(A), along with HA(VM), are summarized in Table 4.1. Of the humic acids studied in this work, the two commercial humic acids had the highest ash contents of 25% and 20% for HA(A) and HA(F), respectively. HA(ML) had the lowest ash content of 14%. Ash content analysis on an unwashed sample of HA(ML) showed that the HCl-HF washing procedure had reduced the ash content of HA(ML) from 30% to 14%.

The ash content of HA(VM) of 76% is also reported in this table, and is very high in comparison to the humic acids investigated in this study. There are two main reasons for this. First, a different soil was used for the extraction of humic acid in the work of Maguire, 1994 compared to the soil used in this work. Second, and more importantly, although the same extraction procedure was used in both works, soil washing with a HCl-HF mixture was not performed in the work of Maguire, 1994, thus contributing to the high ash content.

Chiou et al. (1983) found no effect of inorganic material in terms of adsorption for  $f_{oc}$  greater than 0.01. Onken and Traina (1997) found that dominance of the inorganic material, in terms of condensation and adsorption, was not observed for  $f_{oc}$  greater than  $3 \times 10^{-5}$ . Hence, it was assumed that the ash content had a negligible effect on the interactions between the contaminants and the organic material.

## 4.2 Chemical Functional Groups

Saleh and Chang (1983) described humic substances as a carbon skeleton consisting of a broken network of poorly condensed aromatic rings with an appreciable



**Table 4.1: Experimental Values for Physical and Chemical Characteristics of Humic Acids**

<b>Humic Acid</b>	<b>Ash Content (%)</b>	<b>Total Acidity (meq/g)</b>
HA(ML)	14	6.73
HA(F)	20	4.32
HA(A)	25	2.63
HA(VM)	76	-

**Table 4.2: Average Total Acidity (Senesi and Chen, 1989)**

	<b>Carboxyl (meq/g)</b>	<b>Phenolic Hydroxyl (meq/g)</b>	<b>Total Acidity (meq/g)</b>
Humic Acid	1.5-5.7	2.1-5.7	3.6-11.4
Fulvic Acid	5.2-11.2	0.3-5.7	5.8-16.9

number of disordered aliphatic chains and alicyclic structures. Attached to the carbon skeleton are several oxygen containing functional groups such as carboxyl, phenolic and methoxy groups. It is the presence of these functional groups which renders them able to chemically bind with various organic compounds. Saleh and Chang (1983) presented NMR analysis showing that the aliphatic moieties of humic substances are represented by branched aliphatics with methylene carbons  $\alpha$ ,  $\beta$ , and  $\gamma$  from the end of an alkyl chain or an aromatic ring. They also suggested that the aromatic moieties in humic substances include a significant amount of substituted aromatics.

Humic substances are rich in oxygen content with most of the oxygen occurring in functional groups. Therefore, the functional groups in humic substances are often referred to as oxygen-containing functional groups.

#### 4.2.1 Total Acidity

The results of chemical analysis for total acidity of HA(ML), HA(F) and HA(A) are shown in Table 4.1. Total acidity is the sum of the carboxyl groups (COOH) and phenolic OH (or acidic OH).

A phenolic group has an OH group attached to an aromatic ring. This OH group consists of a strong electronegative oxygen bonded to an electropositive hydrogen, thus creating a permanent dipole capable of hydrogen bonding. The hydrogen from the phenol group is capable of giving up a proton and therefore this group contributes to the total acidity of humic substances. The ability of the phenolic group to give up a proton is due to the ability of the phenolic group to stabilize by resonance. Because the phenolic

group is able to dissociate, this group can occur in the ionic state and therefore ion-dipole bonding is possible (Lemke, 1992). Phenolic groups contribute to the hydrophilic nature of the humic substance.

A carboxyl group consists of a carbonyl group ( $C=O$ ) and hydroxyl group, both of which are polar groups capable of hydrogen bonding. Carboxyl groups are capable of stronger hydrogen bonding due to the greater acidity of the group and because of the additional bonding sites (i.e. both the carbonyl and hydroxyl group). Carboxyl groups add to the hydrophilic nature of humic substances.

Quantitative determination of functional groups using ion-exchange methods, such as the barium hydroxide method used to determine total acidity, must be interpreted with caution. Some problems include: insolubility of humic acids in water and most organic solvents; oxidation and reduction reactions; interactions with reagents used for forming derivatives; and the nonstoichiometric nature of the reactions (Stevenson, 1994). However, the information determined is still valuable in terms of a qualitative measure of the differences in total acidity between HA(ML), HA(F) and HA(A).

A great variability was noticed between each type of humic acid with HA(ML) having the highest total acidity, followed by HA(F), and finally, HA(A) with the lowest. Table 4.2 gives average values for carboxyl and phenolic hydroxyl groups in humic and fulvic acids found in soil as presented by Senesi and Chen (1989). The results in Table 4.1 indicated that HA(ML) has a characteristically high total acidity and is approaching the acidity found in fulvic acids. HA(F) has an average concentration of total acidity for a soil humic acid, whereas HA(A) has a characteristically low total acidity for a humic acid.

#### 4.2.2 NMR Spectroscopy Results

Great variability was observed in the NMR spectrums obtained for HA(F) and HA(ML) as shown in Figures 4.1 and 4.2, respectively. The relative area under the curve divided into the range of chemical shift described in Figure 3.3 are shown in Table 4.3 and are a measure of the %TOC occurring in the given group.

The NMR results indicate that HA(F) is much more aliphatic in nature compared to HA(ML) with approximately 72% of its carbon occurring in aliphatic groups. The largest amount of carbon in HA(ML) also occurs in aliphatic groups with just over 30% of its carbons occurring in aliphatic groups; however, this value is considerably less dominating than that observed for aliphatic carbon in HA(F). About half of the aliphatic structure in humic substances consists of n-fatty acids esterified to phenolic OH groups. The rest is made up of “loosely” held fatty acids and alkanes which seem to be physically adsorbed on the humic materials and which are not structural humic components, and possibly aliphatic chains joining aromatic rings (Schnitzer, 1978).

For both HA(F) and HA(ML), the second largest amount of carbon occurred in the aromatic group, i.e. 26% of the carbon in HA(ML) and about 14% of the carbon in HA(F). This is not surprising since part of the humic acid skeleton is described as a network of poorly condensed aromatic rings (Saleh and Chang, 1983). The aromatic ring is a 6-membered ring with a cloud of delocalized electrons above and below the ring. Because of their high electron density and flat nature, aromatic groups show a somewhat stronger capacity to bond through van der Waals attraction than a corresponding cyclic

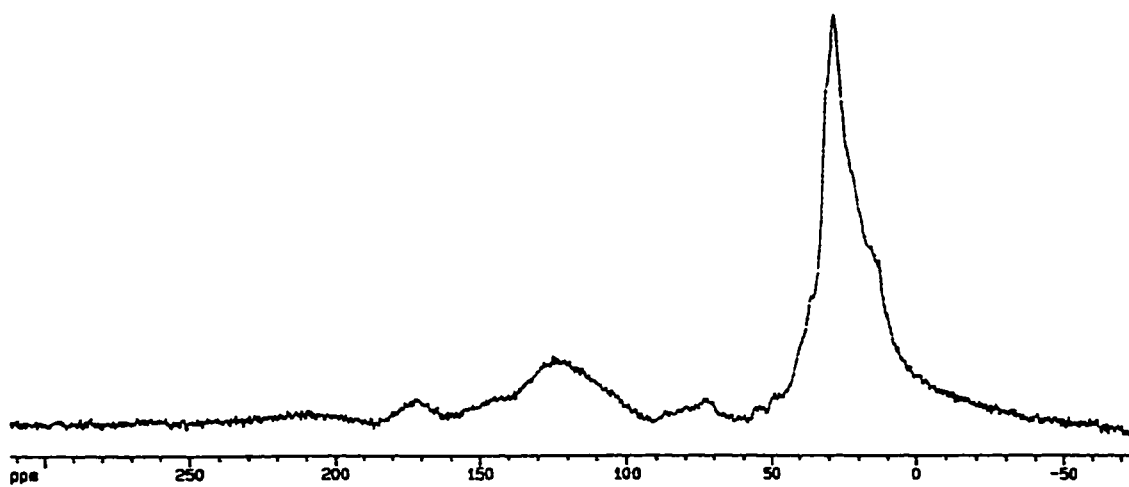


Figure 4.1 NMR Spectrum for HA(F)

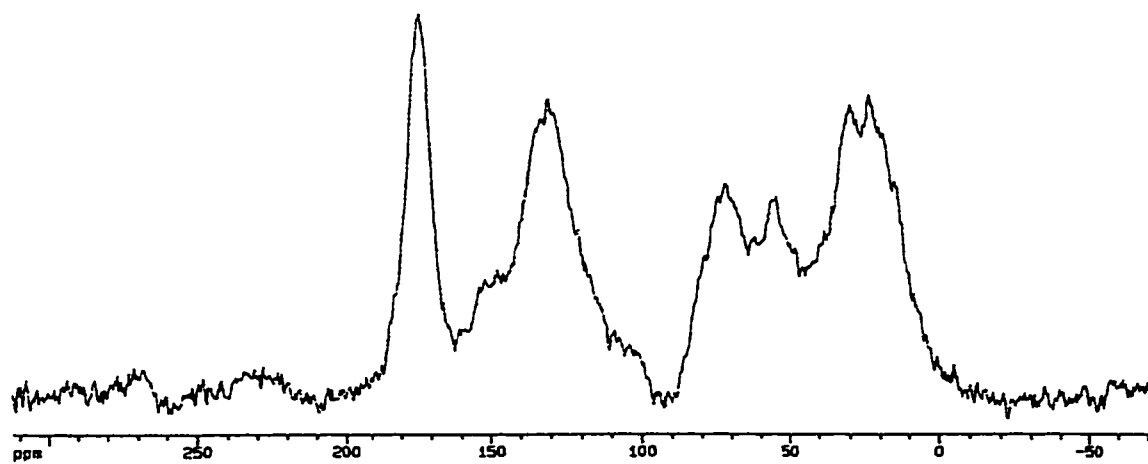


Figure 4.2 NMR Spectrum for HA(ML)

**Table 4.3: %TOC in Various Organic Functional Groups in HA(F) and HA(ML) by  $^{13}\text{C}$ -NMR Analysis**

Organic Group	HA(F)	HA(ML)
Aliphatic (0-50)	72.03	30.97
Carbohydrate (50-96)	5.29	20.39
O-C-O (96-108)	0	1.54
Aromatic (108-145)	13.84	25.86
Phenolic (145-162)	3.88	3.43
Carboxyl (162-190)	2.95	16.07
Ketonic (190-220)	2.00	1.73

hydrocarbon (Lemke, 1992). Aliphatic and aromatic sections of the humic structure are important because they contribute to the hydrophobic nature of the molecule.

The phenol groups are important because they increase the acidity of the humic molecule and also increase the hydrophilic nature of the molecule. Both HA(ML) and HA(F) have approximately the same phenolic content of 3.4% and 3.8%, respectively. Thus, phenolic group contributes equally to the total acidity calculated for HA(ML) and HA(F).

16% of the total carbon in HA(ML) occurs in carboxyl group compared to only 3% in HA(F). The carboxyl group contributes significantly to the total acidity. Therefore, these results are consistent with the results of total acidity presented in Section 4.2.1, which show that HA(ML) has a much higher total acidity than HA(F).

Only 5% of the TOC in HA(F) occurs as carbohydrate ( $C(H_2O)_n$ ) compared to 20% in HA(ML). Carbohydrate groups add to the hydrophilic nature of the humic acid.

Overall, the  $^{13}C$ -NMR results indicate that approximately 40% by mass of HA(ML) consists of polar functional groups compared with only 14% for HA(F). Therefore, HA(ML) can be described as being more polar or hydrophilic in nature. Likewise, HA(F) can be described as comparably non-polar and more hydrophobic in nature.

$^{13}C$ -NMR results of HA(ML) are comparable to those presented by Chiou et al. (1998) who gave the following data for organic carbon in SOM:  $20 \pm 5\%$  aromatic,  $25 \pm 6\%$  alkyl,  $40 \pm 10\%$  O-alkyl (i.e. carbohydrate)  $15 \pm 5\%$  carboxyl-amide-ester.

Analysis on HA(A) was not performed in this study; however, MacCarthy and Malcolm (1989) present a CPMAS  $^{13}C$ -NMR spectrum for Aldrich humic acid. They

found that all the NMR spectra for commercial humic acids investigated in their research were very similar to this Aldrich spectrum. MacCarthy and Malcolm's spectrum for Aldrich humic acid is also very similar to the spectrum of HA(F) conducted in this study.

### **4.3 Humic Acid DSC Thermograms**

Figures 4.3, 4.4, and 4.5 show DSC thermograms for clean HA(ML), HA(F) and HA(A), respectively. Each DSC thermogram represents a 7.8 mg sample run with an empty sample reference. The repeatability in each case is good. Any deviation is due to the heterogeneous nature of the humic acid itself.

#### **4.3.1 Dehydration**

Each humic acid DSC thermogram (HA(ML), HA(F) and HA(A)) is characterized by an initial endothermic peak which starts at approximately 50 °C and ends at approximately 200 °C. This endothermic event represents the desorption of bound water from the humic acid structure and is consistent with the findings of Schnitzer and Kodama (1972). Bound water is the water that is intimately bound to the soil particle, either trapped in void spaces or attached by hydrogen bonds. Energy must be added to the system to remove this water (Yong, 1992).



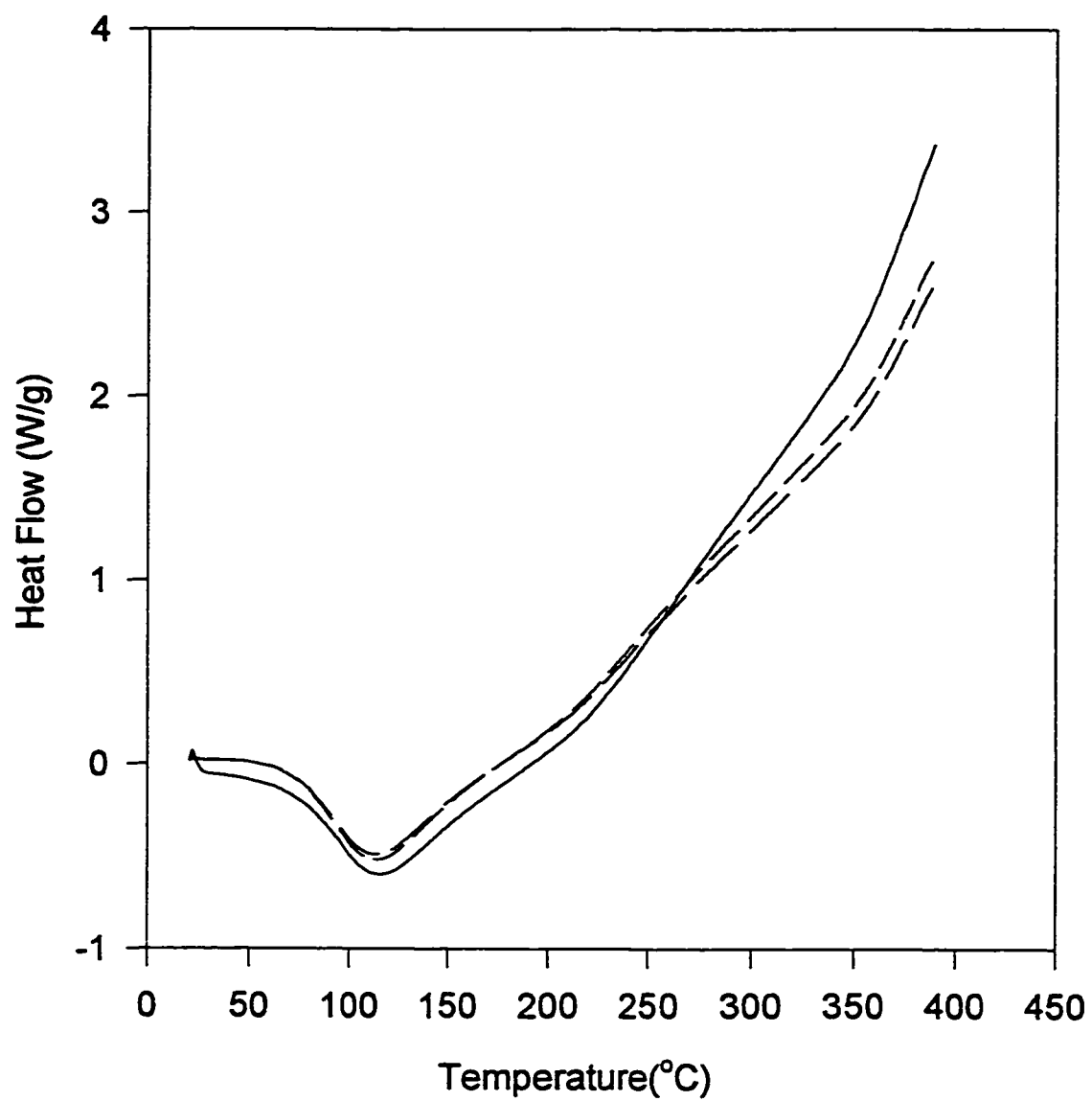


Figure 4.3: DSC Thermograms for Clean HA(ML)

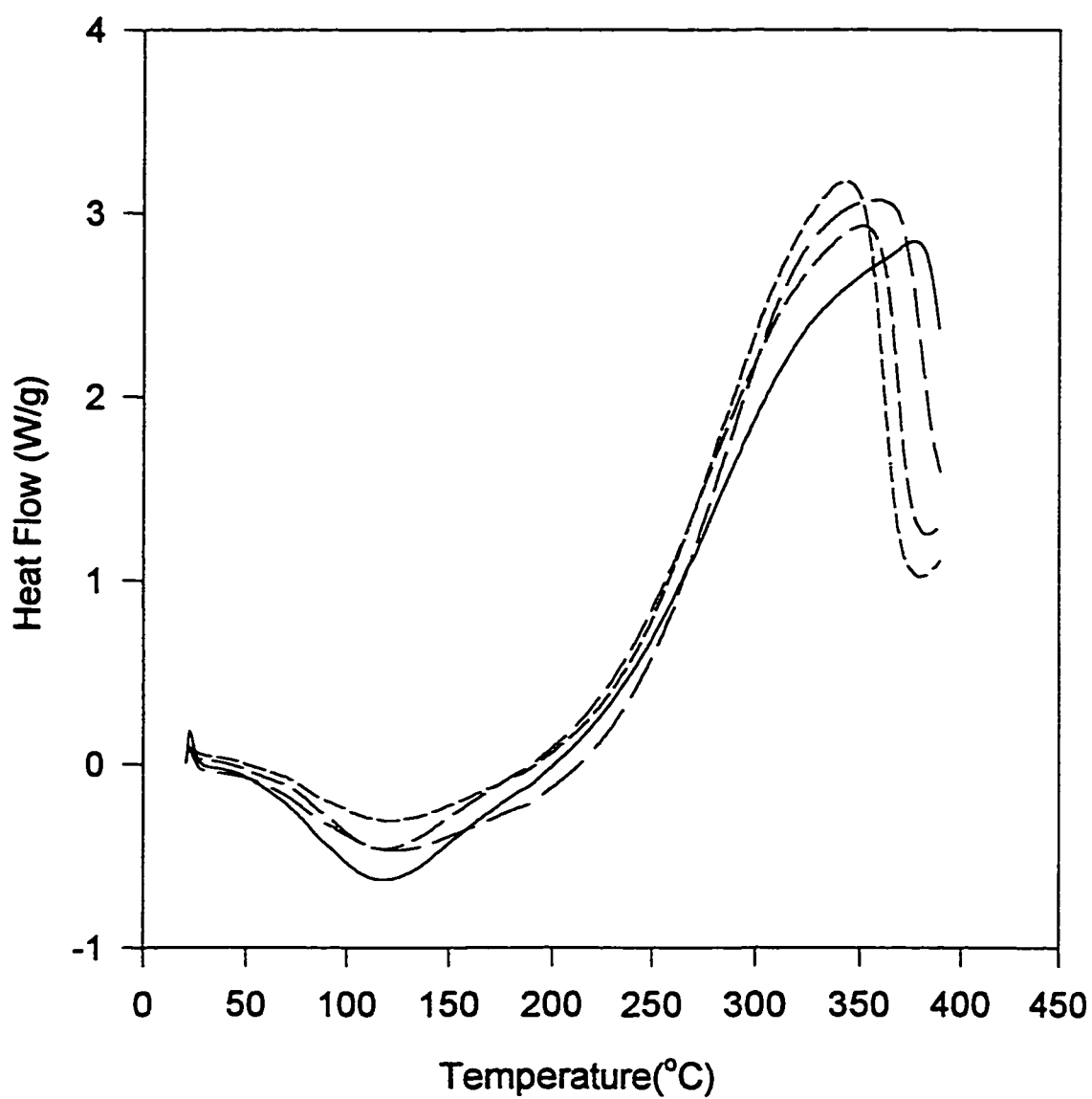


Figure 4.4: DSC Thermograms for Clean HA(F)

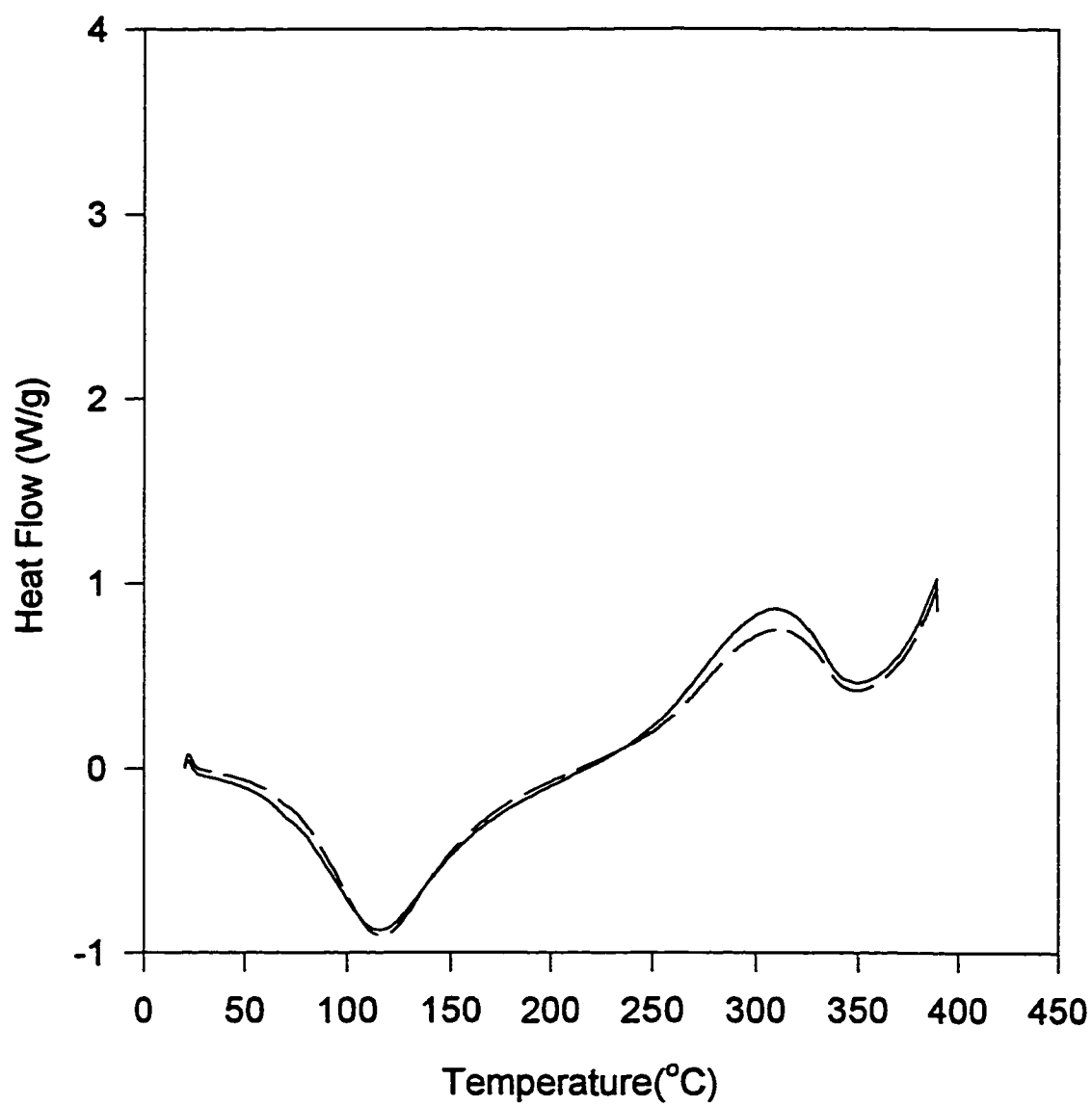


Figure 4.5: DSC Thermograms for Clean HA(A)

#### 4.3.2 Cleavage of Terminal Functional Groups

Immediately after the dehydration endotherm, the curve rises into an exothermic peak for all three humic acids. This second peak can be attributed to the cleavage of terminal functional groups, particularly decarboxylation, cleavage of acetyl groups and demethylation of methoxyl groups (Flaig et al., 1972).

Distinct exothermic peaks are visible for HA(F) and HA(A), however, only the beginning of the exothermic peak is visible for HA(ML). This exothermic peak begins earlier for HA(ML) compared to HA(F) and HA(A). For the HA(F) case, this exothermic peak starts at approximately 220°C and ends at 385°C with a maximum heat flow at 310°C. In comparison, HA(A) shows an exothermic peak starting at 220°C and ending at 355°C with a maximum heat flow at 310°C. Finally, HA(ML) exhibits the beginning of a large exothermic peak that starts at approximately 180°C, but does not reach a maximum before the DSC limit temperature of 390°C.

The great variability in these DSC thermograms are not surprising considering the observed differences in the chemical structure of HA(A), HA(F) and HA(ML) as determined by total acidity and  $^{13}\text{C}$ -NMR analysis. The large exothermic event observed in HA(ML) is to be expected considering the large amount of functional groups being evolved in comparison to HA(F) and HA(A). Variability in DSC thermograms for different humic acids is a common finding in literature (Flaig et al., 1975; Schnitzer and Kodama, 1972; Schnitzer and Hoffman, 1964).

### 4.3.3 Breakdown of Aromatic Structure

Schnitzer and Kodama (1972) identified the third exothermic peak in DSC analysis as decomposition of the aromatic humic acid backbone which occurs at temperatures over 400 °C. The DSC thermogram for HA(A) in Figure 4.5 shows the beginning of a third exothermic peak starting at 350°C. This peak does not summit before the temperature limit of the DSC. These exothermic peaks are not visible for HA(ML) or H(FA). Because analysis of the evolved volatiles from the thermal process was not available, it is not clear whether this peak on the HA(A) curve is the beginning of thermal decomposition of the humic acid backbone. Because this peak starts at a relatively low temperature, it is likely another peak indicating cleavage of terminal functional groups.

## **4.4 TGA Analysis**

### 4.4.1 Mass Loss Experiments

Results of mass loss by TGA analysis for HA(ML) and HA(F) are shown on an ash-free basis in Figure 4.6. For comparison, also shown in Figure 4.6 is the mass loss data for Maguire's humic acid (HA(VM)) as generated in Maguire, 1994. This information is also on an ash-free basis.

HA(ML) experienced a total mass loss of approximately 44% by 400°C and 56% by 500°C. HA(F), on the other hand, experienced a total mass loss of approximately

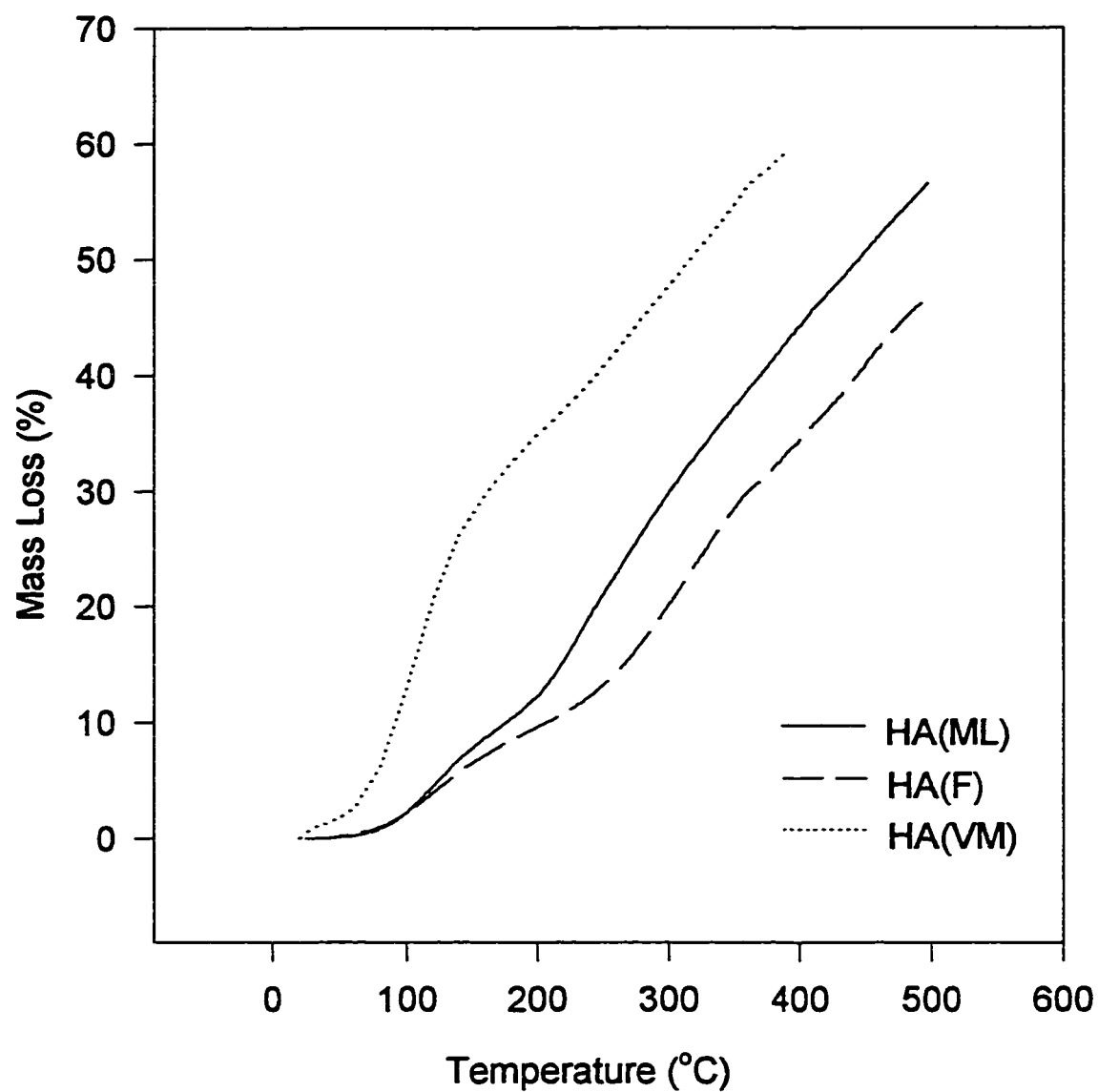


Figure 4.6: % Mass Loss of Humic Acids with Temperature by TGA

34% by 400°C and 46% by 500°C. Since the majority of the mass loss can be attributed to the cleavage of terminal functional groups, the increased mass loss of HA(ML) compared to HA(F) further supports the findings of the total acidity tests and NMR analysis which indicated higher terminal functional group concentration on HA(ML).

In comparison, HA(VM) experienced a total mass loss of almost 60% by 390°C on an ash-free basis assuming 76% ash as determined from ash content analysis. TGA was not performed on HA(VM), but was determined by simulated experiments of thermogravimetry utilizing the DSC furnace Maguire (1994). Therefore, the shape of the mass loss curve is different for HA(VM) versus HA(F) and HA(ML).

#### 4.4.2 Differential Mass Loss Curves

According to Flaig et al. (1975), plots of differential mass loss versus temperature by TGA should reveal the same information as DSC plots. Figure 4.7 shows the rate of % mass change of HA(ML) and HA(F) with temperature.

Like the DSC thermograms, dehydration peaks are observed for HA(ML) and HA(F) in the TGA thermograms presented in Figure 4.7. Both peaks reach a maximum rate at approximately 125°C.

The main exothermic peak indicating decomposition attributed to the loss of terminal functional groups can also be observed in the rate of % mass change curve generated by TGA. For the HA(F) case, the exothermic peak starts at approximately 210°C and ends at 375°C with a maximum rate of mass loss at approximately 310°C.

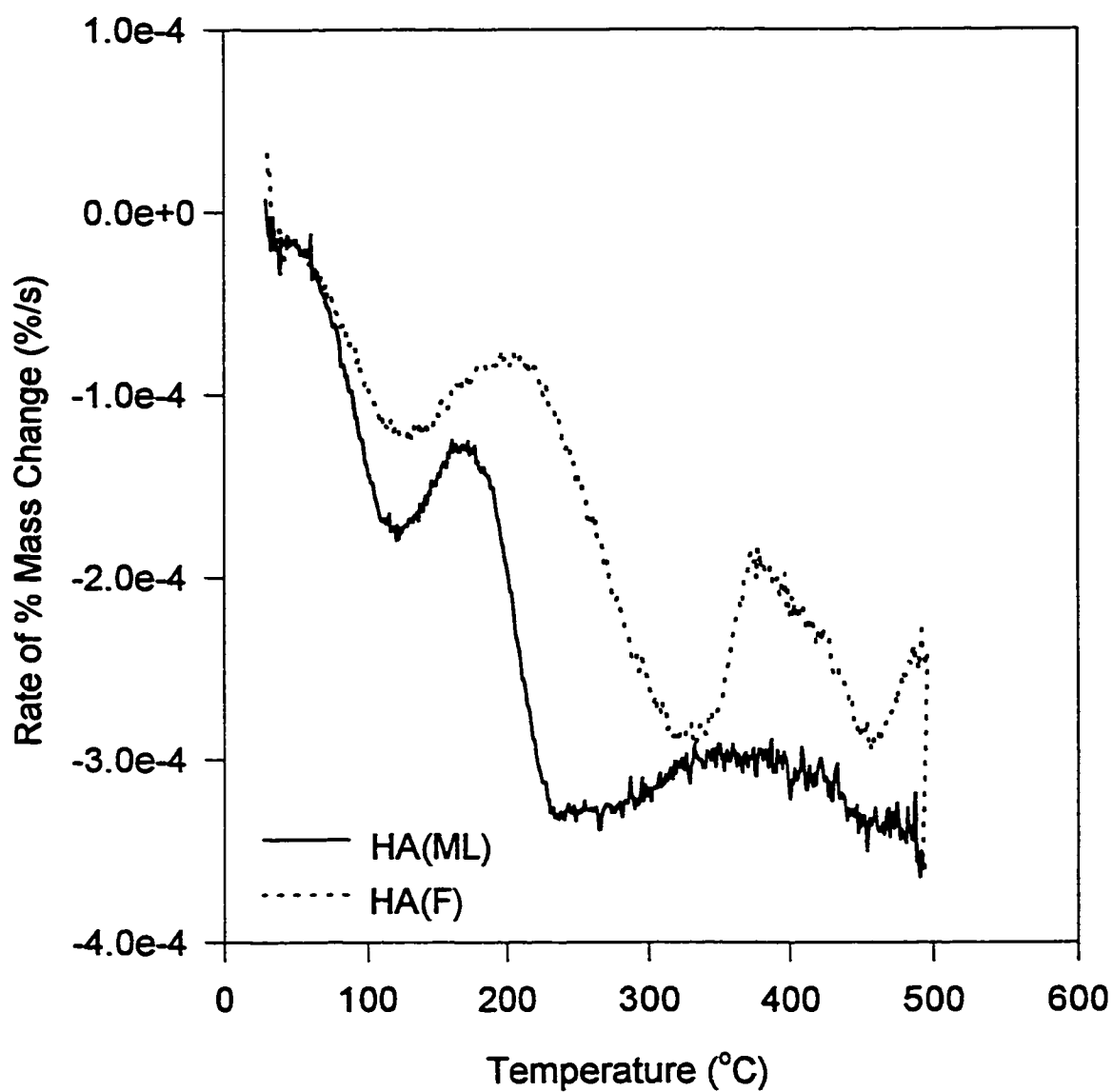


Figure 4.7: Differential Mass Loss of Humic Acids with Temperature by TGA



For HA(ML), the exothermic peak begins at approximately 180°C and a maximum rate of mass loss is observed at 210 °C. This maximum rate was not observed on the DSC thermogram. This may be due to the gradual decay of the curve to a constant rate of mass loss at 500°C.

Because TGA analysis was completed up to 500°C rather than 400°C for DSC (due to the temperature limit of the DSC12E) decomposition of the humic acid backbone could be observed. According to Flaig et al. (1975), this should occur at temperatures above 400°C. A third region of increased rate of mass loss was observed on the HA(F) curve. This peak occurs between 375°C and 500°C. Due to the high temperature at which this peak occurs, it is very likely that this mass loss is due to the breakdown of the aromatic humic acid backbone. At temperatures up to 500°C, an obvious rate of mass loss peak due to decomposition of the humic backbone was not observed for HA(ML).

#### **4.5 Summary**

Structure of humic acid plays a very important role in the sorption of organic contaminants. Many oxygen containing functional groups add to the hydrophilic and thus polar nature of the humic material. Conversely, aromatic or aliphatic sections of the humic acid contribute to the hydrophobic or non-polar nature of the macromolecule. The presence of regions of both high and low polarity is a feature common to all structural models for humic substances (Aochi and Farmer, 1997). These polar and non-polar groups are thoroughly mixed throughout the humic structure (Grabber, 1998).

Polar function groups are capable of intermolecular bonding causing crosslinking of the humic structure. The amount of crosslinking affects the density of the material and therefore the size and amount of void spaces capable of trapping organic molecules. Aochi and Farmer (1997) showed evidence supporting the existence of discrete regions in the macromolecular structures that are more polar, more dense and more tightly coiled than others. Non-polar compounds are less effective than polar compounds at interrupting these polar contacts (Grabber and Borisover, 1998).

Ganaye et al. (1997) attributed the difference in polarity or aromaticity of soil organic matter to the observed variations in  $K_{oc}$  values determined in partitioning experiments. Chiou et al. (1997) also stated that disparity between partition coefficients reflects compositional differences in the humic material.

$^{13}\text{C}$ -NMR results indicate that 40% by mass of HA(ML) consists of polar functional groups, compared with only 13% for HA(F). Thus, HA(ML) should have a more dense cross-linked structure. However, this structure probably “loosens” as functional groups are eliminated at higher temperatures.

## CHAPTER 5

### DSC RESULTS FOR HUMIC ACID-CONTAMINANT MIXTURES

#### 5.1 Anthracene on Humic Acid

Figures 5.1 through 5.3 show the DSC thermograms obtained for HA(ML), HA(F) and HA(A), each contaminated with 3% and 7% by mass anthracene. The humic acid-contaminant mixtures are illustrated as solid lines and glass-anthracene curves are shown as dotted lines. Each humic acid-anthracene curve is compared to the equivalent glass-anthracene curve in which no interaction between the glass beads and the anthracene is assumed to occur. Thus, differences between the contaminant-glass thermograms and the contaminant-humic acid thermograms can be attributed to interactions between the contaminant and the humic acid.

##### 5.1.1 Anthracene on HA(ML)

HA(ML) is the humic acid extracted from a whole soil using the Schnitzer procedure as described in Section 3.2. Figure 5.1 shows DSC thermograms, in duplicate, describing anthracene-HA(ML) interactions at concentrations of 3% and 7% by weight anthracene. The melting point of anthracene, as shown by the first sharp endothermic

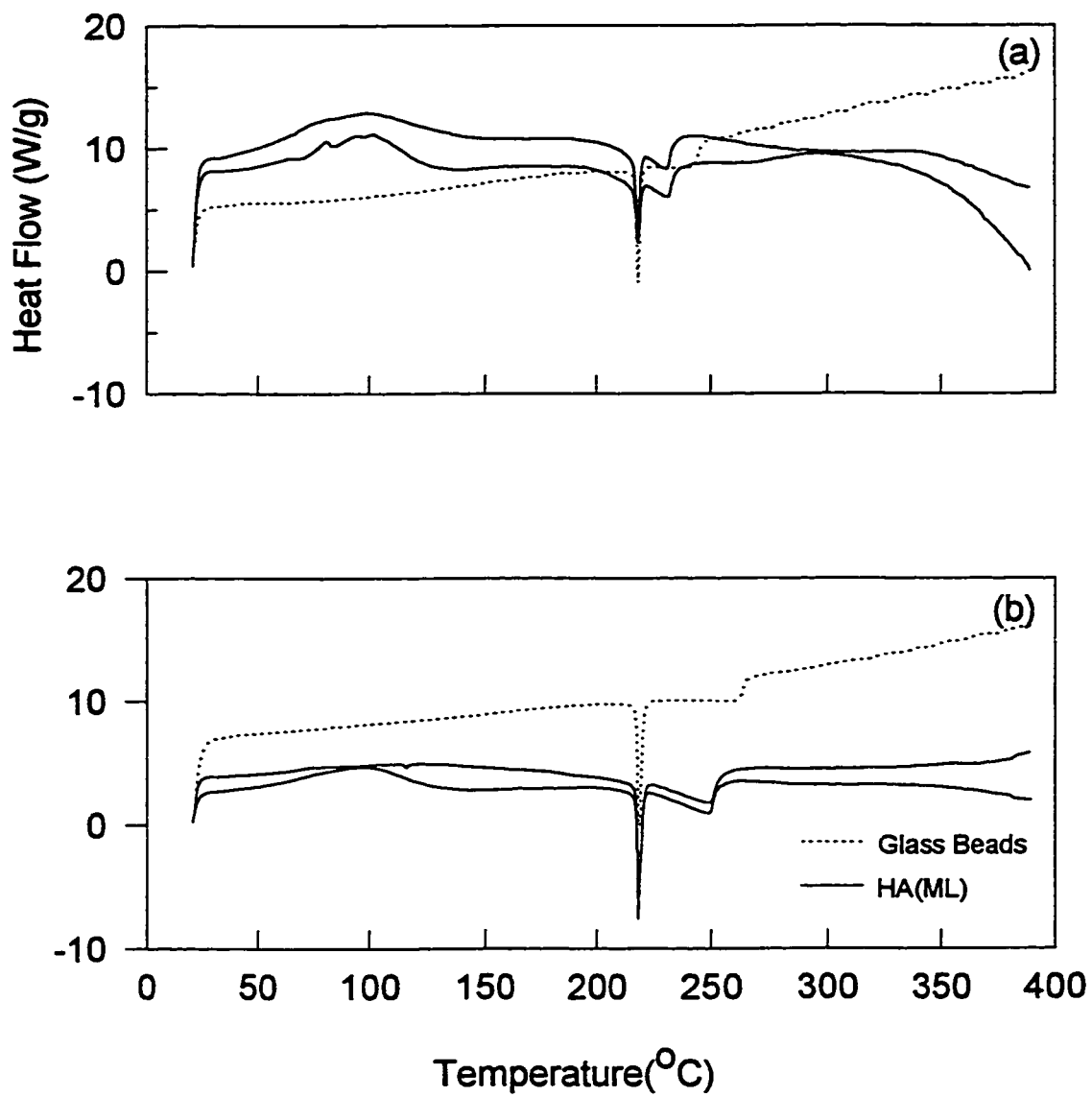


Figure 5.1 DSC Thermograms for Anthracene in HA(ML). (a) 3% anthracene in HA(ML). (b) 7% anthracene in HA(ML).

peak, coincides for HA(ML)-anthracene and glass-anthracene at 216°C, the melting point of pure anthracene.

As described in Section 2.5.3, Maguire et al. (1995) presented a model indicating that the presence or absence of a contaminant vaporization peak on a contaminant-humic substance DSC thermogram indicated immiscible or miscible behaviour, respectively. In Figure 5.1a and 5.1b, anthracene vaporization peaks were observed for both the 3% and 7% anthracene HA(ML)-anthracene mixtures, respectively, thus indicating an immiscible system. This finding is in contrast to Maguire et al. (1995) who, as illustrated in Figure 2.8a, found no vaporization peak on DSC thermograms for anthracene-humic acid mixtures. However, an anthracene concentration of only 0.8% was used in Maguire et al., 1995. Clearly, miscibility of anthracene with HA(ML), at the concentrations presented in this work, is not supported for HA(ML)-anthracene mixtures.

The anthracene vaporization peaks observed for glass-anthracene and HA(ML)-anthracene are qualitatively and quantitatively different, thus indicating an interaction between HA(ML) and anthracene. Vaporization of anthracene from the glass-anthracene appears to occur immediately after melting at 227 °C. This can be observed from the negative deviation from the initial baseline. Vaporization of anthracene from HA(ML)-anthracene also appears to begin immediately after melting of the anthracene; however, the rate of heat flow to the sample, as observed visually from the initial slope of the vaporization peak, is greater for the HA(ML)-anthracene case than the glass-anthracene case. This indicates that a greater amount of energy is being added to the HA(ML)-anthracene sample than to the glass-anthracene sample during the anthracene

vaporization process. This is most likely due to physico-chemical interactions between anthracene and HA(ML).

Vaporization of anthracene is complete sooner in the anthracene-HA(ML) case than the anthracene-glass beads case. In the case of 3% anthracene, anthracene has completely vaporized from the glass beads at 250°C, whereas all of the anthracene has vaporized from HA(ML) by 238°C. Also, for 7% anthracene on HA(ML), anthracene has completely vaporized from the glass at 270°C, whereas all of the anthracene has vaporized from HA(ML) by 255°C. Maguire et al. (1995) stated that a condition of immiscibility is the vaporization of the contaminant before the boiling temperature of the pure contaminant. Therefore, the complete vaporization of anthracene from the HA(ML)-anthracene mixture, before the complete vaporization of pure anthracene from the anthracene-glass mixture, is a further indication of immiscibility.

#### 5.1.2 Anthracene on HA(F)

HA(F) is Fluka humic acid, a commercial humic acid. Figure 5.2 shows DSC thermograms describing anthracene-HA(F) interactions at concentrations of 3% and 7%. In contrast to the HA(ML)-anthracene case illustrated in Figure 5.1, the melting point of anthracene does not coincide for HA(F)-anthracene and glass-anthracene. Instead, the melting point is depressed for the HA(F)-anthracene case. This depression increases as the concentration of anthracene on HA(F) decreases. Thus, the increasing concentration of humic acid causes further depression of the contaminant melting point. The onset of melting of anthracene occurs at approximately 198°C and 174°C for the 7% and 3%

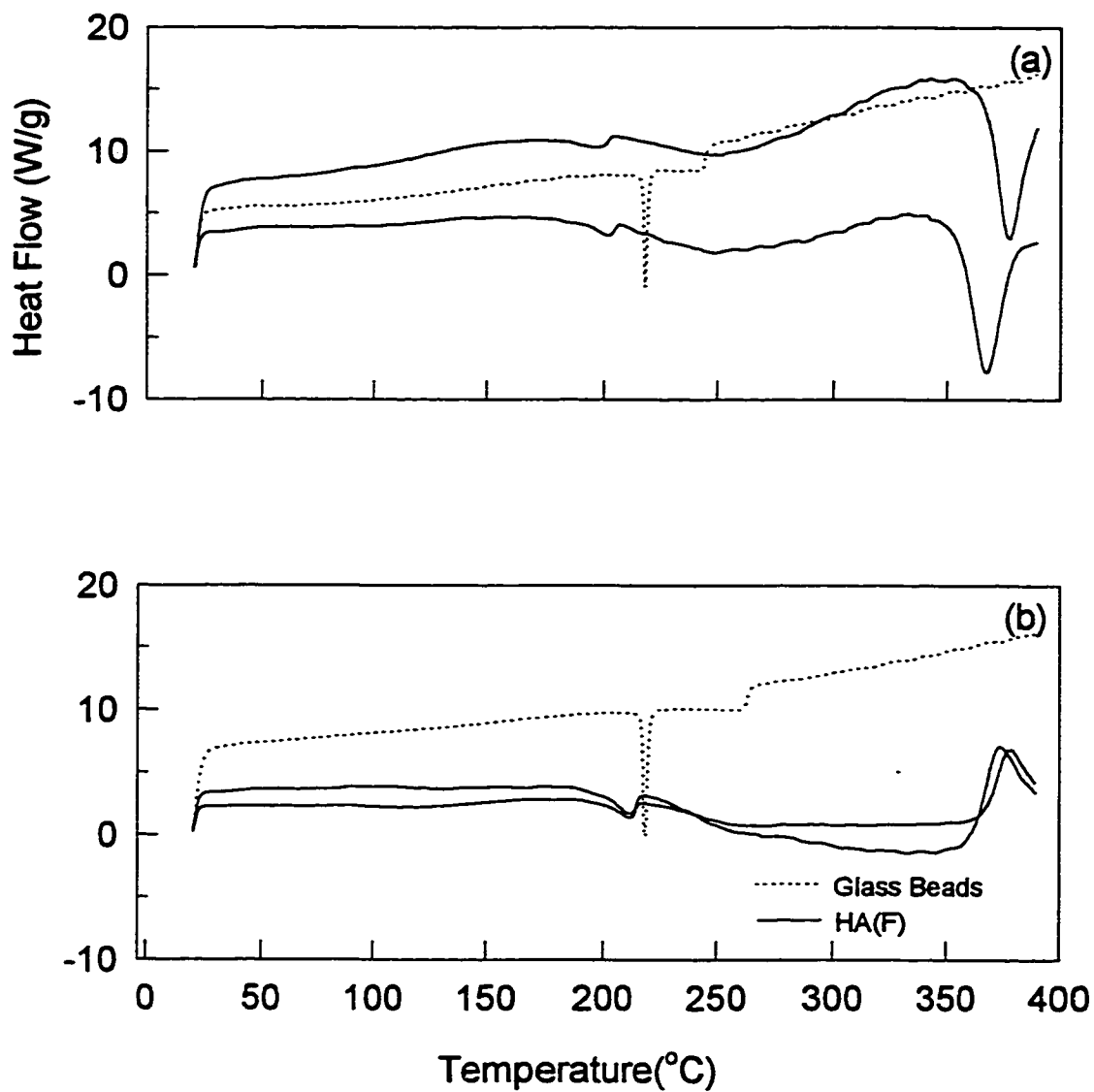


Figure 5.2 DSC Thermograms for Anthracene in HA(F). (a) 3% anthracene in HA(F). (b) 7% anthracene in HA(F).

HA(F)-anthracene cases, respectively. These represent melting point depressions of 18°C and 42°C for the 7% and 3% HA(F)-anthracene cases, respectively. As well, as the melting peak becomes more depressed, it becomes shorter and broader. These results indicate a strong solid-solid interaction between HA(F) and anthracene.

In comparison, Figures 2.8a-2.8c illustrate DSC thermograms for 0.8% anthracene on humic acid, fulvic acid and humin as presented by Maguire et al. (1995). The peaks presented in Maguire's work are not as distinct as those presented in this work since empty crucibles were used as references in Maguire's study, as opposed to humic acid references in this study. Maguire et al. (1995) showed that both fulvic acid and humin exhibited very small anthracene melting peaks. However, no anthracene melting peak was visible for humic acid. It is very likely that a depression of melting point along with broadening of the melting peak occurred in Maguire's experiments. Therefore, the results of melting point with HA(F) may be consistent with Maguire (1994). Unfortunately, only 0.8% anthracene runs were conducted in Maguire's work.

Consistent with Maguire (1994), distinct vaporization peaks were not observed for anthracene-HA(F). The HA(F)-anthracene interaction is unique in that a very long, broad endothermic peak was observed on the DSC thermogram. The endothermic events for both 3% and 7% anthracene start immediately after melting and continue until 330°C and 370°C, respectively. At this point it is uncertain what these peaks mean. However, these odd peaks could indicate miscibility as it is not a "distinct" peak as is predicted in the calculations by Maguire et al. (1995). Another possible explanation could be that a large amount of energy is required to remove the anthracene from the HA(F) due to increased interactions between the aromatic PAH and the aromatic structure of HA(F).



As illustrated in Figure 5.2, the endpoint of each HA(F)-anthracene thermogram contains a sharp endothermic peak or exothermic peak for 3% and 7% anthracene, respectively. These peaks do not have a significant meaning. As shown in Figure 4.4, pure HA(F) shows a large exotherm in its DSC thermogram, with a maximum heat flow at 310°C. This peak is not very reproducible due to the heterogeneous nature of humic acid. Therefore, it is to be expected that there would be some differences between the HA(F) used in the sample and that used in the reference. Because an HA(F) reference was used, the DSC results presented are based on the mass of the contaminant. Since the mass of contaminant is very small relative to the mass of humic acid, small changes in heat flow occurring due to the heterogeneity of the humic acid or due to small differences in the mass of humic acid in the sample and reference, become exaggerated. This exaggeration is more dramatic at the lower contaminant concentrations. Thus, these peaks are insignificant.

If these large peaks are in fact anthracene vaporization curves, then vaporization is completed sooner for the glass-anthracene than the HA(F)-anthracene case. According to Maguire et al. (1995), the absence of a vaporization peak indicates miscibility between the contaminant and the HA(ML). Also, Maguire et al. (1995) indicated that in a miscible system, temperatures above the boiling point of the contaminant are required to vaporize the contaminant. Therefore, it is quite likely that these large peaks are indicating miscibility.

### 5.1.3 Anthracene on HA(A)

HA(A) is Aldrich humic acid, a commercial humic acid obtained from Aldrich Chemical Company, Ltd. Figure 5.3 shows DSC thermograms describing anthracene-HA(A) interactions at concentrations of 3% and 7%, respectively. In contrast to the HA(ML)-anthracene case, but similarly to the HA(F)-anthracene case, the melting point of anthracene is depressed in the solid-solid mixture. Again, this depression increases with decreasing anthracene concentration; however, the interaction is not as large as the case for HA(F)-anthracene. The onset of melting of anthracene occurs at approximately 210°C and 196°C for the 7% and 3%, cases respectively. This corresponds to a melting point depression of only 6°C and 20°C, respectively. Again, the peaks become shorter and broader as the melting point is depressed. This melting peak depression indicates solid-solid interaction, although not as strong as the HA(F)-anthracene case.

Only small anthracene vaporization peaks can be observed for the 7% HA(A)-anthracene curve and no obvious anthracene vaporization peak can be observed for the 3% HA(A)-anthracene case. The fact that there are no peaks for the 3% anthracene case indicates that a miscible solution is formed at this concentration. The small peaks that are observed at 7% anthracene could indicate that the solubility limit had been reached and that the small vaporization peak observed is a result of vaporization of the residual immiscible fraction. As seen in Figure 2.8a, Maguire et al. (1995) did not observe vaporization peaks for anthracene-humic acid mixtures.

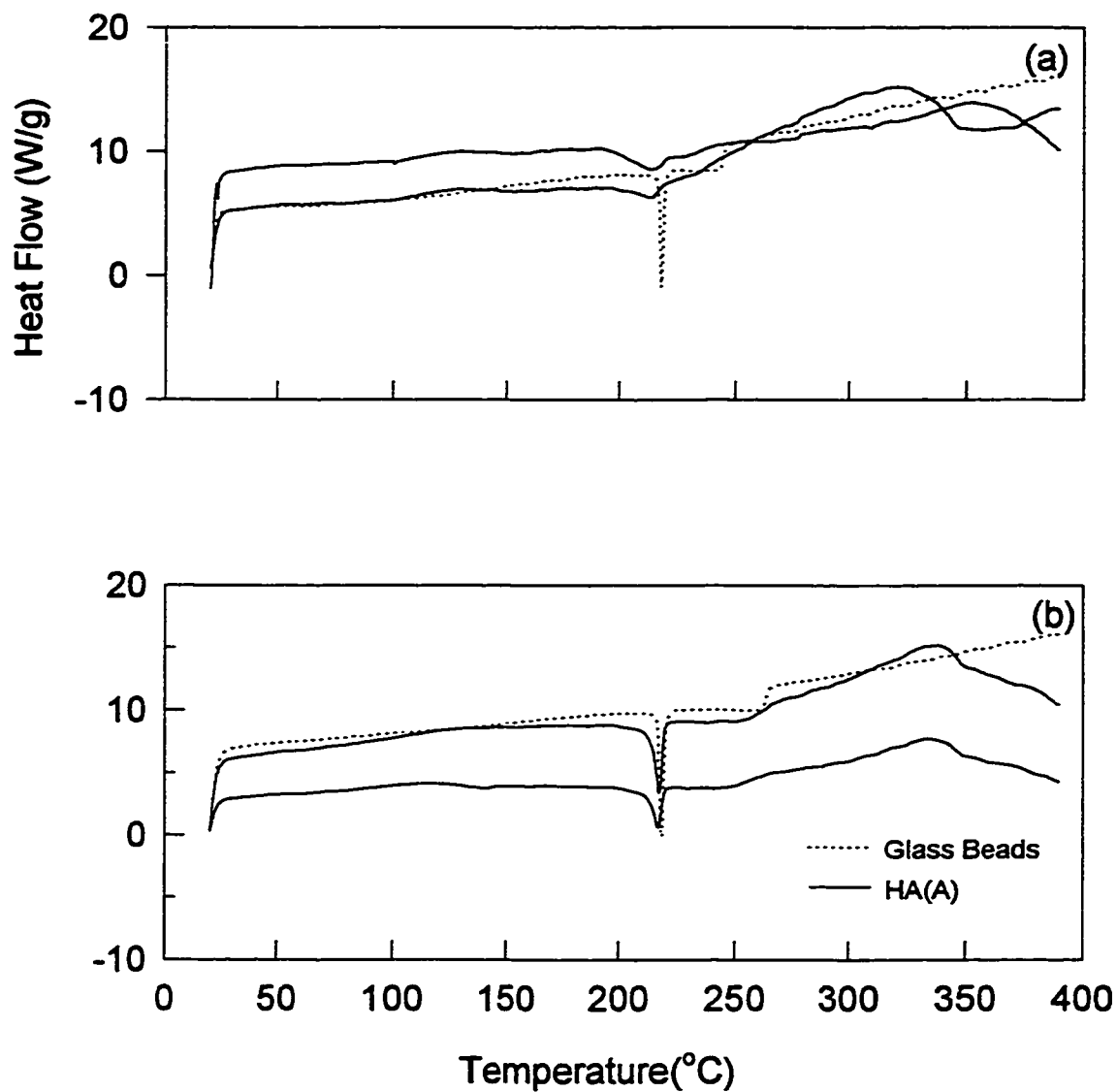


Figure 5.3 DSC Thermograms for Anthracene in HA(A). (a) 3% anthracene in HA(A). (b) 7% anthracene in HA(A).

#### 5.1.4 Constant Concentration of Anthracene on HA(ML), HA(F) and HA(A)

To illustrate different interactions between anthracene and HA(ML), HA(F) and HA(A), a constant anthracene concentration of 7% will be used for comparison. 7% contaminant concentration was chosen as the basis of comparison since data is available for each contaminant and each humic acid at this concentration, and because, in general, the repeatability of the experiments is better at the 7% contaminant concentration than at the 3% contaminant concentration.

Figures 5.1b, 5.2b and 5.3b show DSC thermograms for 7% anthracene on HA(ML), HA(F) and HA(A), respectively. As mentioned earlier, melting point depressions were observed for 7% anthracene on HA(F) and HA(A), as illustrated in Figures 5.2b and 5.3b; however, no melting point depression was observed for 7% anthracene on HA(ML), as observed in Figure 5.1b. This indicates that solid-solid interactions exist between anthracene and HA(F) and HA(A), but not between anthracene and HA(ML). For the cases of HA(F)-anthracene and HA(A)-anthracene, the onset of melting occurs at approximately 198°C and 210°C, respectively, corresponding to melting point depressions of 18°C and 6°C, respectively. This indicates that stronger solid-solid interactions occur between HA(F) and anthracene than between HA(A) and anthracene. Also, the smaller and broader nature of the HA(F)-anthracene melting peak compared to the HA(A)-anthracene case is a further indication of the stronger solid-solid interaction occurring between HA(F) and anthracene compared to HA(A) and anthracene.

In terms of miscible/immiscible behaviour, anthracene and HA(ML) formed an immiscible mixture. This can be observed from the distinct anthracene vaporization peak

seen in Figure 5.1b. The complete vaporization of anthracene from HA(ML) at a lower temperature than complete vaporization of anthracene from the glass beads is a further indication of immiscibility. In comparison, anthracene seems to exhibit miscible behaviour with HA(F), as shown in Figure 5.2b by the lack of a distinct anthracene vaporization peak for the HA(F)-anthracene mixture. Finally, anthracene seems to exhibit partial miscibility with HA(A), as shown in Figure 5.3b. Very small anthracene vaporization peaks can be observed for 7% anthracene on HA(A). These peaks are much smaller than the corresponding glass-anthracene vaporization peak. This indicates that anthracene may have limited miscibility in HA(A) and the small vaporization peak may be the result of vaporization of the residual immiscible anthracene fraction.

These results indicate that in terms of solid-solid interactions, the strength of these interactions from weakest to strongest is: HA(ML), HA(A) and HA(F). As well, anthracene exhibits varying solubilities in the humic acids ranging from immiscible in HA(ML), partially miscible in HA(A) and miscible in HA(F).

## 5.2 Fluorene on Humic Acids

Figures 5.4 through 5.6 show the DSC thermograms obtained for HA(ML), HA(F), and HA(A) contaminated with 3%, 7% and 10% by mass fluorene. The results for humic acid-contaminant mixtures are illustrated as solid lines, in duplicate. Glass-fluorene curves are shown as dotted lines. Each humic acid- fluorene curve is compared to the equivalent glass- fluorene curve in which no interaction between the glass beads and the fluorene is assumed to occur.

### 5.2.1 Fluorene on HA(ML)

Figure 5.4 shows DSC thermograms obtained for 3%, 7% and 10% fluorene on HA(ML), respectively. The melting point of fluorene coincides for HA(ML)-fluorene and glass-fluorene at 116°C. Therefore, like anthracene on HA(ML), no depression of the melting point and, thus, no solid-solid interaction was observed for this PAH and HA(ML).

According to the model by Maguire et al. (1995), as presented in Section 2.5.3, the presence of fluorene vaporization peaks for all concentrations of fluorene on HA(ML) indicates an immiscible HA(ML)-fluorene system. As well, the fact that vaporization is complete before complete vaporization of the pure contaminant further supports the idea of immiscibility between fluorene and HA(ML). For the HA(ML)-fluorene system, vaporization is complete at 215°C, 240°C and 235°C for the 3%, 7% and 10% cases, respectively. In comparison, vaporization for the glass-fluorene case was complete at 216°C, 246°C, and 248°C for the 3%, 7% and 10% concentrations, respectively. Qualitatively, the fluorene vaporization peak for both HA(ML)-fluorene and glass-fluorene are very similar. However, vaporization of fluorene is complete at a lower temperature in the HA(ML) system than the glass-fluorene system.

According to results presented by Maguire et al. (1995), and repeated in Figure 2.7a, fluorene formed a miscible mixture with humic acid. Thus, these results for HA(ML)-fluorene do not support Maguire's findings.

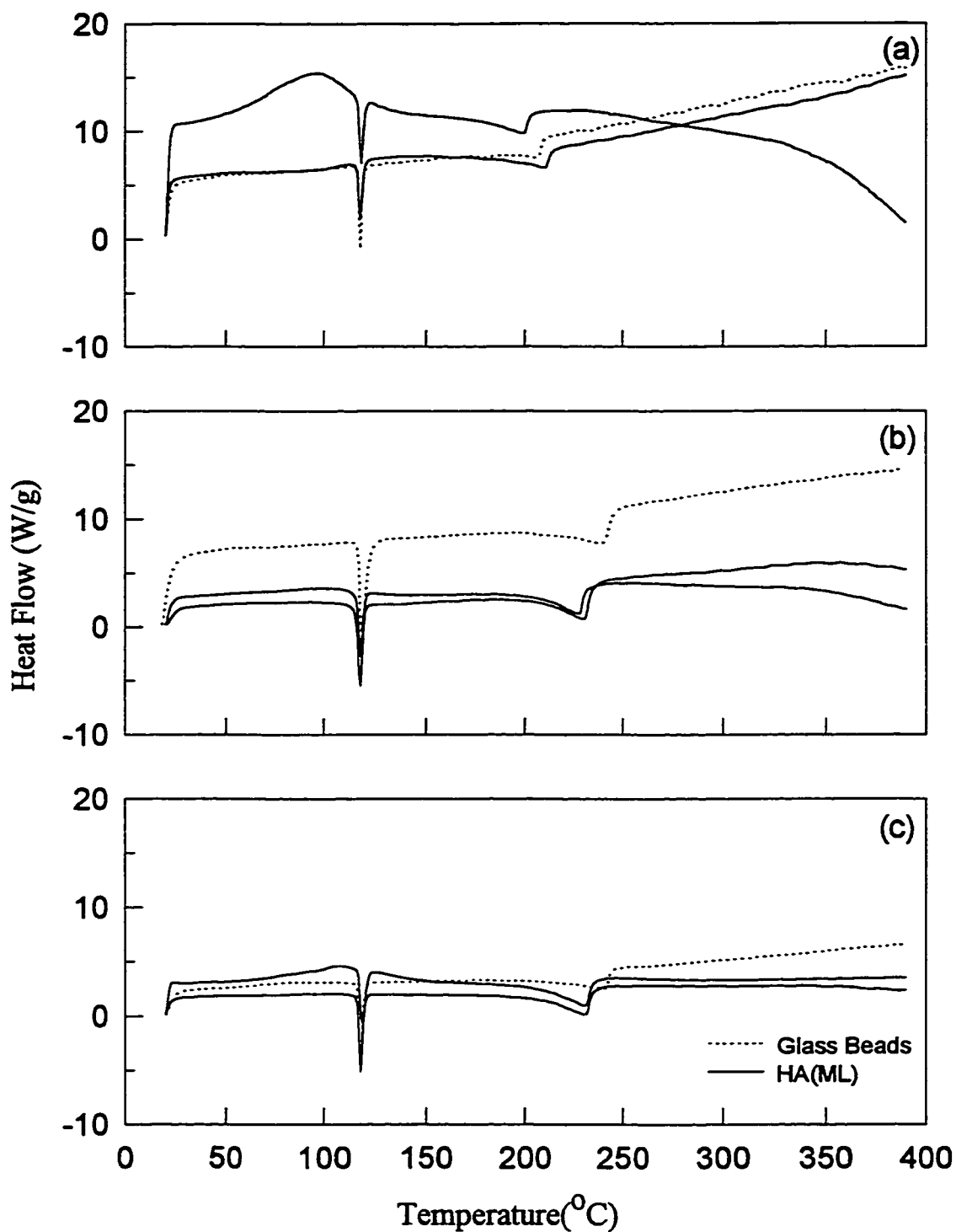


Figure 5.4 DSC Thermograms for Fluorene in HA(ML). (a) 3% fluorene in HA(ML). (b) 7% fluorene in HA(ML). (c) 10% fluorene in HA(ML).

The crossing of the DSC thermograms observed after the fluorene vaporization peaks in Figures 5.4a and 5.4b are considered insignificant due to the exaggeration of the heat flow value as discussed in Section 5.1.2.

### 5.2.2 Fluorene on HA(F)

Figure 5.5 shows DSC thermograms describing HA(F)-fluorene interactions at concentrations of 3%, 7% and 10%, respectively. In contrast to the HA(ML) case, the melting point of fluorene in the HA(F)-fluorene system does not always coincide with the melting point of fluorene in the glass-fluorene system. Instead, the melting point becomes more depressed as the concentration of fluorene decreases or the concentration of HA(F) increases. The onset of melting occurs at 114°C, 112°C and 85°C for 10%, 7%, and 3% fluorene concentrations, respectively. This represents melting point depressions of 2°C, 4°C, and 31°C. The peaks also become broader as the melting point depression increases. The melting point depression indicates a solid-solid interaction between fluorene and HA(F); however, this interaction is not as strong as the solid-solid interaction observed for anthracene and HA(F) in Figure 5.2.

Distinct vaporization curves are not observed for the HA(F)-fluorene mixtures. Very weak peaks can be identified for 10% and 7% fluorene; however, no peaks are observed for the 3% case. Since the lack of distinct vaporization peaks indicates miscible systems, it is likely that a 3% solution created a miscible system; however, the solubility limit has been exceeded at 10% and 7%, resulting in an immiscible phase. As the concentration increases from 7% to 10%, the vaporization peaks become slightly sharper



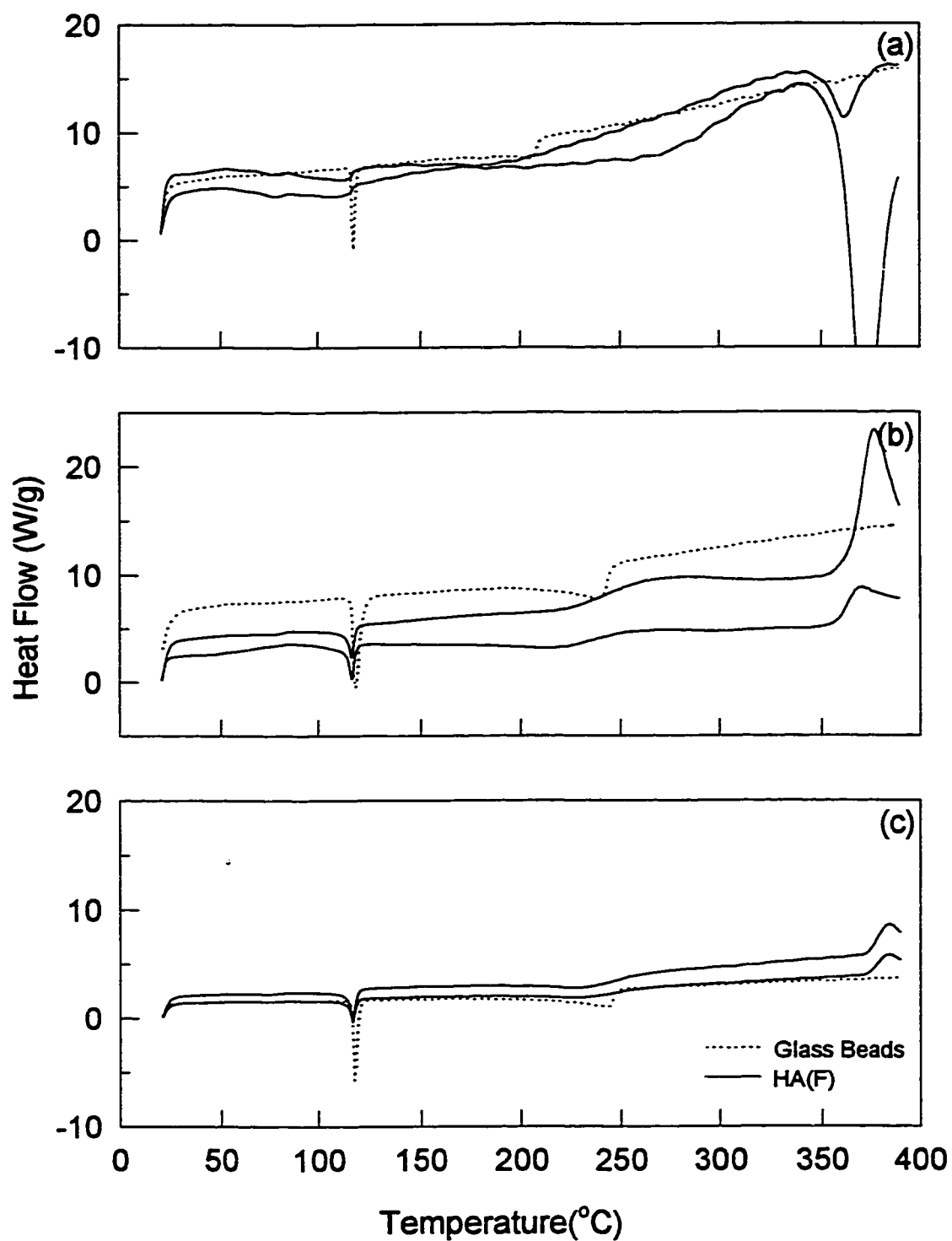


Figure 5.5 DSC Thermograms for Fluorene in HA(F). (a) 3% fluorene in HA(F). (b) 7% fluorene in HA(F). (c) 10% fluorene in HA(F).

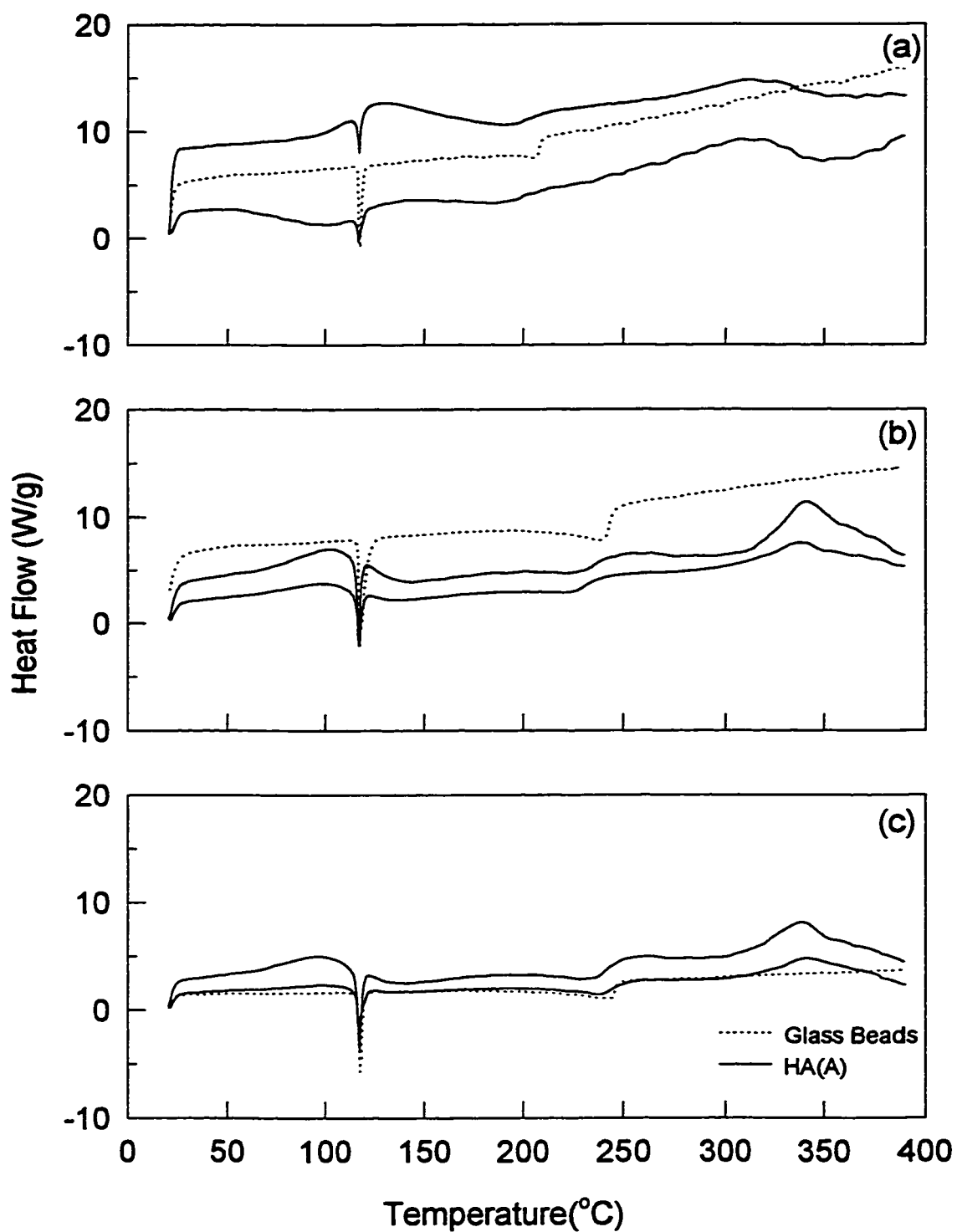
and becomes closer to the glass-fluorene thermogram. Although different concentrations, vaporization is complete at 258°C for both the 7% and 10% concentration. The onset of vaporization appears to occur earlier for 7% fluorene case compared to the 10% fluorene case. Actual values for the onset of vaporization temperatures were difficult to determine due to the gradual slope of the of the vaporization peak.

The HA(F)-fluorene results presented here are consistent with those reported by Maguire et al. (1995) and reproduced in Figure 2.7a. Maguire (1994) showed that at concentrations 3% and lower, miscible mixtures were formed between fluorene and humic acid. Maguire (1994) also presented a 4% fluorene-humic acid thermogram which was said to exhibit miscible behaviour; however, a very small peak can be observed just over 200°C. This is approximately the same temperature at which a small peak was observed for the 7% and 10% fluorene HA(F)-fluorene mixtures. This suggests a miscibility limit for fluorene in humic acid.

Again, the peaks at the end of the thermograms illustrated in Figures 5.5a-5.5c are insignificant due to exaggeration of small changes due to the low contaminant mass used to calculate the heat flow.

### 5.2.3 Fluorene on HA(A)

Figure 5.6 illustrates DSC thermograms describing HA(A)-fluorene interactions at concentrations of 3%, 7%, and 10%, respectively. For the 3% and 10% cases, the



**Figure 5.6** DSC Thermograms for Fluorene in HA(A). (a) 3% fluorene in HA(A). (b) 7% fluorene in HA(A). (c) 10% fluorene in HA(A).

melting point of fluorene coincides for the HA(A)-fluorene and glass-fluorene thermograms. A slight melting point depression was observed at 7%. It is unclear as to why only the 7% case showed the depression. This indicates that if any solid-solid interactions were occurring, they were very weak.

Weak fluorene vaporization curves were observed for all concentrations of HA(A)-fluorene. These peaks are much smaller than the glass-fluorene vaporization peaks, and become sharper and qualitatively more similar to the glass-fluorene mixture as the fluorene concentration increases from 3% to 10%. The presence of vaporization peaks suggests an immiscible system; however, the increasing sharpness of the peaks with increasing concentration may indicate that a miscible solution is being formed up to a certain concentration and that the residual fluorene is immiscible with the humic acid.

The increasing sharpness of the fluorene vaporization peaks with increasing fluorene concentration observed in the HA(A)-fluorene mixture is similar to the HA(F)-fluorene mixture. An approximate miscibility limit of 3% fluorene was observed in the HA(F)-fluorene mixture. The miscibility limit for the HA(A)-fluorene mixture is lower than 3%. Therefore, fluorene is likely more miscible in HA(F) than in HA(A).

#### 5.2.4 Constant Concentration of Fluorene on HA(ML), HA(F) and HA(A)

A 7% concentration of fluorene on HA(ML), HA(F) and HA(A) will be used to compare different interactions between fluorene and the respective humic acids. Figures 5.4b, 5.5b and 5.6b show DSC thermograms for 7% fluorene on HA(ML), HA(F) and HA(A), respectively.

Again, as seen in Figure 5.4b, no melting point depression was observed for 7% fluorene on HA(ML), thus indicating no solid-solid interactions. In comparison, only a very slight melting point depression can be observed in Figure 5.6b for the HA(A)-fluorene mixture, thus indicating very weak solid-solid interactions. Finally, for the case of HA(F)-fluorene, the onset of vaporization of fluorene occurs at approximately 112°C, which corresponds to a melting point depression of only 4°C. This indicates weak solid-solid interactions.

With respect to miscible/immiscible behaviour, fluorene and HA(ML) formed an immiscible mixture at the 7% fluorene concentration as can be observed from the distinct fluorene vaporization peak seen in Figure 5.4b. Immiscibility of HA(ML) and fluorene is further supported by the complete vaporization of fluorene from HA(ML) at a lower temperature than the complete vaporization of fluorene from glass beads. In comparison, 7% fluorene seems to exhibit limited miscibility with HA(F). This can be observed from the very small fluorene vaporization peaks observed in Figure 5.5b. These peaks are much smaller than the corresponding glass-fluorene vaporization peak, indicating vaporization of the residual immiscible fluorene fraction. Likewise, 7% fluorene seems to exhibit limited miscibility with HA(A), as observed from the small fluorene vaporization peak in Figure 5.6b. This peak is smaller than the corresponding glass-fluorene vaporization peak, but is larger than the fluorene vaporization peak observed for HA(F)-fluorene in Figure 5.5b. The larger size of this peak may indicate a larger residual immiscible fraction thus inferring a lower miscibility limit for fluorene in HA(A) compared to HA(F).

These results indicate that in terms of solid-solid interactions between the humic acids and fluorene, the strength of these interactions from weakest to strongest is: HA(ML), HA(A) and HA(F). Also, varying solubilities of fluorene in the humic acids were observed with the range of increasing solubility of fluorene as: HA(ML), HA(A) and HA(F). Both of these findings are consistent with those for the anthracene-humic acid cases.

### **5.3 Discussion of PAH and Humic Acid Results**

PAHs have been found to have enhanced partitioning in humic substances compared to other nonpolar organics due to the compatibility of the cohesive energy density or solubility parameters of PAHs with those of the aromatic components in humic substances (Chiou et al., 1988). Thus, chemical composition of the humic acid will have an appreciable effect on the interaction between a PAH and the humic acid.

Based on DSC results using a different soil with a different extraction technique, Maguire (1994) introduced the idea that humic acids form miscible mixtures with humic acid, but immiscible mixtures with fulvic acid and humin. Although this may be true in Maguire's study, the results of this study show that Maguire's findings cannot be generalized for different humic acid samples. First, humic acids and fulvic acid have been described as having a range of properties; therefore, they should also have a range of miscibility characteristics with PAHs. Second, the PAH itself has an effect on the interaction between the PAH and the different humic acids. Third, solubility limits seem

to exist for PAHs and humic acids. In the following sections, an attempt is made to explain the results in Figures 5.1 to 5.6 on the basis of these concepts.

### 5.3.1 Effect of Humic Acid Structure

Chemical characterization of HA(ML), HA(F), and HA(A) show that these humic acids are chemically different. The results of chemical characterization of these humic acids are shown in Chapter 4. Partially miscible to miscible characteristics are observed for PAHs with HA(A) and HA(F); whereas, immiscible characteristics are observed for HA(ML).

Chiou et al. (1998) suggested that the increased partitioning of PAHs into humic substances is due to compatibility between the aromatic nature of the PAH and the aromatic backbone of the humic acid. According to NMR analysis presented in Chapter 4, HA(ML) has a significantly larger aromatic concentration than HA(F) and HA(A). Therefore, one would initially suppose that partitioning should be greater in HA(ML) than in HA(F) and HA(A), which is contradictory to the results presented in this work. However, this apparent contradiction can be explained by the presence of polar functional groups.

Another factor that is important to note is that HA(ML) has a much higher concentration of polar functional groups. Ganaye et al. (1998) stated that differences in both aromaticity and polarity of soil organic matter could explain the differences in partitioning coefficients between humic substances and organic contaminants. The high polar functional group concentration in HA(ML) contributes to its hydrophilic nature,

which is not compatible with a nonpolar organic compound such as anthracene or fluorene. Chemical interactions, such as hydrogen bonds, between the functional groups of the humic acid increase the cross-linking in the macromolecular structure. Polar compounds are capable of disrupting these contacts; however, nonpolar compounds are unable to do so (Graber, 1998). Therefore, the large aromatic fraction of HA(ML) may be inaccessible to the PAHs due to the large concentration of polar functional groups. Consistent with this theory, HA(F) and HA(A) show increased interactions between PAH and humic acid both in terms of solid-solid interactions and solubility of PAH in humic acid. The less polar nature of these humic acids allow for increased interaction between the humic acid and the PAH.

Maguire (1994) suggested that PAHs form miscible mixtures with humic acids and immiscible mixtures with fulvic acids. This work did not investigate the effect of polarity of the humic substance on thermal interactions with PAHs. Neither chemical nor structural analysis were completed on Maguire's humic and fulvic acids; however, in general, it is known that fulvic acids have a characteristically higher total acidity than humic acids. Therefore, it can be inferred from the work of Maguire (1994) that increased polarity of the humic substance may decrease the miscibility of a PAH in a humic substance. This would be consistent with the results found in the present study.

### 5.3.2 Effect of PAH Structure

The PAH itself has an effect on the interactions between HA(F) and HA(A). Anthracene displayed more interactions than fluorene with HA(F) and HA(A) both in



terms of solid-solid interactions and increased solubility. Anthracene has a higher molecular weight than fluorene; however, its physical structure may make it more compatible with humic acid. Anthracene consists of three condensed aromatic rings thus creating a planar molecule. Fluorene on the other hand, consists of two planar aromatic rings covalently bonded at the 1 and 2 carbon positions, plus a CH<sub>2</sub> group. Due to the tetrahedral bonding shape of carbon, this results in a more kinked and irregular molecule. Therefore, the planar molecule may have easier access to humic acid than the kinked molecule. This is supported by Chiou et al. (1998) who stated that the enhanced partitioning ability of PAHs with organic matter could be attributed to their planar molecule structures which allow them to gain a closer approach to the aromatic components of the humic substance or to enhance their mutual attractions through  $\pi$ - $\pi$  interactions.

### 5.3.3 Effect of PAH Concentration

Finally, the concentration of PAH has an effect on the interaction between PAHs and humic acids. Solubility limits are observed above which the mixture becomes immiscible. This is consistent with the rubbery/glassy model. According to this model, partitioning occurs first in the rubbery section of the humic acid and the remaining portion may interact physically with the glassy section (Xing and Pignatello, 1997).

## 5.4 Dodecane on Humic Acids

Figures 5.7 and 5.8 show the DSC thermograms obtained for HA(ML) and HA(F) contaminated with 3%, 7% and 10% by mass dodecane. Duplicate or triplicate runs of the humic acid-contaminant mixtures are illustrated on each graph as solid lines and glass-dodecane curves are shown as dotted lines. Each HA-dodecane curve is compared to the equivalent glass-dodecane curve in which no interaction between the glass beads and the dodecane is assumed to occur.

### 5.4.1 Dodecane on HA(ML)

Figure 5.7 shows DSC thermograms obtained for 3%, 7% and 10% dodecane on HA(ML). Obviously, these thermograms show no melting peaks since dodecane is a liquid at room temperature.

A distinct vaporization peak is observed for all concentrations of dodecane on HA(ML). This indicates an immiscible dodecane-HA(ML) system. However, this vaporization peak exhibits much different behaviour than glass-dodecane.

The vaporization peak of pure dodecane on glass-dodecane is a uniform endothermic peak showing no sign of an exotherm indicating decomposition of dodecane. For all concentrations of dodecane on HA(ML), an exothermic reaction is observed as a positive deviation from the vaporization endotherm, thus indicating decomposition of dodecane. For the 3% dodecane case in Figure 5.7a, this endothermic reaction occurs consistently at 129°C for all runs. This repeatability is not observed for the 7% or the

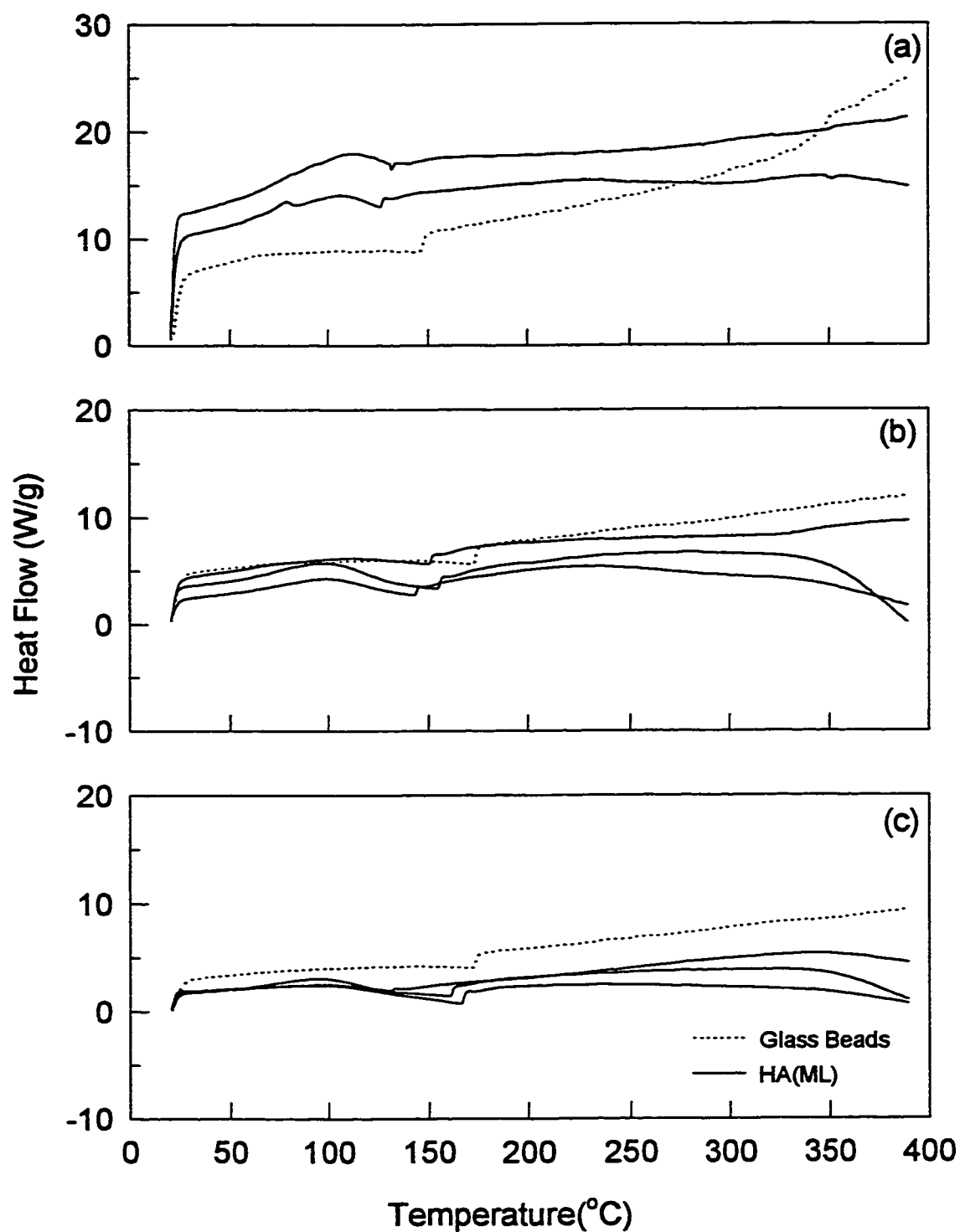


Figure 5.7 DSC Thermograms for Dodecane in HA(ML). (a) 3% dodecane in HA(ML). (b) 7% dodecane in HA(ML). (c) 10% dodecane in HA(ML).

10% case. These positive deviations from the vaporization endotherm for three different trials occur at 146°C, 154°C, and 157°C for 7% dodecane and at 132°C, 160°C and 168°C for 10% dodecane. The lack of repeatability of the location of these exothermic reactions is possibly due to the heterogeneous nature of the humic acid.

These exothermic reactions occur at temperatures much higher than the flash point temperature of dodecane (71°C), which indicates auto-oxidation of dodecane in the presence of O<sub>2</sub>. This eliminates the possibility that auto-oxidation of dodecane was occurring due to the presence of residual O<sub>2</sub> in the void space of the sealed crucible.

These exothermic reactions likely occur due to decomposition of the dodecane. HA(ML) is relatively polar due to its high concentration of polar functional groups. Because dodecane, C<sub>12</sub>H<sub>26</sub>, is a non-polar straight chain aliphatic, it is incompatible with the polar functional groups of HA(ML). This incompatibility could cause instability in the dodecane molecule causing it to decompose at lower temperatures.

#### 5.4.2 Dodecane on HA(F)

Figure 5.8 shows DSC thermograms for 3%, 7%, and 10% dodecane on HA(F) respectively. The results for HA(F)-dodecane are significantly different from those for HA(ML)-dodecane mixtures. Small dodecane vaporization peaks are observed for the 3% dodecane on HA(F) case. As the concentration is increased to 7% and 10%, the vaporization peaks become sharper and approach the shape of the glass-dodecane curve. Because lack of a distinct vaporization peak indicates a miscible mixture, it appears that dodecane is partially miscible in HA(F). As the concentration of dodecane increases, the

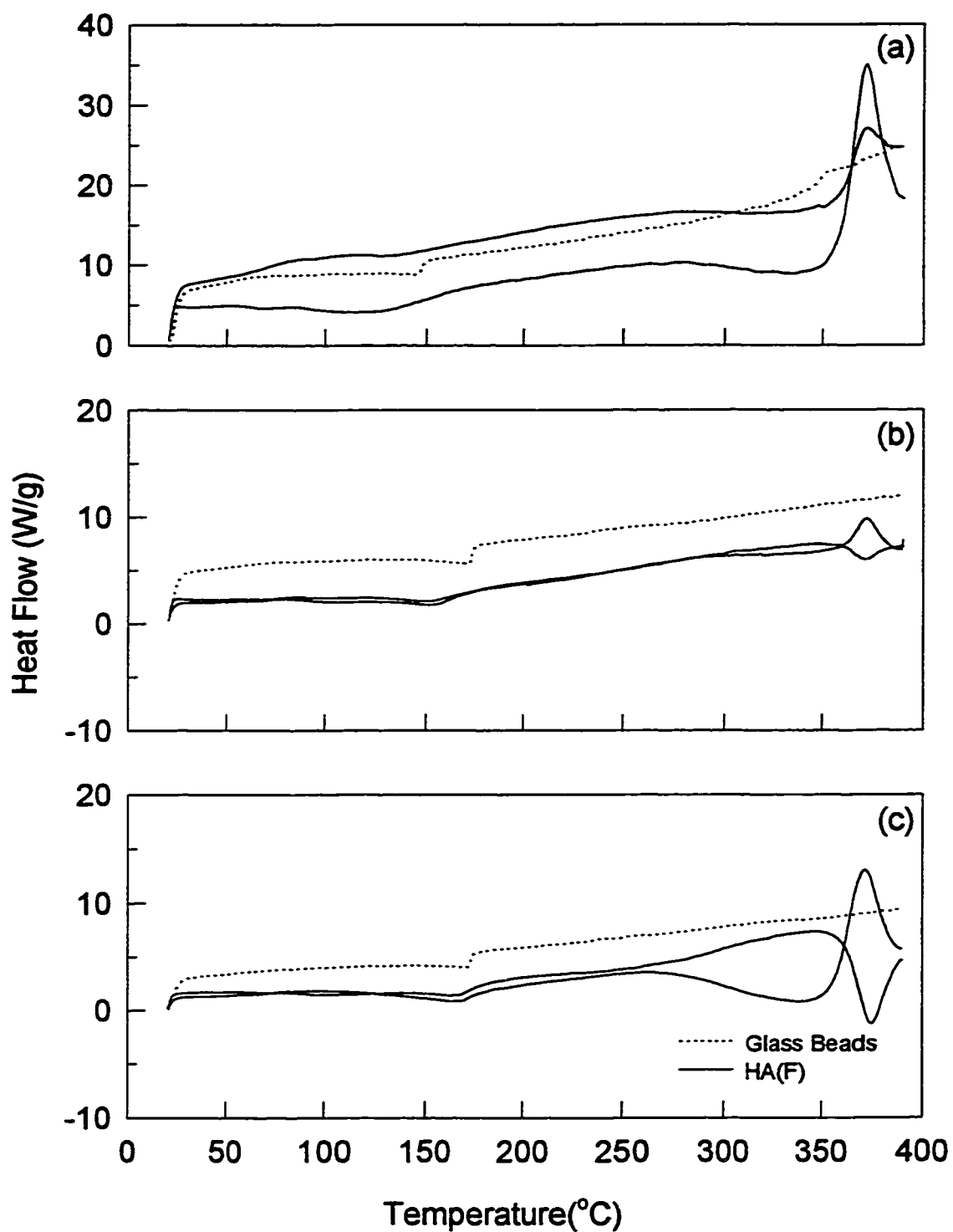


Figure 5.8 DSC Thermograms for Dodecane in HA(F). (a) 3% dodecane in HA(F). (b) 7% dodecane in HA(F). (c) 10% dodecane in HA(F).

presence of sharper vaporization peaks indicates immiscibility. Therefore, the miscibility limit is likely just under 3% dodecane.

It is also important to note that no exothermic decomposition of the dodecane occurs in the HA(F)-dodecane mixture. Because HA(F) is more hydrophobic in nature, due to its lower concentration of polar functional groups as compared to HA(ML), dodecane is more compatible with HA(F) than HA(ML) and therefore is more stable. For this reason, it is not surprising to see a partially miscible system between dodecane and HA(F).

#### 5.4.3 Constant Concentration of Dodecane on HA(ML) and HA(F)

A 7% concentration of dodecane on HA(ML) and HA(F) will be used to compare different interactions between dodecane and the respective humic acid. Figures 5.7b and 5.8b show DSC thermograms for 7% dodecane on HA(ML) and HA(F), respectively.

As seen in Figure 5.7b, distinct endothermic peaks are observed for the vaporization of 7% dodecane from HA(ML), thus indicating an immiscible system. In comparison, as seen in Figure 5.8b, dodecane vaporization peaks can also be observed on the 7% dodecane-HA(F) thermograms. However, these vaporization peaks are much smaller than the dodecane peak for the respective 7% dodecane-glass case. This suggests partial miscibility between dodecane and HA(F).

As explained previously, decomposition of dodecane was detected as determined by the small exothermic reactions observed during the vaporization process in Figure 5.7b. This decomposition occurred despite the fact that no decomposition was observed

in pure dodecane in the temperature range studied. In comparison, decomposition of dodecane was not observed in the HA(F)-dodecane mixture as shown in Figure 5.8b.

These results indicate that, first, the more favourable interactions between HA(F) and dodecane compared to HA(ML) and dodecane create a partially miscible system which does not destabilize the dodecane molecule. Second, incompatibility between HA(ML) and dodecane creates an immiscible system and destabilizes the dodecane molecule causing decomposition at an earlier temperature.

## **5.5 Hexadecane on Humic Acid**

Figures 5.9 and 5.10 show the DSC thermograms obtained for HA(ML) and HA(F) contaminated with 3%, 7% and 10% by mass hexadecane. Duplicate runs of the humic acid-contaminant mixtures are illustrated as solid lines and glass-hexadecane curves are shown as dotted lines. Each humic acid-hexadecane curve is compared to the equivalent glass-hexadecane curve in which no interaction between the glass beads and the hexadecane is assumed to occur.

### **5.5.1 Hexadecane on HA(ML)**

Figure 5.9 shows DSC thermograms obtained for 3%, 7% and 10% hexadecane on HA(ML). Again, no melting peaks are observed on the thermograms as the melting point of hexadecane is below room temperature.

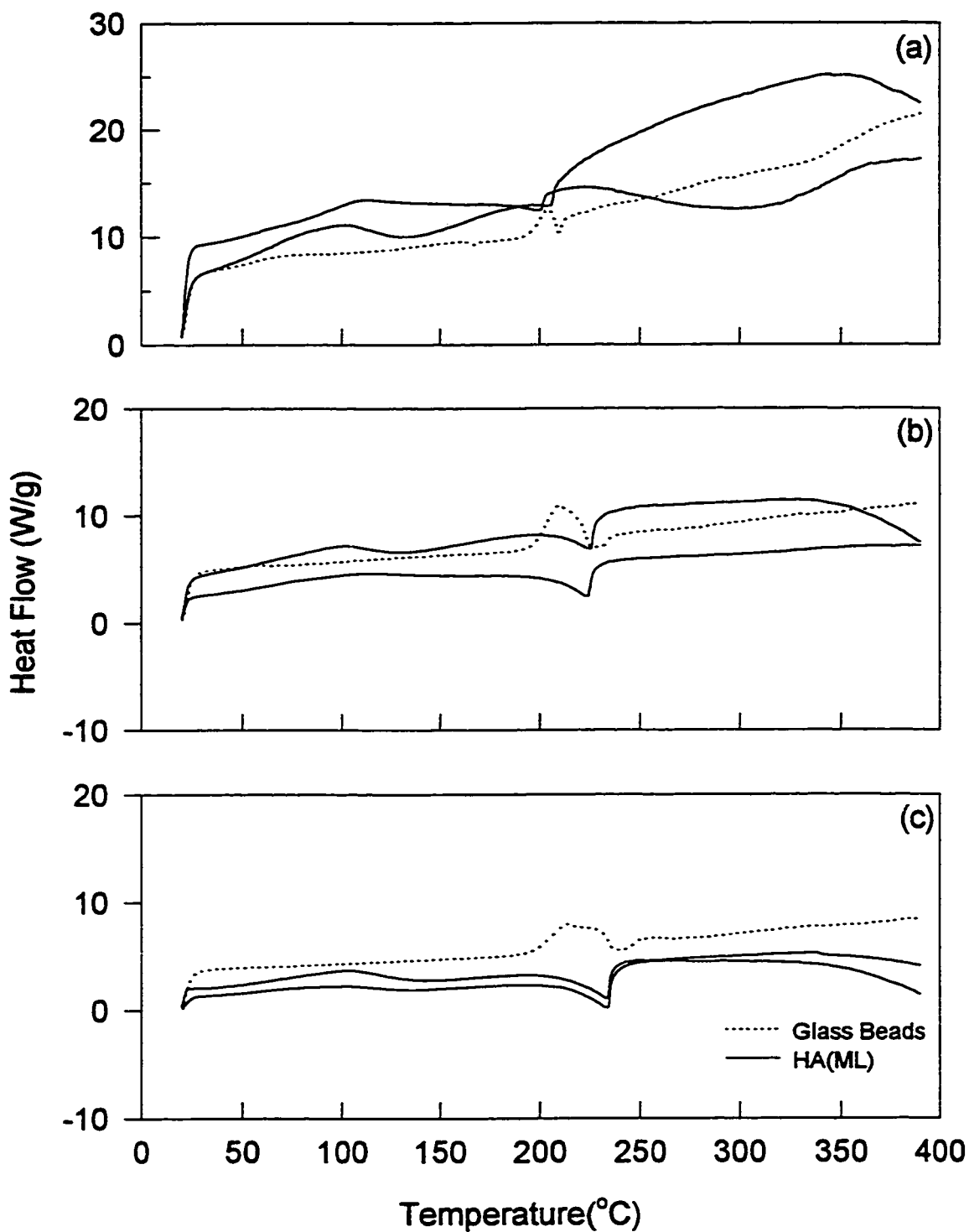


Figure 5.9 DSC Thermograms for Hexadecane in HA(ML). (a) 3% hexadecane in HA(ML). (b) 7% hexadecane in HA(ML). (c) 10% hexadecane in HA(ML).



Decomposition of pure hexadecane on glass beads can be observed as an exothermic peak for all equivalent concentrations of hexadecane on glass. Each thermal event is characterized by an initial exothermic peak followed by an endothermic peak. The first is likely due to exothermic decomposition and the second is likely a vaporization peak. The ranges of the exothermic peaks are 196-212°C, 198-230°C, and 194-242°C for 3%, 7%, and 10% equivalent weights of hexadecane on glass, respectively. The ranges of the endothermic peaks are 212-214°C, 230-240°C, and 242-259°C for 3%, 7%, and 10% equivalent weights of hexadecane on glass, respectively.

For some reason, the decomposition of hexadecane is less pronounced when it is associated with HA(ML). This contradicts the original assumption for dodecane on HA(ML) which suggested that the polar functional groups destabilized the dodecane molecule. In the case of HA(ML)-hexadecane, HA(ML) appears to stabilize the hexadecane molecule. This is unexpected since hexadecane is similar in structure to dodecane with four extra bonded carbons.

#### 5.5.2 Hexadecane on HA(F)

Figure 5.10 shows DSC thermograms for 3%, 7%, and 10% hexadecane on HA(F). No decomposition of the hexadecane can be observed in any thermogram describing HA(F)-hexadecane interactions. Thus, HA(F) seems to stabilize the hexadecane molecule. This is to be expected since the hydrophobic nature of the HA(F) would lead to favourable interactions between HA(F) and hexadecane. Only small vaporization peaks can be observed for the 3% hexadecane case. These peaks become

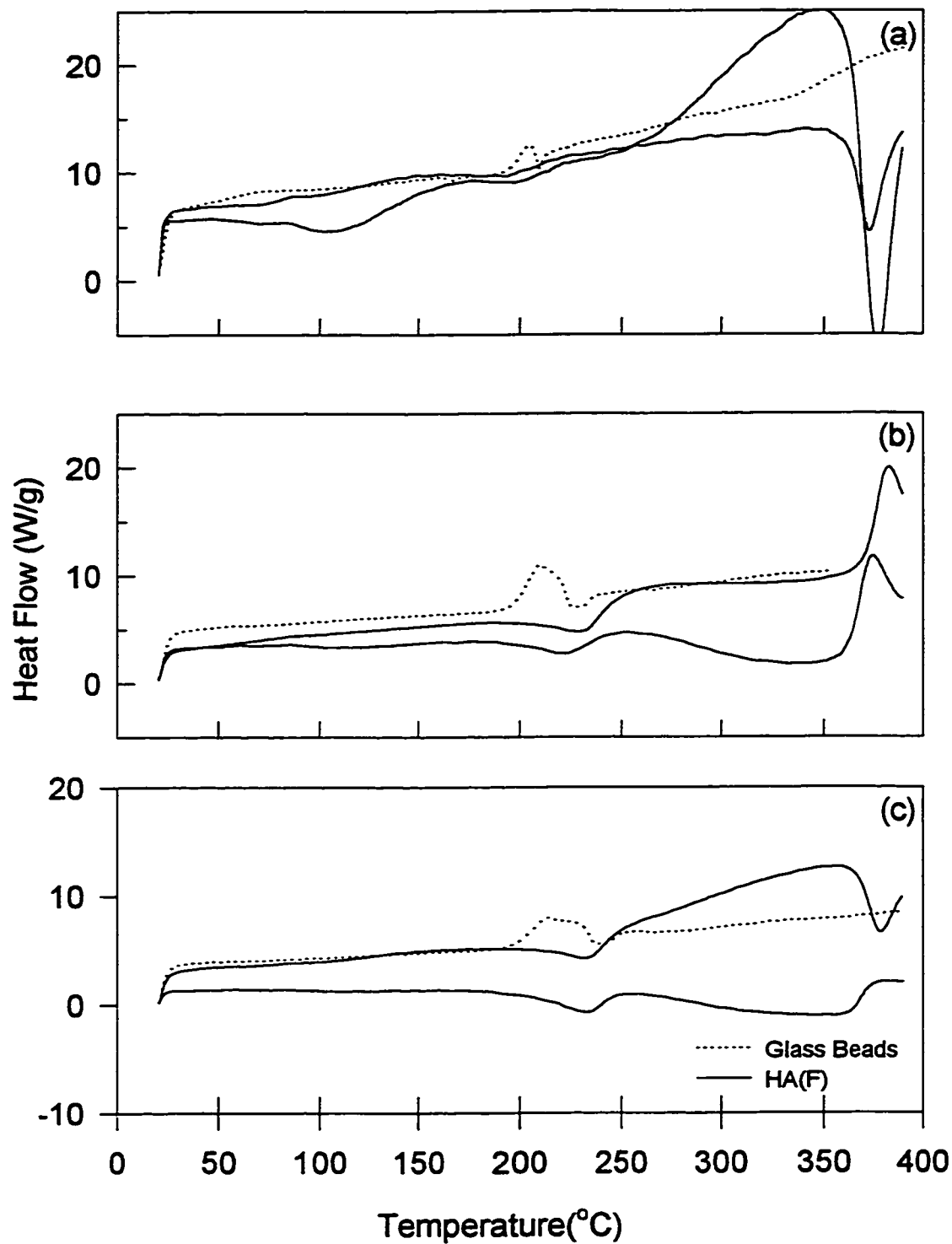


Figure 5.10 DSC Thermograms for Hexadecane in HA(F). (a) 3% hexadecane in HA(F). (b) 7% hexadecane in HA(F). (c) 10% hexadecane in HA(F).

much larger at 7% and 10% hexadecane concentration. This suggests that the 7% and 10% concentrations are forming immiscible mixtures with HA(F). The miscibility limit may have just been reached at the 3% hexadecane concentration as observed by the very small vaporization peak.

Again, the large peaks observed at the ends of the thermograms in Figures 5.10a-5.10b are considered insignificant due to the exaggeration of small changes due to the low contaminant mass used to calculate the heat flow.

### 5.5.3 Constant Concentration of Hexadecane on HA(ML) and HA(F)

A 7% concentration of hexadecane on HA(ML) and HA(F) will be used to compare different interactions between hexadecane and the respective humic acid. Figures 5.9b and 5.10b show DSC thermograms for 7% hexadecane on HA(ML) and HA(F), respectively.

Figure 5.9b shows the DSC thermogram for a 7% hexadecane HA(ML)-hexadecane mixture. An immiscible HA(ML)-hexadecane system is observed by the distinct hexadecane vaporization peak. As mentioned previously, no decomposition of HA(ML) in the HA(ML)-hexadecane system was observed, although decomposition of hexadecane in the pure form on glass beads did show a large exothermic peak indicating decomposition of the hexadecane. The same phenomenon is observed for the 7% hexadecane-HA(F) system illustrated in Figure 5.10b. A distinct vaporization peak indicates an immiscible system, but the lack of a decomposition peak indicates stabilization of the hexadecane molecule on HA(F).

When comparing the 7% hexadecane-HA(ML) system to the 7% hexadecane-HA(F) system, the vaporization peaks seem larger in the case of hexadecane-HA(ML). This may indicate that hexadecane has a slightly higher partial solubility in HA(F) compared to HA(ML). This is reasonable to expect due to the larger aliphatic fraction of HA(F).

## **5.6 Discussion of Straight Chain Aliphatic and Humic Acid Results**

Different interactions are expected for aliphatic hydrocarbons on humic acids compared to PAHs on humic acids. Aliphatic hydrocarbons are thought to have less favourable partitioning characteristics than PAHs due to their lower solubility parameters (Chiou et al., 1998). As in the case of PAHs and humic acids, the humic acid-aliphatic mixture results will be discussed in terms of the effect of humic acid structure, the effect of contaminant structure and the effect of concentration.

### **5.6.1 Effect of Humic Acid Structure**

Like HA(ML)-PAH mixtures, immiscible behaviour was observed for both dodecane and hexadecane on HA(ML). This is explained in terms of the high polarity of HA(ML) compared to HA(F) and HA(A). Dodecane appeared to be very incompatible with HA(ML). The high polarity of the humic acid seemed to reduce the thermal stability of the dodecane molecule. It is interesting, however, that the same effect was not observed for hexadecane. Although hexadecane showed decomposition in the pure form

on glass beads, association with HA(ML) seemed to stabilize this molecule. It is difficult to confirm thermal decomposition of the contaminant as the products of these reactions could not be analyzed and/or quantified.

NMR analysis in Chapter 4 shows that HA(F) has a large aliphatic section (72% by mass of total organic carbon) compared to HA(ML) (31% by mass of total organic carbon). Therefore, it is expected that HA(F) would have more favourable interactions with aliphatic hydrocarbons. HA(F) seemed to stabilize the aliphatic molecule since no exothermic peaks were observed during decomposition. As well, smaller peaks were observed for both dodecane and hexadecane on HA(F) compared to HA(ML) indicating the possibility of limited miscibility of the aliphatic in the less polar HA(F).

#### 5.6.2 Effect of Aliphatic Structure

Both dodecane and hexadecane are long chain aliphatic hydrocarbons having carbon chain lengths of 12 and 16, and molecular weights of 170 and 226 kg/kmol, respectively. Chiou et al. (1998) stated that there is a significant reduction in solubility of nonPAH, nonpolar solutes in humic substances with increasing solute molecular weight. Dodecane and hexadecane both formed immiscible mixtures with HA(ML) and displayed limited miscibility up to an aliphatic concentration of 3% with HA(F). However, it is difficult to determine the relative extent of solubility of these two compounds in humic acid using these experiments.

### 5.6.3 Effect of Aliphatic Concentration

Like the PAH-humic acid mixtures, aliphatic solubility limits in humic acid were observed, particularly in the HA(F)-aliphatic mixtures.

## **5.7 O-chlorophenol on Humic Acids**

Figures 5.11 and 5.12 show the DSC thermograms obtained for HA(ML) and HA(F) contaminated with 3% and 7% by mass o-chlorophenol. Repeated runs of the humic acid-contaminant mixtures are illustrated as solid lines. Glass-o-chlorophenol curves are shown as dotted lines. Each humic acid-o-chlorophenol curve is compared to the equivalent glass-o-chlorophenol curve in which no interaction between the glass beads and the o-chlorophenol is assumed to occur. Melting peaks are not observed for o-chlorophenol mixtures as o-chlorophenol is a liquid at room temperature.

### 5.7.1 O-chlorophenol on HA(ML)

Figures 5.11 shows DSC thermograms obtained for 3% and 7% o-chlorophenol on HA(ML). Repeatable results for 3% o-chlorophenol-HA(ML) were not obtainable in the four trials. This could be due to the heterogeneous nature of the humic acid and the low concentration of o-chlorophenol. Repeatable results were obtained, however, for the 7% chlorophenol. In this case, large vaporization peaks were obtained indicating immiscible behaviour between the o-chlorophenol and the humic acid. As well, complete

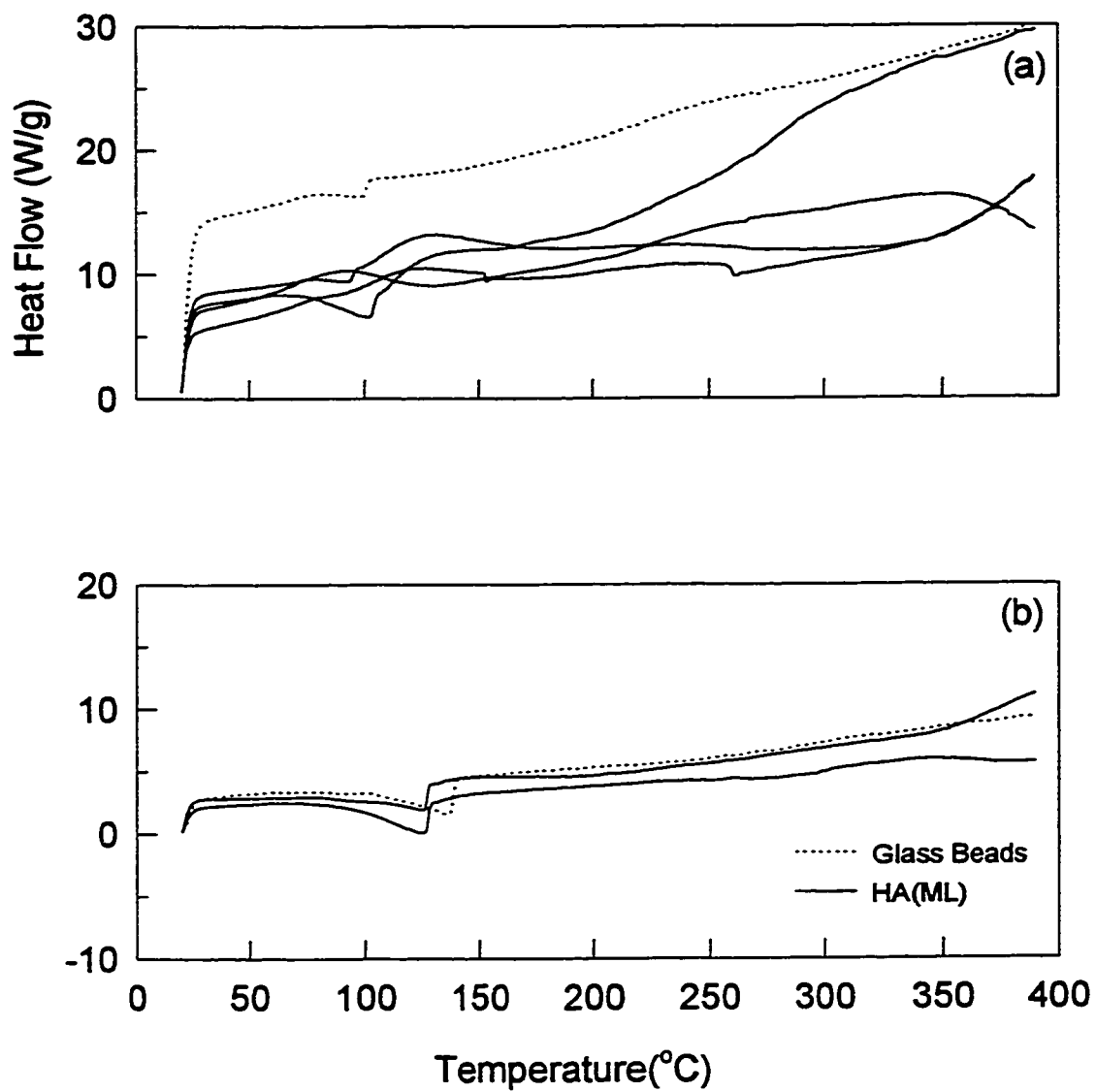


Figure 5.11 DSC Thermograms for O-chlorophenol in HA(ML). (a) 3% o-chlorophenol in HA(ML). (b) 7% o-chlorophenol in HA(ML).

vaporization of o-chlorophenol in HA(ML)-o-chlorophenol occurs before complete vaporization of o-chlorophenol in glass-o-chlorophenol. Complete vaporization of 7% o-chlorophenol occurs at 128°C and 143°C for HA(ML)-o-chlorophenol and glass-o-chlorophenol, respectively. The complete vaporization of o-chlorophenol from the HA(ML)-o-chlorophenol mixture before complete vaporization of pure o-chlorophenol also supports immiscibility.

### 5.7.2 O-chlorophenol on HA(F)

Figure 5.12 shows DSC thermograms obtained for 3% and 7% o-chlorophenol on HA(F). For the case of 3% o-chlorophenol, no obvious vaporization peak can be observed. This indicates miscible interactions between HA(F) and o-chlorophenol. As the concentration increases to 7% o-chlorophenol, small vaporization curves can be observed. This suggests that o-chlorophenol forms a miscible mixture with HA(F) up to a concentration of approximately 3%, after which an immiscible mixture is formed.

### 5.7.3 Constant Concentration of O-chlorophenol on HA(ML) and HA(F)

A 7% concentration of o-chlorophenol on HA(ML) and HA(F) will be used to compare different interactions between o-chlorophenol and the respective humic acid. Figures 5.11b and 5.12b show DSC thermograms for 7% o-chlorophenol on HA(ML) and HA(F), respectively.



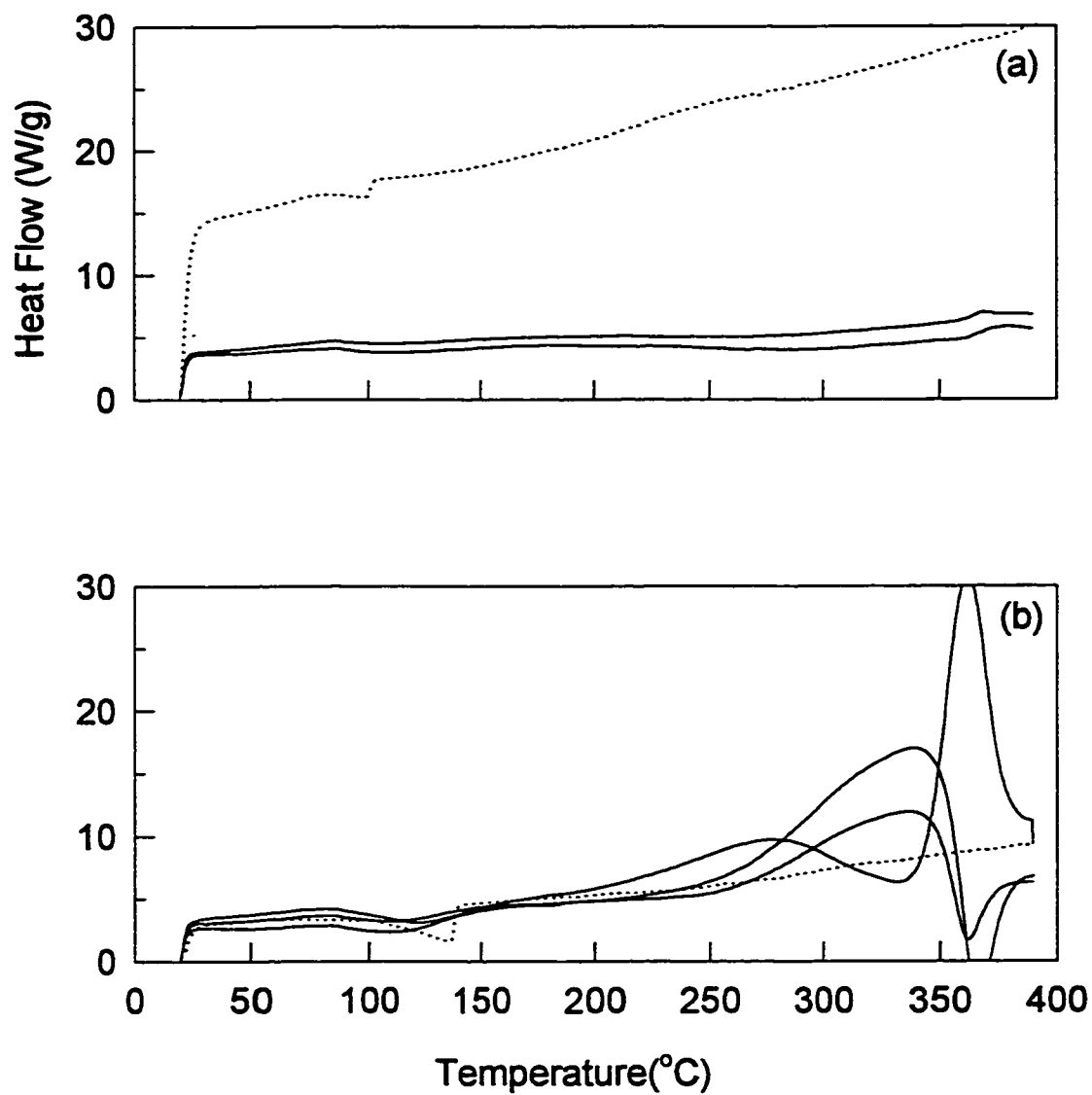


Figure 5.12 DSC Thermograms for O-chlorophenol in HA(F). (a) 3% o-chlorophenol in HA(F). (b) 7% o-chlorophenol in HA(F).

As seen in Figure 5.11b, 7% o-chlorophenol forms an immiscible mixture with HA(ML). This is evident from the distinct o-chlorophenol vaporization peaks which indicate complete vaporization of o-chlorophenol from the HA(ML) before complete vaporization of o-chlorophenol from the glass beads. In comparison, only small o-chlorophenol peaks were observed in Figure 5.12b which shows DSC thermograms for 7% o-chlorophenol on HA(F). These vaporization peaks are much smaller than the respective 7% equivalent o-chlorophenol. This suggests that o-chlorophenol exhibits limited miscibility in HA(F).

Thus, these results indicate that o-chlorophenol has a higher solubility in HA(F) than HA(ML).

## **5.8 Discussion of Polar Organic and Humic Acid Results**

Previously it was stated that the accessibility of nonpolar compounds to the aliphatic and aromatic regions of the humic acid macromolecule was limited since these compounds were unable to disrupt polar linkages within the molecule (Grabber, 1998). Conversely, Grabber (1998) stated that polar molecules were able to disrupt cross-linkages in the humic material thus allowing polar interactions between the polar compound and the humic material. This suggests that the interaction between o-chlorophenol and HA(ML) should be stronger than the interaction between HA(ML) and PAHs or aliphatic hydrocarbons due to the formation of hydrogen bonds between polar functional groups. However, like PAH-HA(ML) and aliphatic-HA(ML), immiscible behaviour was observed between o-chlorophenol and HA(ML).

As well, the ability of o-chlorophenol to form hydrogen bonds with polar functional groups also suggests that the interaction between o-chlorophenol and HA(ML) should be stronger than the interaction of o-chlorophenol with HA(F). Instead of a strong interaction with HA(ML), o-chlorophenol exhibited immiscible behaviour with HA(ML) and miscible behaviour with HA(F).

Therefore, it seems that o-chlorophenol did not disrupt polar linkages in HA(ML) to form its own linkages. This may be due to the short time between contamination of HA(ML) with o-chlorophenol and the DSC runs. These samples were run on the DSC immediately after contamination due to the relatively high vapour pressure of o-chlorophenol.

There are two possible explanations for the miscibility with HA(F). First, because o-chlorophenol is a much smaller molecule than the other contaminants presented in this study, its small size could have lead to favourable interactions between o-chlorophenol and HA(F). Second, although it has been emphasized that HA(ML) has a much higher polar functional group concentration, HA(F) still has 13% by mass of its total organic carbon in polar functional groups, as discussed in Chapter 4. Because this number is lower than the 40% by mass polar functional groups in HA(ML), there may be less cross-linking in HA(F) compared to HA(ML). Therefore, the polar functional groups in HA(F) may be accessible to o-chlorophenol for hydrogen bonding.

## 5.9 Cooling Thermograms

In order to confirm that all of the contaminant in the contaminant-humic acid mixture had been completely removed during the DSC vaporization process, corresponding crystallization thermograms were completed using a DSC program which decreased the temperature from 390°C to 60°C using a cooling rate of 10°C/min. It was reasoned that if any contaminant remained in the mixture, it should recrystallize at the same temperature as the contaminant melting point, as determined in the DSC heating thermogram (Maguire, 1994).

Figure 5.13 shows some examples of cooling thermograms for fluorene on HA(F) and HA(ML). As seen in this figure, no peak representing recrystallization of fluorene can be observed, thus indicating complete removal of the contaminant.

## 5.10 Summary

The results presented clearly indicate that the type of contaminant, concentration of the contaminant and the type of humic acid all have an effect on the interaction between the contaminant and the humic acid.

In general, it was found that all of the contaminants investigated formed immiscible mixtures with HA(ML). The NMR results presented in Chapter 4 showed that HA(ML) had a high concentration of polar functional groups and, therefore, the hydrophilic nature of this humic acid was incompatible with the highly hydrophobic PAH and aliphatic contaminants. Strong interactions between PAHs and humic acids are

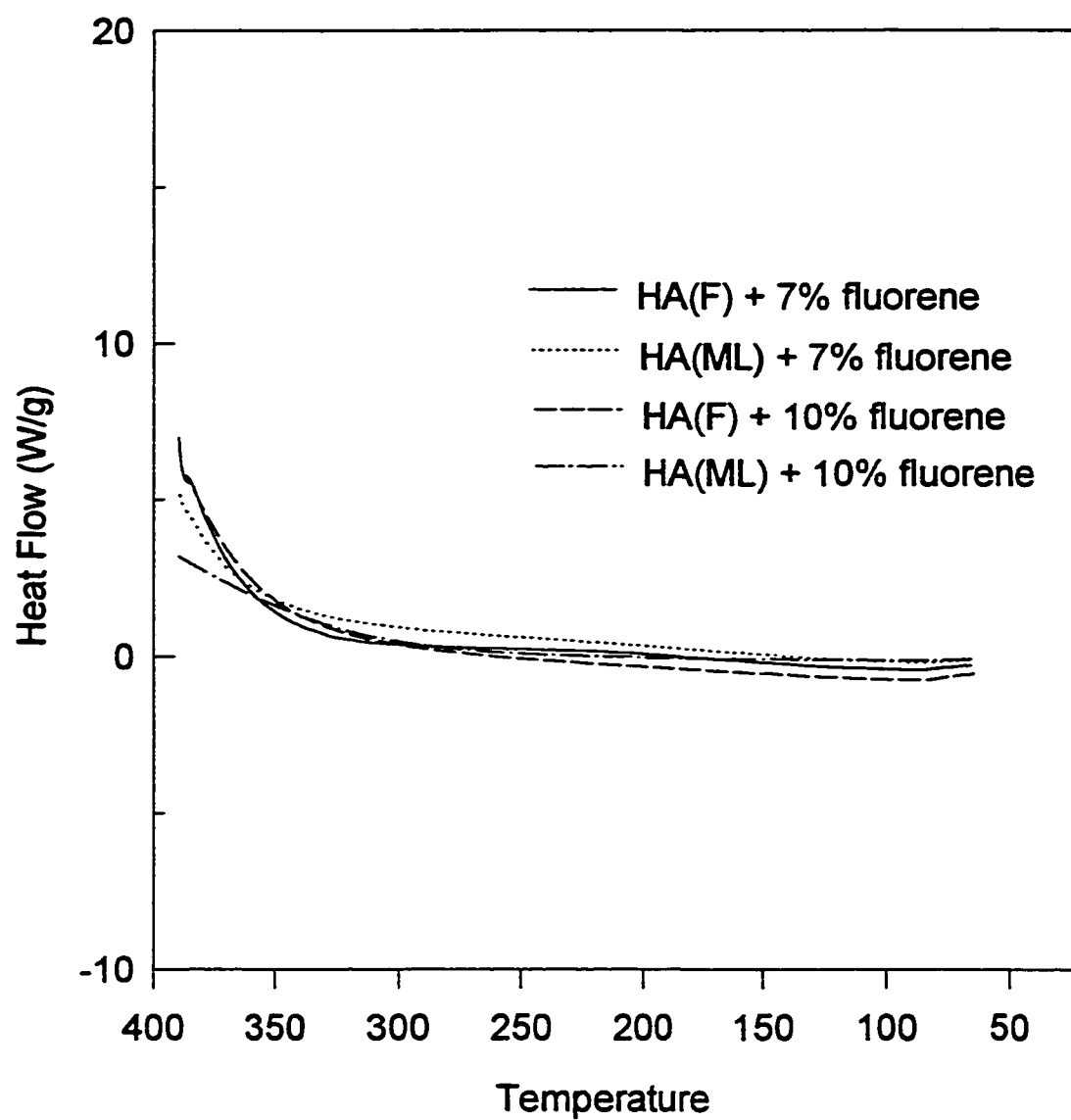


Figure 5.13 DSC Cooling Thermograms

expected due to compatibility between the aromatic structure of the PAH and aromatic components of humic acid. However, the high concentration of polar functional groups in HA(ML) seemed to prevent access of the PAHs to the aromatic regions of HA(ML).

The same effect of the polar functional groups was observed for the aliphatic contaminants. The incompatibility between the polar functional groups and the dodecane was observed by the destabilization of the dodecane molecule when associated with HA(ML).

It was surprising that HA(ML) also formed an immiscible mixture with o-chlorophenol since it was expected that hydrogen bonds could be formed between the contaminant and the polar functional groups of HA(ML). This result suggests that the polar groups of HA(ML) are interacting with each other forming cross-linkages which could not be broken by the o-chlorophenol molecule.

Both HA(F) and HA(A) formed miscible to partially miscible mixtures with the contaminants investigated in this study. NMR analysis of HA(F) and HA(A) indicated that these commercial humic acids had a much lower concentration of polar terminal functional groups compared to HA(ML). Therefore, although the aromatic component of HA(F) was smaller than that of HA(ML), accessibility of the PAHs to these site was greater in HA(F) due to the lower concentration of polar functional groups. The strong interactions between PAHs and the aromatic components in HA(F) and HA(A) can be observed from the solid-solid interactions which occurred in the HA(F)-PAH and HA(A)-PAH mixtures, which were not observed for the other contaminants.

Limited miscibility between HA(F) and the aliphatic hydrocarbons, namely dodecane and hexadecane, was suggested from the slightly smaller aliphatic vaporization

curves when associated with HA(F) compared to glass beads. Although HA(F) had a very large aliphatic component, solubility of these aliphatic contaminants into the aliphatic regions of HA(F) was limited due to the large size of the contaminants.

Finally, o-chlorophenol exhibited a relatively large solubility in HA(F). This was likely due to the small size of the molecule and due to interactions between the polar contaminant and the accessible polar functional groups in HA(F) due to limited cross-linking in HA(F).

The results for HA(ML) do not support the findings of Maguire (1994) who discovered that PAHs formed miscible mixtures with humic acids. However, the results for HA(F) and HA(A) show limited miscibility to immiscible behaviour with the contaminants investigated. The results presented here do not dispute Maguire's findings, but merely emphasize the importance of the effect of humic acid structure on the interaction between humic acids and organic contaminants.

## CHAPTER 6

### CONCLUSIONS AND RECOMMENDATIONS

#### 6.1 Conclusions

Due to the unique behaviour between PAHs and humic acid, the effect of humic acid structure, contaminant structure and contaminant concentration on the interactions between organic contaminants and humic acid were studied. This work was an extension of the work of Maguire (1994) performed in our laboratory, who had investigated the interactions between PAHs and humic acid, fulvic acid and humin, and proposed that whereas fulvic acid and humin formed immiscible mixtures with PAHs, humic acid formed miscible mixtures with these compounds. The miscible behaviour between humic acids and PAHs has implications on the temperature and time requirements for a thermal desorption process.

Differential scanning calorimetry (DSC) tests were completed on binary mixtures of three humic acids (HA(ML), HA(F) and HA(A)) and three different types of contaminants (PAH, aliphatic hydrocarbon and polar organic). Specifically, anthracene and fluorene were used as PAHs, dodecane and hexadecane were used as aliphatic hydrocarbons and o-chlorophenol was used as a polar organic. DSC thermograms of the contaminant-humic acid mixtures were compared to the equivalent concentration of contaminant on glass beads, thus taking into account the effects of pre-boiling vaporization due to the small mass of contaminant which caused shifts in the location of



the vaporization peak depending on concentration. Although repeatability of the DSC thermograms was not very good in term of the heat flow measurements, in general, repeatability was good in terms of the shape, size and location of the contaminant vaporization peaks.

Chemical characterization was completed on the humic acids used in this study. Chemical functional group analysis showed that total acidity increased from HA(A) to HA(F) to HA(ML). NMR analysis was performed on HA(ML) and HA(F) which showed that 40% by mass of the total organic carbon in HA(ML) occurred as polar terminal functional groups, compared to 13% in HA(F). According to Senesi and Chen (1989) similar results are expected for HA(A) as HA(F). These results lead to the conclusion that HA(ML) is much more hydrophilic in nature than HA(F) and HA(A).

HA(ML) formed immiscible mixtures with all of the contaminant investigated in this study. This lead to the conclusion that the large concentration of polar functional groups was inhibiting access of the non-polar contaminants, specifically PAHs and aliphatic hydrocarbons, to the aromatic and aliphatic sections of HA(ML), with which these contaminants could interact. Despite the polar nature of o-chlorophenol, which was expected to be capable of hydrogen bonding with HA(ML), immiscible mixtures of HA(ML) and o-chlorophenol were formed. This was likely due to high cross-linking in the HA(ML) molecule which could not be broken by o-chlorophenol.

Very strong interactions existed between PAHs and HA(F) and HA(A) due to the accessibility of the PAHs to the aromatic section of the humic acid molecule. This was concluded from the strong solid-solid interactions along with the limited miscibility to miscible behaviour between the PAHs and HA(F) and HA(A). The aliphatics used in this

study had only limited solubility in HA(F) due to their large size. Finally, although HA(F) was emphasized to have a low concentration of polar functional groups, the small amount present are capable of interacting with polar organics. The lack of polar functional groups in HA(F) likely results in decreased cross-linking making these groups more accessible for bonding.

The conclusions presented here do not always support the findings of Maguire (1994) who stated that PAHs form miscible mixtures with humic acid and immiscible mixtures with fulvic acid and humin. Maguire's findings cannot be disputed by these conclusions since chemical characterization of Maguire's humic fractions was not completed. The emphasis in this work was the importance of the effect of humic acid structure on the interaction between humic acids and different organic contaminants.

One consistency between this work and the work of Maguire (1994) is the effect of decreasing solubility of non-polar contaminants with increasing polarity of the humic material. Although the polarity of Maguire's humic fractions was not determined, it is known, in general, that fulvic acid has a characteristically higher total acidity than humic acids. HA(ML) in this work behaved similarly to fulvic acid in Maguire's work, whereas HA(F) and HA(A) exhibited behaviour similar to the humic acid used in Maguire's work.

Whereas in Maguire (1994), for the case of simplicity, only completely miscible and completely immiscible systems were considered, the concept of limited solubility of the contaminants in humic acid was also introduced in this thesis. It was also concluded that the different types of contaminants (PAHs, aliphatic hydrocarbons and polar organic) interact differently with humic acid. As well, the structure of the individual contaminant

with the give classification of contaminants also interacts differently with a given humic acid.

## **6.2 Significance of Results to the Thermal Desorption Process**

The results presented here have significance to the application of thermal desorption. First, information is given which indicates the temperatures needed to effectively remove a given organic contaminant from soil, depending on whether it forms a miscible or immiscible mixture with humic acid. In an immiscible system, contaminants may be removed at temperatures lower than the pure component boiling point. In comparison, temperatures higher than the pure contaminant boiling point may be required to effectively remove the organic contaminant from the soil.

As well, this thesis provides information concerning the prediction of the formation of miscible, partially miscible or immiscible mixtures of organic contaminants and humic acid based on the structure of the humic acid. In general, it was determined that as the polarity of the humic acid increases, the solubility of non-polar organic contaminants in the humic acid decreases. Thus, if predictions can be made concerning the solubility of the contaminant in humic acid, then an effective temperature for the thermal desorption process can also be predicted.

### 6.3 Recommendations

All soils contain a certain amount of organic material and, therefore, knowledge of the interactions between organic contaminants and humic material is essential in understanding the fate of these contaminants in the environment and in soil remediation processes. The heterogeneous nature of humic material makes research in this area complex. However, increased knowledge of the mechanisms of sorption of contaminants to humic material and the factors affecting these mechanisms will lead to the creation of predictive models for environmental processes such as remediation by thermal desorption. Presented below are some recommendations for future research in this area.

1. Although TGA was performed on the clean humic acid samples, mass loss data generated by TGA would be useful if run in conjunction with DSC for all of the contaminant-humic acid mixtures. This way, heat flow values could be related to actual mass remaining rather than initial mass.
2. Analysis of the evolved volatiles and vapor phase composition from the DSC is also important. Integration of a gas chromatograph or mass spectrometer with the DSC would allow for complete mass balances to be performed for the runs. As well, useful information concerning the decomposition products of the aliphatic compounds could be obtained.
3. A larger variety of contaminants should be investigated. In particular, more polar organic compounds should be investigated. For example, for the case of o-chlorophenol, the short time between initial contamination of the humic acid and

the DSC run due to the high volatility of the contaminant could be corrected by using m-chlorophenol or p-chlorophenol which both occur as a solid at room temperature.

4. Humic acids should be extracted from different soils using different extraction techniques to further investigate the effect of humic acid structure on its interaction with organic contaminants. Although the use of commercial humic acids in this work was effective for the investigation of the importance of structural differences in humic acids, the applicability of these commercial humic acids to natural humic acids is questionable.
5. More information concerning the phase behaviour of humic acid is required. This way, the results presented here could be validated using a more accurate model.

## Chapter 7

### REFERENCES

- Aochi, Y. O. and Farmer, W. J. (1997) "Role of Microstructural Properties in the Time-Dependent Sorption/Desorption Behaviour of 1,2-Dichloroethane on Humic Substances" Environmental Science and Technology. 31, 9, 2520-2526.
- ASTM (1995) "Standard Test Methods for Moisture, Ash, and Organic Matter of Peat and Other Organic Soils", D 2974-87.
- Bowser, W. E., Kjearsgaard, A. A., Peters, T. W. and Wells, R. E. (1962) "Soil Survey of the Edmonton Sheet (83-H)" University of Alberta Bulletin No. SS-4, Alberta Soil Survey Report No. 21. University of Alberta, Edmonton, Alberta.
- Briggs, G. G. (1974) "A Simple Relationship Between Soil Adsorption of Organic Chemicals and Their Octanol-Water Partition Coefficients" Proceedings of the 7<sup>th</sup> British Insecticide and Fungicide Conference 1973. The Boots Company, Inc., Nottingham.
- Cassel, B. and DiVito, M. P. (1994) "Use of DSC to Obtain Accurate Thermodynamic and Kinetic Data" American Laboratory. January, 14-16.
- Chin, Y. P. and Weber, W. J. Jr. (1989) "Estimating the Effects of Dispersed Organic Polymers on the Sorption of Contaminants by Natural Solids. 1. A Predictive Thermodynamic Humic Substance-Organic Solute Interaction Model" Environmental Science and Technology. 23, 8, 978-984.
- Chiou, C. T., McGroddy, S. E. and Kile, D. E. (1998) "Partition Characteristics of Polycyclic Aromatic Hydrocarbons on Soils and Sediments" Environmental Science and Technology. 32, 2, 264-269.
- Chiou, C. T., Porter, P. E., and Schmedding, D. W. (1983) "Partition Equilibria of Nonionic Organic Compounds between Soil Organic Matter and Water" Environmental Science and Technology. 17, 4, 227-231.
- Cook, R. L. (1997) "A Structural Metal Binding Study of Laurentian Fulvic Acid" PhD Dissertation, University of Calgary, Calgary, Alberta.
- Cook, R. L. and Langford, C. H. (1998) "Structural Characterization of a Fulvic Acid and a Humic Acid Using Solid-State Ramp-CP-MAS <sup>13</sup>C Nuclear Magnetic Resonance" Environmental Science and Technology. 32, 5, 719-725.

- Flaig, W., Beutelspacher, H., and Rietz, E. (1975) "Chemical Compostion and Physical Properties of Humic Substances". Soil Components: Volume 1 Organic Components. Ed. Gieseking, J. E., Springer-Verlag, New York, 1-211.
- Friend, D. (1996) Remediation of Petroleum Contaminated Soils. National Academy Press, Washington, D. C.
- Ganaye, V. A., Keiding, K., Vogel, T. M., Viriot, M.-L., and Block, J.-C. (1997) "Evaluation of Soil Organic Matter Polarity by Pyrene Fluorescence Spectrum Variations" Environmental Science and Technology. 30, 10, 2701-2706.
- Garbarini, D. R. and Lion, L. W. (1986) "Influence of the Nature of Soil Organics on the Sorption of Toluene and Trichloroethylene" Environmental Science and Technology. 20, 12, 1263-1269.
- Gauthier, T. D., Seltz, W. R., and Grant, C. L. (1987) "Effects of Structural and Compositional Variations of Dissolved Humic Materials on Pyrene  $K_{oc}$  Values" Environmental Science and Technology. 21, 3, 243-247.
- Goodrum, J. W. (1997) "Rapid Measurements of Boiling Point and Vapor Pressure of Short-Chain Triglycerides by Thermogravimetric Analysis" IAOCS. 74, 8, 947-950.
- Goodrum, J. W. and Siesel, E. M. (1996) "Thermogravimetric Analysis for Boiling Points and Vapour Pressure" Journal of Thermal Analysis. 46, 1251-1258
- Graber, E. R. and Borisover, M. D. (1998) "Hydration-Facilitated Sorption of Specifically Interacting Organic Compounds by Model Soil Organic Matter" Journal of Environmental Science and Technology. 32, 2, 258-263.
- Karickhoff, S. W., Brown, D. S. and Scott, T. A. (1979) "Sorption of Hydrophobic Pollutants on Natural Sediments" Water Research. 13, 241-248.
- Kile, D. E., Chiou, C. T., Zhou, H., Li, H., and Xu, O. (1995) "Partition of Nonpolar Organic Pollutants from Water to Soil and Sediment Organic Matters" Environmental Science and Technology. 29, 5, 1401-1406.
- Laforanara, P., Oberacker, D. and dePercin, P. (1991) "Thermal Desorption Treatment" EPA Report EPA/504/2-91-008.
- Lambert, S. M. (1967) "Functional Relationship Between Sorption in Soil and Chemical Structure" Journal of Agriculture and Food Chemistry. 15, 4, 572-576.

- Leboeuf, E. J. and Weber, W. J. (1997) "A Distributed Reactivity Model for Sorption by Soils and Sediments. 8. Sorbent Organic Domains: Discovery of a Humic Acid Glass Transition and an Argument for a Polymer-Based Model" Environmental Science and Technology. 31, 6, 1697-1702.
- Lemke, T. L. (1992) Review of Organic Functional Groups: Introduction to Medicinal Organic Chemistry Second Edition, Lea and Febiger, Philadelphia.
- Lighty, J. S., Pershing, D. W., Cundy, V. A. and Linz, D. A. (1988) "Characterization of Thermal Desorption Phenomena for the Cleanup of Contaminated Soil" Nuclear Chemical Waste Management. 8, 225-237.
- MacCarthy, P. and Malcolm, R. L. (1989) "The Nature of Commercial Humic Acids" Aquatic Humic Substances: Influence on Fate and Treatment of Pollutants. Eds. Suffet, I. H. and MacCarthy, P., Advances in Chemistry Series 219, American Chemical Society, Washington, DC.
- MacIntyre, W. G. and Smith, C. L. (1984) "Comment on Partition Equilibria of Nonionic Organic Compounds between Soil Organic Matter and Water" Environmental Science and Technology. 18, 4, 295-297.
- Maguire, V. (1994) "Thermal Desorption of Contaminated Soils: A Study of Soil Fractions-Contaminant Interactions" MSc Thesis, University of Calgary, Calgary, Alberta.
- Maguire, V., Svrcek, W. Y., Mehrotra, A. K. and Razzaghi, M. (1995) "A Study of Interactions Between Soil Fractions and PAH Compounds in Thermal Desorption of Contaminated Soils" The Canadian Journal of Chemical Engineering. 73, 844-853.
- Means, J. C., Wood, S. G., Hassett, J. J. and Benwart, W. L. (1980) "Sorption of Polynuclear Aromatic Hydrocarbons by Sediments and Soil" Environmental Science and Technology. 14, 12, 1524-1528.
- Mehrotra, A. K., Maguire, V. and Svrcek, W. Y. (1996) "Interactions Between Soil Fractions and PAH Compounds in Thermal Desorption of Contaminated Soils" The 5<sup>th</sup> World Congress of Chemical Engineering. 3, 570-575.
- Mingelgrin, U. and Gerstl, Z. (1983) "Reevaluation of Partitioning as a Mechanism of Nonionic Chemicals Adsorption in Soils" Journal of Environmental Quality. 12, 1, 1-11.
- Onken, B. M. and Traina, S. J. (1997) "The Sorption of Pyrene and Anthracene to Humic Acid-Mineral Complexes: Effect of Fractional Organic Carbon Content" Journal of Environmental Quality. 26, 126-132.



- Saleh, F. Y. and Chang, D. (1983) "Cross Polarization Carbon-13 Nuclear Magnetic Resonance and Fast Atom Bombardment Mass Spectrometry of Fractionated Fulvic Acid" Analytical Chemistry. 55, 6, 862-866.
- Schnitzer, M. (1982) "Organic Matter Characterization" Methods of Soil Analysis Part 2 Chemical and Microbiological Properties Second Edition. Eds. Page, A. L., Miller, R. H. and Keeney, D. R. American Society of Agronomy, Madison, Wisconsin.
- Schnitzer, M. (1978) "Humic Substances: Chemistry and Reactions" Soil Organic Matter. Eds. Schnitzer, M. and Khan, S. U., Elsevier Scientific Publishing Company, New York.
- Schnitzer, M. and Desjardins (1962) "Molecular and Equivalent Weights of Organic Matter of a Podzol" Soil Science Proceedings. 26, 362-365.
- Schnitzer, M. and Hoffmann, I. (1964) "Pyrolysis of Soil Organic Matter" Soil Science Society Proceedings. 28, 520-525.
- Schnitzer, M. and Kodama, H. (1972) "Differential Thermal Analysis of Metal-Fulvic Acid Salts and Complexes" Geoderma. 7, 93-103.
- Schnitzer, M. and Schulten, H. R. (1995) "Analysis of Organic Matter in Soil Extracts and Whole Soils by Pyrolysis-Mass Spectrometry" Advances in Agronomy. 55, 167-217.
- Schnitzer, M. and Wright, J. R. (1957) "Extraction of Organic Matter from Podzolic Soils by Means of Dilute Inorganic Acids" Canadian Journal of Soil Science. 37, 1, 89-95.
- Senesi, N. and Chen, Y. (1989) "Interactions of Toxic Organic Chemicals with Humic Substances" Toxic Organic Chemicals in Porous Media. Eds. Z. Gerstl, Y. Chen, U. Mingelgrin and B. Yaron, Springer-Verlag, New York, 37-90.
- Seyler, A. J. (1976) "Parameters Affecting the Determination of Vapor Pressure by Differential Thermal Methods" Thermochimica Acta, 17, 129-136.
- Smith, M. T. (1997) "Treatment of Contaminated Soils by Batch Thermal Desorption" MSc. Thesis, University of Calgary, Calgary, Alberta.
- Sparks, D. L. (1995) Environmental Soil Chemistry. Academic Press, Toronto.
- Stevenson, F. J. (1994) Humus Chemistry Genesis, Composition and Reactions Second Edition. John Wiley and Sons, Inc., Toronto.

- Stott, D. E. and Martin, J. P. (1990) "Synthesis and Degradation of Natural and Synthetic Humic Materials in Soil" Humic Substances in Soil and Crop Sciences: Selected Readings. Eds. MacCarthy P., Clapp, C. E., Malcolm, R. L. and Bloom, P. R., American Society of Agronomy, Inc., Soil Science Society of America, Inc., Madison, Wisconsin.
- TA Instruments (1994) "Vapor Pressure Measurements Made Easier" The TA Hotline. Vol. 1.
- Tan, K. H. (1985) "Scanning Electron Microscopy of Humic Matter as Influenced by Methods of Preparation" Soil Science Society of America Journal. 49, 1185-1191.
- Tan, K. H. (1978) "Formation of Metal-Humic Acid Complexes by Titration and their Characterization by Differential Thermal Analysis and Infrared Spectroscopy". Soil Biology and Biochemistry. 10, 123-129.
- Tan, K. H., Hajek, B. F. and Barshad, I. (1986) "Thermal Analysis Techniques". Methods of Soil Analysis: Part 1 Physical and Mineralogical Methods Second Edition. Ed. Klute, A. American Society of Agronomy, Madison, Wisconsin.
- Troxler, W. L., Cudahy, J. J., Zinc, R. P., Yezzi, J. J. Jr., and Rosenthal, S. I. (1993) "Treatment of Nonhazardous Petroleum-Contaminated Soils by Thermal Desorption Technologies" Air and Waste. 43, 1512-1525.
- Valenti, M. (1994) "Cleaning Soil Without Incineration" Mechanical Engineering. May Issue.
- Voice, T. C. and Weber, W. J. (1983) "Sorption of Hydrophobic Compounds by Sediments, Soil and Suspended Solids- 1 Theory and Background" Water Resources. 17, 10, 1433-1441.
- Watson, E. S., O'Neil, M. J., Justin, J., and Brenner, N. (1964) "A Differential Scanning Calorimeter for Quantitative Differential Thermal Analysis" Analytical Chemistry. 36, 7, 1233-1237
- Weed, S. B. and Weber, J. B. (1975) "Pesticide-Organic Matter Interactions" Pesticides in Soil and Water. ed. Guenzi, W. D., Soil Science Society of America, Inc. Madison, Wisconsin.
- Wershaw, L. R. (1993) "Model for humus in Soils and Sediments" Environmental Science and Technology. 27, 5, 814-816.
- Xing, B. and Pignatello, J. J. (1997) "Dual-Mode Sorption of Low-Polarity Compound in Glassy Poly(Vinyl Chloride) and Soil Organic Matter" Environmental Science and Technology. 31, 792-799.

## APPENDIX A

### CALCULATIONS FOR DATA PROCESSING

#### A.1 Calculations

Differential thermal calorimetry (DSC) is a thermal analysis technique in which the differential energy required to keep both a sample and a reference at the same temperature is measured, while being subjected to a controlled heating program. The measurement signal,  $U$ , is recorded in  $\mu\text{V}$ . The calorimetric sensitivity ( $E(T)$ ) is a calibration constant in  $\mu\text{V/mW}$  and is a measure of the number of  $\mu\text{V}$  required for a heat flow to the sample of 1 mW. Thus, the heat flow per unit mass to the sample ( $Q$ ) at any given time can be calculated by:

$$Q = \frac{U}{E(T) \times m} \quad (\text{A.1})$$

where  $m$  is the sample mass (mg) and  $T$  is temperature ( $^{\circ}\text{C}$ ).

By integration, the enthalpy change ( $\Delta H$ ) of the sample can be calculated by:

$$\Delta H = \frac{\int U dt}{E(T) \times m} \quad (\text{A.2})$$

where  $\Delta H$  is the enthalpy change of the sample in mJ and  $t$  is time.  $E(T)$  can be resolved into a temperature dependent and temperature independent component according to:

$$E(T) = E_{in} \cdot E_{rel} \quad (A.3)$$

where  $E_{in}$  is the value of  $E$  at 156.6 °C, the melting point of indium, and is determined during calibration using the TA89E software.  $E_{rel}$  is a function of temperature and is determined by the material and design of the METTLER DSC12E.  $E_{rel}$  can be determined using the equation:

$$E_{rel} = A + BT \quad (A.4)$$

where  $A$  is 1.078 and  $B$  is  $-5.512 \times 10^{-4}$  and  $T$  has units of °C.

After  $E_{in}$  is found through calibration, the heat flow  $Q$  in mW/mg can be calculated using:

$$Q = \frac{U}{E_{in} \cdot E_{rel} \cdot m} \quad (A.5)$$

## A.2 Data Processing

The TA89E software presents the data in graphical form and the data files are stored in machine language format. Each file contains information concerning the mass of the sample ( $m$ ) the calorimetric sensitivity ( $E_{in}$ ), the temperature ( $T$ ) and the

measurement signal, ( $U$ ). The data was extracted from this format and imported into a spreadsheet program. The data was read and numbers calculated using the BASIC program as shown in A.3.

Every line of the raw data file consists of four entries, two of which are zero or a small integer value (i.e. 0, 1, 2, 3 or 4). Lines 1 to 37 contain constant values such that the constant occurs in one of the four columns and remaining three columns have values of zero.  $E_{ln}$  occurs on line 3 and  $m$  occurs on line 4. The column number is not consistent for  $E_{ln}$  or  $m$  and therefore the BASIC program extracts the value by determining the non-zero column value.

The experimental values of  $T$  versus  $U$  are recorded from line 38. The column number in which these values occur is not consistent; however,  $T$  and  $U$  are always recorded consecutively. Since both  $T$  and  $U$  are real numbers and because the other two columns contain zero or small integer values,  $T$  and  $U$  can be extracted by first setting all integer values to zero, and then determining the product of each consecutive data entry. Columns with a non-zero product can be identified and recorded as  $T$  and  $U$ .

The data files obtained from each run are very large and must be reduced before being imported into a spreadsheet program. This is done by printing each  $n^{\text{th}}$  data point where  $n$  is an integer number.

### A.3 BASIC Program

Listed below is the BASIC program used to process the DSC data. To run this program a “\*.out” file must be created using the METTLER system software TA89E.

This data file can be obtained by printing the data to a file using the "Print Data" option under the "Data" menu. This program results in 3 files: "\*.dat", "\*.cln", and "\*.red". The "\*.red" file can be imported into a spreadsheet program such as EXCEL.

```

10 CLS
20 input "enter input file WITHOUT EXTENSION", S$
21 D$="C:\MICHELLE\"+S$+".OUT"
22 OPEN D$ FOR INPUT AS #5
23 A$="c:\MICHELLE\"+s$+".DAT"
24 open A$ for output as #6
25 for I=1 to 20000
26 if eof(5) then 444
27 on error goto 444
28 input #5,a,b,c,d
29 print #6,i,a,b,c,d
30 next i
444 close #5:close #6
31 beep:beep
32 print
33 print "Done Reading...Now Cleaning"
34 open A$ for input as #1
35 B$="c:\MICHELLE\"+S$+".CLN"
36 open B$ for output as #2
46 aa=1.078
47 bb=-5.512e-4
50 write "Writing File... "
60 print: print "Please wait !"
70 FOR I=1 TO 20000
71 IF EOF(1) THEN 180
80 ON ERROR GOTO 180
81 INPUT #1,AA,A,B,C,D
82 if I<37 then print #2,AA,A,B,C,D
501 IF A=1 OR A=2 OR A=3 OR A=4 THEN A=0
502 IF B=1 OR B=2 OR B=3 OR B=4 THEN B=0
503 IF C=1 OR C=2 OR C=3 OR C=4 THEN C=0
504 IF D=1 OR D=2 OR D=3 OR D=4 THEN D=0
91 if i=3 and a>0 then ein=a
92 if i=3 and b>0 then ein=b
93 if i=3 and c>0 then ein=c
94 if i=3 and d>0 then ein=d
95 if i=11 and a>0 then m=a
96 if i=11 and b>0 then m=b
97 if i=11 and c>0 then m=c

```

```

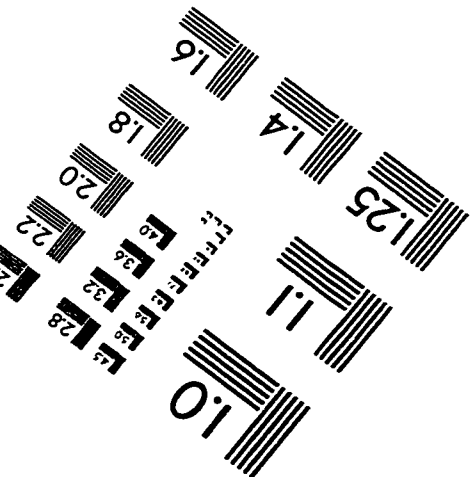
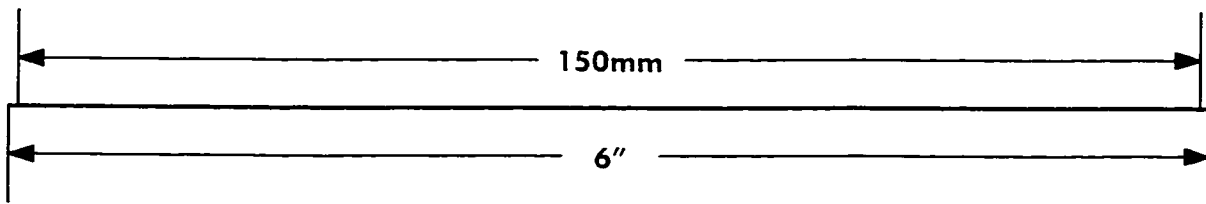
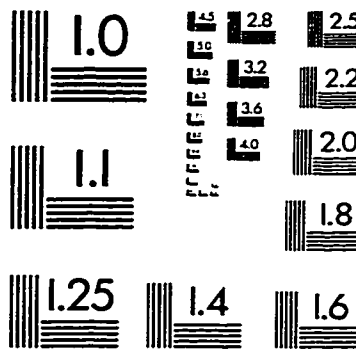
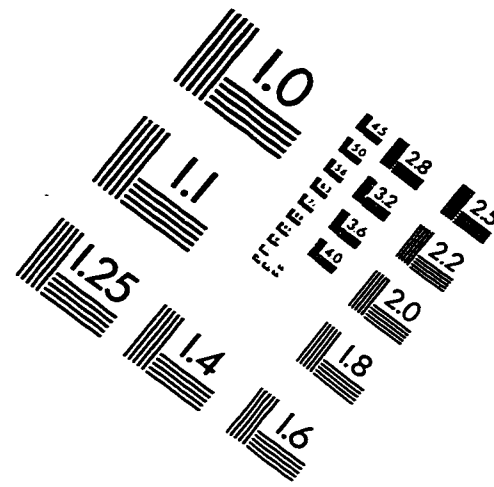
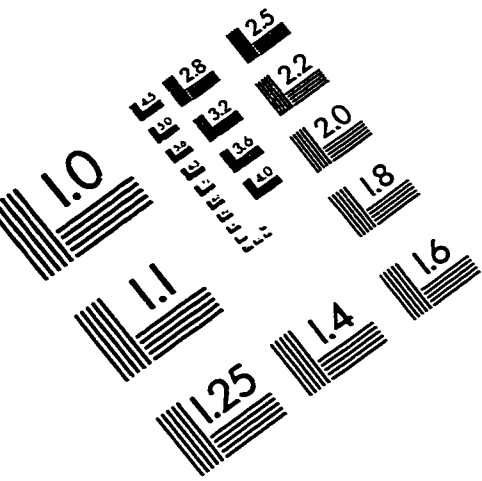
98 if i=11 and d<>0 then m=d
100 P1=A*B:P2=B*C:P3=C*D:P4=D*A
110 IF I<37 THEN 170
120 IF P1>0 OR P1<0 THEN PRINT #2,A,-B
130 IF P2>0 OR P2<0 THEN PRINT #2,B,-C
140 IF P3>0 OR P3<0 THEN PRINT #2,C,-D
150 IF P4>0 OR P4<0 THEN PRINT #2,D,-A
170 NEXT I
171 print , ein
172 print , m
180 close #1:close #2
181 beep:beep
185 print
186 print "Done Cleaning...now reducing!"
187 open b$ for input as #3
188 c$="c:\MICHELLE\"+S$+".RED"
189 open c$ for output as #4
190 for J=1 to 20000
191   if eof(3) then 200
192   if J<37 then
193     input #3,aa,a,b,c,d
194     print #4, AA,A,B,C,D
195   else
196     INPUT #3,t,h
197     s=s+1
198   end if
199 next J
200 close #3
201 n=s/1400
202 m=int(n)+1
203 open b$ for input as #3
204 for K=1 to s+36
213   if K<37 then
214     input #3, aa,a,b,c,d
205   else
206     input #3, t,h
207     if k=37 then 300
208 v=v+1
209 if v<m then 310
300 print #4, t,h
301 v=0
302 end if
310 next k
311 close #3
312 close #4
313 BEEP:BEEP

```

```
314 PRINT "ALL DONE!"  
315 END
```



# IMAGE EVALUATION TEST TARGET (QA-3)



APPLIED IMAGE, Inc.  
1653 East Main Street  
Rochester, NY 14609 USA  
Phone: 716/482-0300  
Fax: 716/288-5989

© 1993, Applied Image, Inc., All Rights Reserved

